UC Riverside

UC Riverside Electronic Theses and Dissertations

Title

Novel Image-Based Analysis of Bone Teratogenesis Using Human Embryonic Stem Cell Model

Permalink

https://escholarship.org/uc/item/0rx7h119

Author

Martinez, Ivann Kenneth Carvajal

Publication Date

2014

Peer reviewed|Thesis/dissertation

eScholarship.org Powered by the California Digital Library
University of California

UNIVERSITY OF CALIFORNIA
RIVERSIDE

Novel Image-Based Analysis of Bone Teratogenesis Using Human Embryonic Stem Cell Model

A Dissertation submitted in partial satisfaction
of the requirement for the degree of

Doctor of Philosophy

in

Cell, Molecular, and Developmental Biology

by

Ivann Kenneth Carvajal Martinez

December 2014

Dissertation Committee::

Dr Nicole I. zur Nieden, Chairperson
Dr. Prudence Talbot
Dr. Jin Nam

Copyright by
Ivann Kenneth Carvajal Martinez
2014

The Dissertation of Ivann Kenneth Carvajal Martinez is approved:

_____

_____

_____

Committee Chairperson

University of California, Riverside

Acknowledgement

“Experience is a brutal teacher, but you learn, my God, do you learn” C.S. Lewis. Obtaining this PhD. has been challenging to say the least, but I am lucky and thankful for several people for all the assistance I received, whether they were obvious or subtle. I truly appreciate all the lessons that you have imparted and advise that you have given to me over the course of this endeavor.

For my dream giver, Dr. Judy Brusslan, I wanted to thank you for taking me into your lab and giving me a home throughout whole college career. Your lab allowed me to develop the confidence and technical know-how to survive through graduate school. It was through your lab that I develop lifelong friendships and a lab family. You have opened so many doors for me that I can honestly say that without your guidance and mentorship I would have never started down this path. You have been a lifelong mentor to me even after I left your lab. You have encouraged me to endure and put me back on track when I lost my way, Thank you so much. I still remember the day you told me that you dreamed for me to get into graduate school and get my PhD, that was the day I first realized that it is possible for me to make this dream a reality. I am truly blessed to have you as my lifelong mentor.

To my summer mentor, Dr. Julia Bailery-Serres, I want to say thank you for being my mentor during my time at UC Riverside for the summer NSF-REU program. I have learned so much from you and my graduate mentor Dr. Christina Branco-Price. You have expanded my views about research and helped me see what its like to be a graduate student and prepared me to undertake the challenge of a PhD.

My graduate whisperer, Dr. Linda Walling, even though I did not end up in your lab, you have been a very important mentor to me during my time here at UC Riverside. You have provided me with the will to continue during my darkest times as a graduate student, and advice whenever I needed it. I was not even your student, but you have been always been there for me. As a graduate students and a person, your support has meant so much to me.

My graduate cheerleader, Dr. Kelly Young, you have been an inspirational teacher to me both as a student, as an undergraduate and graduate. Thank you for being a wonderful teacher and person. You have inspired many of your students to do great things. You have helped me remember to love the science and the joy of pursuing it. You have taught me so much by being the wonderful teacher and person. You valued your students and found ways to polish them and shine like diamonds. Due to your encouragement, I found a way to balance the challenges and reward of a obtaining a PhD.

My graduate committee members, Dr. Prue Talbot and Dr. Jin Nam, your guidance have been a tremendous help to me during my time in UC Riverside. You have offered me great advice to improve my work and thesis. You have been available to me whenever I needed your guidance; I am lucky to have both of you as member of my committee. You have kept me from failing and have advanced my progress. I honestly could not have done this with your knowledge and expertise.

My PI and mentor Dr. Nicole zur Nieden, I am lucky and honored to have worked under your guidance and tutelage. I could not have asked for a better PI and mentor. You have taught me so much during my time in your lab. You have shared your expertise and educated me on how to be successful in our field. You have been a great friend, and offered me compassion when I needed it. I excelled as a leader and a member of you lab because you found a way to bring out the best in me, even when I didn't think I could. You believed in my potential and have nurtured it. You had my back through thick and thin. Thank you so much. I can honestly say I would not have succeeded in this endeavor without you. Thank you for helping me achieve the dreams that my undergraduate mentor dared me to achieve.

I am thankful for my years that I have spent in your labs and as a member of your lab families. For everything we shared. For every chance we have to grow. I promise to take the best of you with me and lead by your example wherever I go.

Dedication

I dedicate this thesis to my family, to Mary, my grandmother, to Rommel, my father, to Nellie, my mother, and to Cedrick, my brother. You have been my inspiration and my reason to pursue this dream.

I dedicate this to my fellow Brusslanites: Heather, Jennifer, Stephanie, Leticia, Michelle, Gorjana, Scott, Christy, Daisy, Bethel, Robert, Meena, and my undergraduate PI, Dr. Judy Brusslan. You have encouraged me to continue on my pursuit to be a scientist and to be confident as a student and a lab member.

I dedicate this to my fellow lab mates at the zur Nieden Lab: Nicole, Lauren, Devon, Kevin, Beatrice, Beatriz, Antonio, Tiffany, Darcie, and graduate PI Dr. Nicole zur Nieden. You have helped me be the person and scientist capable of being creative, knowledgeable, and resilient. You have helped me learn how to be a better leader and lab member.

ABSTRACT OF THE DISSERTATION

Novel Image-Based Analysis of Bone Teratogenesis Using
Human Embryonic Stem Cell Model

by

Ivann Kenneth Carvajal Martinez

Doctor of Philosophy, Graduate Program in
Cell, Molecular, and Developmental Biology
University of California, Riverside, December 2014
Dr. Nicole I zur Nieden, Chairperson

Development is an important process in the biology of an organism. This process is tightly regulated allowing it to be responsive to signals and resistant to toxicants to prevent the occurrence of congenital diseases. Such toxicants that alter development are teratogens, the identification and characterization of which is of immense importance. Of greatest concern are those teratogens that the embryo is exposed to involuntarily, such as environmental toxicants, the most well known being tobacco smoke. Here, we have devised a novel cellular model for bone development using human embryonic stem cells to screen tobacco products for their potential teratogenicity. This cellular model of bone development can successfully mimic embryonic osteogenesis in humans *in vitro*. Using this method we have tested commercially available tobacco products, both conventional and “harm-reduction”. We have identified that sidestream smoke from all tobacco products has a more detrimental effect on osteoblast differentiation compared to mainstream smoke, which caused no observable changes in osteogenesis. Sidestream

smoke was more potent in disrupting osteogenesis by either lowering levels of calcification through a teratogenic effect or by reducing cell viability through a cytotoxic effect. Harm-reduction products reduced calcification in differentiating human embryonic stem cell osteogenic cultures at lower concentrations than conventional products in the absence of cytotoxicity, suggesting a teratogenic effect. By extension, this data suggests that harm-reduction products offer no reduction in harm towards their effects on bone health. In addition to screening several tobacco products using calcification and cell viability assays, we also created a novel video–based method to determine teratogenic effects on osteogenic differentiation. This method utilizes image analysis technology to automatically segment areas of calcification, the functional property of osteoblasts, from phase contrast images or time-lapse videos. This new method allowed us to quantify the amount of calcium in a kinetic manner without destroying the cultures. Overall, this study has yielded a novel method to establish teratogenicity of chemicals towards bone differentiation using data obtained from images, a method that is more cost-effective, requires less sample and is environmentally safer compared to conventional methods of establishing teratogenic effects of chemicals.

Table of contents

List of Figures

Chapter 2

Chapter 3

Chapter 4

Abbreviation

AA	Ascorbic Acid
Alizarin	Alizarin Red S
ALP	Alkaline Phosphatase
AS	American Spirits
BMC	Bone Mineral Content
C	Camel
Ca^{2+}	Calcium Ion
CB	Camel Blue
CDM	Control Differentiation Medium
CSn	Camel Snus
CYT	Cytotoxic Effect
DAPI	4',6-diamidino-2-phenylindole
DEX	Dexamethasone
DMEM	Dulbecco's Modified Eagle's Medium
ECM	Extracellular Matrix
ESC	Embryonic Stem Cells
EST	Embryonic Stem Cell Test
FBS	Fetal Bovine Serum
hESCs	Human Embryonic Stem Cells
hiPSCs	Human Induced Pluripotent Stem Cells
IC_{50}	Inhibition of Cell Viability
ID_{50}	Inhibition of differentiation
M	Marlboro Red
MatLab	Matrix Laboratory
MG	Marlboro Gold
MS	Mainstream Smoke
MSn	Marlboro Snus
MTT	3-[4,5-dimethylthiazol-2-yl]-2,5-diphenylterazolium bromide
nAChR	Nicotine Acetylcholine Receptors
NEAA	Non-essential amino acids
NNK	4-(methylnitro-samino)-1-(3-pyridyl)-1-butanone
NNN	N'-nitrosonornicotine
NOE	No Observable Effect
OCN	Osteocalcin
OPN	Osteopontin
Osx	Osterix
PAH	Polyaromatic Hydrocarbons
PAH	Polyaromatic Hydrocarbons
PBS	Phosphate Buffered Saline
PE	Puff Equivalent
RIPA	Radio-Immunoprecipitation Assay
ROS	Reactive Oxygen Species
SIDS	Sudden Infant Death Syndromes
SS	Sidestream Smoke

TER	Teratogenic Effect
TSNAs	Tobacco Specific Nitrosamines
VD_3	1,25α-dihydryoxy vitamin D_3
vK	von Kossa
WiCell	WiCell Research Institute
β-GP	β-glycerophosphate

Chapter 1: Introduction to the Thesis

Organogenesis and the Effects of Teratogens on Human Development

Humans are one of the most complex multi-cellular organisms on the planet. Human fetal and growth and development have allowed a fertilized fusion of an ovum and sperm to develop into an embryo. In humans, this development occurs in a nine month span called gestation or pregnancy. This results in the formation of the eleven organ systems found in the human body. Organogenesis, the process of organ development, occurs early during embryogenesis, beginning with gastrulation, a process that results in the formation of the three primary germ layers: the endoderm, the mesoderm, and the ectoderm.

The neural crest, which is often regarded as the 'fourth germ layer' due to its versatile developmental potential, forms at around day 20 of gestation [O'Rahilly and Muller, 2007; https://embryology.med.unsw.edu]. Specifically the cranial neural crest cells have the potential to form bone and cartilage and contribute to skeletal bones in the head. Cardiogenesis begins soon after at day 21 and the heart begins to beat at day 22 to 23, making it the first functioning organ in the developing fetus [https://embryology.med.unsw.edu]. By week 5, organ systems are starting to be formed whereby the cardiovascular system is followed by the respiratory, auditory, and pituitary systems. In week 6, the embryo continues with organ formation to parathyroid, adrenal and thymus glands. In week 5-7, the early mesoderm gives rises to osteoblasts, bone cells that create bones, through a process known as endochondral ossification, which replaces the cartilage framework with bones. This results in the formation of the

appendicular skeleton that later gives rise to the appendages. At week 8, embryogenesis concludes with the final phases of the gastrointestinal tract formation, the head becomes visible, and the axial skeleton forms. In contrast to endochondral bone formation in the appendicular skeleton, the axial skeleton, including the vertebrae and the rib cage, is formed through intramembraneous ossification, which lacks a cartilage framework [https://embryology.med.unsw.edu; O'Rahilly et al, 1980]. Week 9 concludes the first trimester and organ development. The embryo begins to grow until birth at around week 38-40.

During the 1st trimester the developing embryo is most susceptible to effects from environmental sources. In the United States, the Center for Disease Control estimates that 120,000 of babies born will have a congenital birth defect. Birth defects are the leading cause of death in infants, resulting in an estimated 20% of all infant deaths in the country. Some of the most common birth defects are those that affect the central nervous system (2,660 incidents annually), as well as the eye (780), the cardiovascular (6,136), the orofacial (7,088), the gastrointestinal (2,857), and the musculoskeletal (5,889) systems [http://www.cdc.gov/ncbddd/birthdefects/index.html].

The external factors that influence development of an embryo to permanently alter structure or function, restrict the growth, or result in death of the developing embryo, collectively are called teratogens [Gilbert-Barness, 2010]. There are several different types of environmental teratogens that are capable of causing congenital problems. An estimated 10% to 15 % of the congenital disorders has been attributed to environmental teratogens [Brent, 2001; Gilbert-Barness, 2010]. The effect of a teratogen is dependent on its chemical and physical properties, as well as the dose, route of exposure, length of exposure, developmental stage of exposure and susceptibility of the maternal,

embryonic or fetal tissue [Gilbert-Barness, 2010]. Environmental teratogens can come in the form of radiation, infectious agents, disruption in thermal regulation, toxic metals, chemical exposure, as well as consumption of alcohol, tobacco, and other drugs. These environmental teratogens can affect an embryo, as a whole, or different organs, by altering organ development. Thus, it is important to determine and understand how these environmental teratogens can affect a developing embryo.

Modern methods of testing for chemical teratogenicity is accomplished through teratogenicity screening that uses animals, either as *in vivo* models [Cook and Fairweather, 1968; Kochhar, 1980; Fantel, 1982; Schumann, 2010], whole embryo cultures [van der Valk and van der Meijden, 2014; Kim et al, 2013, Casarini et al, 2007], micromass assays [Memon and Pratten, 2013; Hurst et al, 2009; Zou et al, 2012] or stem cells [de Jong et al, 2014; zur Nieden et al, 2004] as an *in vitro* model for development. The latter category of *in vitro* assays will be detailed in chapters 2 and 3 of this thesis.

In this study, we focused on the identification of tobacco products as environmental teratogens and their potential to cause musculoskeletal congenital diseases by affecting osteoblast differentiation using an *in vitro* stem cell differentiation system. We compared the different types of smoke generated from conventional and “harm-reduction” products that are widely available to public consumers by biochemical means and developed a new automatable analysis method through the use of image analysis.

Embryonic Stem Cells: An *In Vitro* Model for Human Embryonic Development

Hallmarks of Pluripotent Stem Cells

Stem cells have recently garnered the attention of the public, policy makers, and scientists because of the promise they hold for the future of medicine and therapeutic uses for treatment towards several diseases such as spinal cord injury, heart disease, diabetes, Parkinson's disease, Alzheimer's disease, Lou Gehrig's disease, lung disease, arthritis, sickle cell anemia, and possibly organ failures. However, there are other potential uses of stem cells apart from regenerative medicine: Stem cells are a powerful tool for laboratory research to understand the intricacies of development, of a cell type, tissue, and organs. In addition, they can be used to create disease models that are imperative for understanding how a disease occurs and progresses, and possibly be used to develop a treatment. Stem cells are also important as a model for drug discovery and for testing toxicity of chemicals, drugs, and environmental toxicants, which is the topic of this thesis.

Stem cells are defined as having the capability to self-renew, as well as the ability to undergo differentiation to become a more specialized cell type [Weissman et al 2001; Smith, 2001]. This definition is somewhat simple and broad, to allow to cover the multiple different kinds of stem cells from different sources. However, this definition of a stem cell does capture in essence the common features between the different kinds of stem cells regardless of their tissue origin.

The description of self-renewal includes the ability of a cell for extensive proliferation, unlike most somatic cells that have been cultured *in vitro*, which have an estimated 80 population doublings before undergoing senescence [Houck et al, 1971;

Hayflick, 1973; Hayflick, 1974; Sherr and DePinho, 2000; Shay et al, 2000]. A notable example of self-renewal capacity was seen in adult hematopoietic stem cells as demonstrated by Iscove and Nawa in 1997, when they serially transplanted adult hematopoetic stem cells into a mouse, have shown that these stem cells can further divide when transplanted to a new host or have been given exogenous cytokines: SCF, c-kit ligand, and Interleukin 11 [Iscove and Nawa, 1997]. Self-renewal also includes the ability to give rise to more stem cells. Stem cells are often viewed to be unspecialized, but also have the ability to differentiate and become specialized. However, it is imperative for stem cells to be capable of dividing without undergoing differentiation, in order to give rise to other unspecialized cells.

The differentiation capacity is also an important property of stem cells and means that stem cells are unspecialized cells capable of undergoing differentiation into a more specialized and distinct cell type. The differentiation capacity, or potency, of a stem cell differs depending on the different type of stem cell and is dictated by its origin as will be detailed in the next section.

Stem Cell Sources: Embryonic Stem Cells versus Adult Stem Cells

There are two general categories of stem cells that differ in their potency: embryonic stem cells and adult stem cells. Adult stem cells are identified to have a more limited differentiation potential, in which it can only develop into cell types that belong to the same embryonic germ layer and thus adult stem cells are described to be multipotent. This is not true for embryonic stem cells, which are pluripotent, because

they are capable of broader differentiation and have the ability to give rise to cell types from all germ layers.

In the adult body, adult stem cells can be obtained from specialized areas, so-called niches, an example of which is the bone marrow that houses both hematopoietic and mesenchymal stem cells. There are several different kinds of recognized adult stem cells that can be found *in vivo* including the already mentioned hematopoietic stem cells [Kau and Turpen, 1983; Medvinsky et al, 1993; Medvinsky and Dzierzak, 1996] and mesenchymal stem cells [Phinney and Prockop; 2007]. A third stem cell type, the endothelial stem cell, is also found in the bone marrow and the lining of blood vessels [Sanada et al, 2014]. In addition, the gut contains intestinal stem cells [Barker et all, 2009; van der Flier and Clevers, 2009], breast tissue contains mammary stem cells [Liu et al, 2005; Prater et al, 2014], neural stem cells are harvested from specific regions of the brain [Alvarez- Buylla et al, 2002; Bjornson et al, 1999], neural crest stem cells can be enriched from skin and gut [Sieber-Blum and Hu, 2008; Kruger et al, 2002] and olfactory stem cells were found to exist in the nose [Murell et al, 2005]. As previously stated, adult stem cells are multipotent and can only give rise to a limited subset of cell types. For example, mesenchymal stem cells give rise to osteoblasts, chondrocytes, myocytes and adipocytes [Jiang et al, 2002]. A disadvantage of adult stem cells is that there is only a small amount of these cells that can be obtained from a person, thus they need to be expanded in culture, which has presented copious problems for researchers.

Another issue that needs to be addressed when harvesting adult stem cells is their purity. In order to properly control for differentiation of adult stem cells into a specific lineage, it is important to control the factors that can direct differentiation. Impurities in adult stem cell populations can lead to unwanted cell to cell signaling that

can affect their differentiation to the targeted cell type. A notable advantage of adult stem cells is the ability to create patient-specific cells, thus reducing immune rejection when transplanted back into the host. This makes adult stem cells a very attractive source for cell-based regenerative medicine. However, adult stem cells are not ideal for the study of development, toxicity testing and drug discovery because of their already mature state. Here, embryonic stem cells offer advantages that are far better suited to early developmental studies.

Embryonic stem cells (ESCs) are obtained from the inner cell mass of a pre-implantation blastocyst [Papaionnou, 2001; Hadjantonakis and Papaioaanou, 2001]. This population of cells in the developing embryo gives rise to the epiblast, which later develops into all the cell types found in the adult organism. *In vitro*, ESCs maintain the capacity to differentiate into the three primary germ layers, a capacity defined as pluripotency. In essence, ESCs can be viewed as *in vitro* model of a developing embryo because of their ability to give rise to all cells in the embryo proper. ESCs are also unique because of their seemingly unlimited proliferative capacity, which by far surpasses that of adult stem cells.

Based on these defining features of ESCs, they are an excellent *in vitro* model for studying developmental processes. In contrast to adult stem cells, their differentiation mimics the complete developmental process from an undefined cell to a final specialized cells, for example, a functional osteoblast. This allows researchers to dissect every stage of development from beginning to end. Drug discovery can use this *in vitro* system as unlimited source of cellular material to develop desired cell types to determine how these chemicals affect the molecular machinery in the cells of a particular organ. This allows researchers to determine probable success of drugs before advancing to clinical

trials. For the same reason, ESCs are excellent models for toxicity testing, during the process of which toxicants or teratogens, for example environmental toxicants, such as tobacco and its components, can be identified that would potentially yield congenital diseases in developing embryos.

Bone Tissue and its Development *in Vivo*

Bones are the rigid organs that make up the body's skeletal frame. There are 206 bones in the adult human body. These bones provide various functions, one of which is to provide the overall structure for the body. They are also essential in providing protection to the body's vital organs, such as the heart, lungs, and brain [Duplomb et al, 2007]. Bones in collaboration with skeletal muscles imparts the body the ability to move. In addition, tiny bones in the ears that can vibrate when sound is perceived relay signals to the brain allowing us to hear. In addition, bone also has important metabolic functions as well as is the site for stem cell niches that allow the body to replace and heal damaged organs.

Metabolically, bones are the storage house for important minerals for the cellular function of the body, such as calcium and phosphorus [Duplomb et al, 2007]. These minerals are essential chemicals that allow for intra- and intercellular signaling. Bones are also important storage sites for growth factors, such as insulin-like growth factors, transforming growth factors, as well as bone morphogenetic proteins. Bones can also play a role in adjusting the pH of the blood by absorbing and releasing alkaline salts. Through the same strategy, bones also play a role in reducing and excreting heavy metals found in the blood that will otherwise affect tissues in the body.

Bones are formed and reshaped through the actions of two cell types found in bone tissue with opposing functions. These bone cells are the osteoclasts that functions to resorb or break down bones [Rouselle and Heymann, 2002]. This is an important role when reshaping bone to allow for proper movement and to fix damage or broken bones. The second class and the focus of this dissertation is the osteoblasts or the bone forming cells. This class of bone cell is responsible in the formation of bone connective tissues by embedding minerals, such as calcium and phosphate on the collagen rich extracellular matrix [Aguila and Rowe, 2005]. The contrasting natures of these two classes of bone cells allow for the formation and development of the rigid and lightweight form of the bodies skeletal frame.

The combined actions of both osteoclasts and osteoblasts results in the formation and structure of all bones found in the human body. There are two distinct methods bones in the skeleton can be physiologically formed through 1) endochondral ossification and 2) intramembranous ossification. Endochondral ossification is dependent on the chondrocyte to create a cartilage-like structure that osteoblasts invade and later mineralize and calcify [Blair et al, 2002]. In fact, the growing portion at the end of the long bone, known as the epiphyseal plate, is composed of chondrocytes. During development, endochondral ossification begins with the creation of primary ossification centers, a step in which osteoblasts invade the cartilage and begin to calcify. This is followed by the development of a secondary ossification site at the distal ends of each bone, as the primary ossification sites are vascularized. The primary ossification sites are remodeled by invading osteoclasts and resorbed and hollowed out to form the bone marrow. Hematopoietic stem cells and mesenchymal stem cells invade and populate the bone-marrow of the developing bone. Lastly, in the secondary ossification centers the

articular cartilage and epiphyseal plate is formed to allow the bones to lengthen. This results in the lightweight and rigid long bones.

Intramembranous ossification does not require the actions of chondrocytes to form a cartilage models. Intramembranous ossification typically occurs in the formation of flat bones that are mainly found in the craniofacial region of the skull as well as trabecular types of bones in the body. Endochondral ossification is typically observed in the bones of the appendicular skeleton. Both Endochondral and Intramembraneous ossification contributes to the formation of the axial skeleton.

Human Embyronic Stem Cell *In Vitro* Differentiation to Model Bone Development

Osteogenesis can be modeled *in vitro* using ESCs [Duplomb et al, 2007; Heng et al, 2004; McClelland Descalzo et al, 2014]. Several methods have been developed to direct the differentiation of ESCs into mature and functional osteoblasts, such as modulating the extracellular matrix in which stem cells are embedded [Heng et al, 2004], the use of co-culture or conditioned media [Heng et al, 2014; Buttery et al, 2001], generation of free radical and reactive oxygen species [Heng et al, 2014; Chae et al, 1999], physical stimuli, such as pulsating electrical field [Heng et al, 2004; Petersson et al, 1982; Yonemori, et al, 1996; Lee and McLeod, 2000], as well as direct genetic manipulation of osteogenic transcription factors [Heng et al, 2004], such as Runx2 [Zelzer et al, 2001], and Osterix [Nakashima et al, 2002; Katagiri and Takahashi, 2002]. The method that will be the focus of this dissertation is the induction of osteogenesis through the addition of a defined chemical milieu [Duplomb et al, 2007; Heng et al, 2004;

McClelland Descalzo et al, 2014] which is also the method that has been described the longest.

Several groups, including our lab, have developed a short list of defined chemical factors to direct differentiation of ESCs to undergo osteogenesis *in vitro* [zur Nieden et al., 2003; Duplomb et al, 2007; Heng et al, 2004]. These osteogenic factors are dexamethasone (DEX) [Sottile et al, 2003; Bielby et al, 2004], 1,25α-dihydryoxy vitaminD_3 (VD_3) [zur Nieden et al, 2003; van Leeuwen et al, 2001], β-glycerophosphate (β-GP) [Sottile et al, 2003; zur Nieden et al, 2003], and ascorbic acid (AA) [Sottile et al, 2003; zur Nieden et al, 2003, Valenti et al, 2014]. DEX is a synthetic steroid that has been shown to promote osteogenic differentiation in mouse and human cells [Buttery et al, 2001; Sottile, 2003]. It has also been shown to be successful in inducing osteogenesis in both embryonic [Buttery et al, 2001; Sottile, 2003] and adult stem cells [Rogers, et al, 1995]. VD_3, the active form of Vitamin D, promotes differentiation and mineralization of emerging osteoblasts [zur Nieden et al, 2003; van Leeuwen et al, 2001; Beresford et al, 1992]. β-GP and AA are critical factors without which the matrix does not calcify [Notoya, 1999].

Osteogenic differentiation of ESCs can be achieved *in vitro* using these osteogenic factors in addition to manipulating the culture environment physically. Mouse ESCs are typically differentiated through the use of a hanging drop culture method. This culture system is comprised of three steps: cells are seeded in the inner part of the petri dish lid as suspended droplets. This forces the cells to aggregate at the bottom of the drop due to gravitational force within three days. These cell aggregates are called embryoid bodies and simulate the formation of a gastrulating embryo. These embryoid bodies are then harvested and grown in suspension for an additional two days, after

which these embryoid bodies are allowed to adhere to gelatin coated plates with the addition of one or more of the identified osteogenic factors.

However, not all protocols require the use of hanging drops to form embryoid bodies but instead directly seed ESCs either into regular petri dishes at low density or into suspension dishes [Trettner et al, 2014], the latter of which seems to primarily be beneficial for the osteogenic differentiation of non-human primate ESCs. Other protocols eliminate the formation of embryoid bodies all together by use of an overgrowth approach and inclusion of osteogenic factors into the media [Karp et al, 2006]. This leads to successful osteogenic differentiation of human embryonic stem cells into mature osteoblasts.

The success of the induction protocol can be verified by assessing hallmark markers of differentiation. One of these markers is the expression of bone-related transcription factors and markers. Osteocalcin, for example, is a structural protein only expressed by mature and functional osteoblasts. It is a secreted protein and is an essential component of the calcified extra-cellular matrix of the bone. Osteocalcin also acts as a hormone to insulin secretion and sensitivity as well as stimulate increase in numbers of insuling-producing cells and reducing fat storage [Lee et al, 2007].

Another hallmark of osteogenesis are the expression of the transcription factors Runx2/Cbfa1, Osterix (Osx), DFosB, and Fra1 [Inoue et al, 2004; Eferi et al, 2004] as well as the bone-specific Alkaline Phosphatase (ALP) and Osteopontin (OPN). Runx2 is the earliest regulator of osteoblast differentiation and belongs the runt-family of transcription factors. It is expressed during the mineralization phase after the establishment of osteoblasts [Nielsen et al, 2001; Choi et al, 1996]. In turn, Osx is a zinc-finger transcription factor that is specifically expressed in osteoblasts [Nakashima, 2002],

but their relationship is such that Runx2 stimulates the expression of Osx. Together then, Runx2 and Osx stimulate the expression of other bone-specific markers, for example OPN, which is a structural protein expressed by mature bone [Kasugai et al, 1992]. OPN plays a role in biomineralization [Addison et al, 2010; Azzopardi et al, 2010; Hunter et al, 2010] and bone remodeling [Choi et al, 2008].

In addition, calcification of the extracellular matrix is an important functional property of osteoblasts in culture, but also *in vivo*. Calcification of the organic part of the matrix results in the hard and rigid construction seen in bones. The extracellular bone matrix is estimated to be composed of 70% inorganic material and 25% organic material and cells, and 5% water. The organic material found in bones are phosphoproteins and glycoproteins including: osteocalcin [Price et al, 1976], OPN [Noda et al, 1988], osteonectin [Fisher et al, 1987], and bone morphogenetic protein [Urist, et al, 1984]. The inorganic material is made of out calcium and phosphate in the form of hydroxyapatite [Legros et al, 1987; Field et al, 1974].

Mineralization of the extracellular matrix can be visualized *in vitro* by using Alizarin Red [Moester et al, 2014] and von Kossa [Meloan and Puchter, 1985] staining to detect the calcium components in the bone matrix. *In vitro*, calcification can also be assessed visually based on its physical appearance on the plate [zur Nieden et al, 2010]. Calcification takes on an appearance of intense black clusters when viewed under phase-contrast microscopy [zur Niedne et al, 2010]. This is due to the amount of calcified bone matrix that forms during the differentiation. This bone matrix prevents the passage of light during microscopy resulting in the black appearance in phase-contrast micrographs. This is an important property that will be exploited in this dissertation to determine the effects of tobacco on bone formation.

Exposure to Tobacco and Smoke and its Potential Effects as a Teratogen

Tobacco is the number one preventable cause of death in the U.S. There is an estimated 480,000 deaths attributed to tobacco use each year including deaths from secondhand smoke [U.S. Department of Health and Human Services , 2014; Centers for Disease Control and Prevention. QuickStats, 2010]. There is a notably more death in men (58%) attributed to smoking than women (42%) [U.S. Department of Health and Human Services , 2014; Centers for Disease Control and Prevention. QuickStats, 2010]. In addition, non-smokers have a 10-year longer life expectancy than smokers. However, this chance can be reduced by 90% if a smoker quits smoking by the age of 40.

Smoking cigarettes and tobacco has been attributed to several types of diseases, the most notable being numerous types of cancer, cardiovascular disease, and respiratory complications [U.S. Department of Health and Human Services , 2014]. In addition, tobacco use has also been linked to increased risk of osteoporosis and reduced bone health, teeth and gum loss, rheumatoid arthritis, cataract and age related macular degeneration, reduced fertility, and type-2 diabetes mellitus [U.S. Department of Health and Human Services , 2014; Centers for Disease Control and Prevention. QuickStats, 2010; U.S. Department of Health and Human Services , 2010].

Tobacco use can also lead to pregnancy-related complications such as premature birth, low birth weight, still birth, and exposure tobacco smoke increases the risk for Sudden Infant Death Syndrome (SIDS) after the baby has been born. Despite of increased awareness of the complications of tobacco use, there is still an estimated 12.9% to 22% of female smokers who consume cigarettes during their pregnancy according to the Center of Disease Control [http://www.cdc.gov/tobacco/osh/index.htm],

warranting the need to test the potential teratogenicity of tobacco products and compare them for their relative toxicity to the unborn.

Cigarette smoke is one of the most complex blends of toxicants found in the environment. It is estimated to contain 7000 chemicals, 69 of which are known carcinogens [U.S Department of Health and Human Services; 2010], including nicotine, tar, polyaromatic hydrocarbons (PAH), tobacco specific nitrosamines (TSNAs), formaldehyde, carbon monoxide, methanol, lead, arsenic, nickel, cadmium, arsenic, and phenols.

Nicotine is regarded to be main component of tobacco and cigarettes. As a chemical, it is known to be a potent stimulant drug. It is also known to be the dependence-property in tobacco and cigarettes that causes addiction. While it can act as a stimulant in low doses, at higher doses of 50-100 mg it can be harmful [Mayer, 2014]. In the body, nicotine acts as an agonist on nicotine acetylcholine receptors (nAChR), except for nAChRα9 and nAChRα10, on which in acts as an antagonist. This results in an increase in blood pressure and heart rate. Nicotine is metabolized in the liver by the cytochrome P450 enzyme mainly into cotinine, but it can also be converted into other metabolites, such as nicotine *N′*-oxide, nornicotine, nicotine isomethonium ion, 2-hydroxynicotine and nicotine glucuronide [“Nicotinic acetylcholine receptors: Introduction". *IUPHAR Database* , 2014].

During later pregnancy, nicotine is also one of the chemicals that has been shown to cross the placenta [Malenka et al, 2009]. It has also been implicated in long term and short term effects on the developing fetus, including impaired brain development, abnormalities of newborn neurobehavior, impaired orientation and

autonomic regulation and abnormalities of muscle tone [Hukkanen et al, 2005]. This suggests that nicotine can potentially also disturb bone development.

In the adult, nicotine consumption form tobacco use and cigarette smoking can lead to complications in bone remodeling and healing, as determined from a reduction in bone mineral content (BMC). In a cohort study to determine the effects of cigarette smoking on bone mass, Gerdhem and Obrant found a significant decrease in BMC in the femoral neck, tibia, calcaneus, as well as in the lumbar spine and bones in the hand [Gerdhem and Obrant, 2002]. In addition, epidemiological studies showed that post-menopausal women lose more cortical bone than non smokers [Behnke and Smith, 2013], suggesting a link between tobacco and osteoporosis. It has been suggested that the effects of nicotine in human bone development is biphasic: high concentrations of >1mmol/L nicotine inhibit proliferation and are toxic, while very low concentrations of 0.01 – 10μmol/L are stimulatory to osteoblasts, upregulating OPN through inducing expression of c-fos and AP1 transcription [Benowitz et al, 2009; Walker et al, 2001]. Nicotine can also reduce bone formation indirectly by lowering serum levels of 25-hydroxyvitamin D and VD_3.

Another product of tobacco use and cigarette smoking that is potentially harmful to bones are reactive oxygen species (ROS). ROS are oxygen-containing molecules that are chemically reactive. ROS are generated naturally by the cells as a by-product of oxygen metabolism [Walker et al, 2001]. ROS plays an essential role in cell signaling as well as homeostasis. During environmental stress like chemical exposure, ROS can increase significantly, and elevation of ROS in the cellular system can lead to oxidative stress. If not corrected, this can lead to cell death [Walker et al, 2001] or inhibited differentiation in a variety of tissue lineages [Need et al, 2002].

Oxidative stresses due to excessive ROS have in fact been implicated also in the reduction of bone formation *in vivo*. Mechanistically, oxidative stress can lead to attenuation of osteogenesis by suppressing the Wnt signaling pathway [Need et al, 2002], which is an important signaling pathway for osteoblast development *in vivo* [Marie and Hay, 2013], but also for the osteogenic differentiation of pluripotent stem cells [Devargayam et al, 2004].

Canonical Wnts, such as Wnt3a, signal through the stabilization of β-catenin [Iyer et al, 2013]. Increased stabilization of β-catenin leads to translocation of this protein from the cytoplasm into the nucleus. Upon entering the nucleus, β-catenin has a high affinity to LEF/TCF transcription factors leading to the occupation of promotors coding for bone-specific proteins, such as osterix, and their subsequent transcription [Monroe et al, 2012]. The existing link between ROS and bone differentiation suggests that exogenous ROS caused by environmental tobacco smoke could potentially lead to a reduction of osteoblastogenesis by modifying Wnt signaling.

Another component of tobacco smoke that possibly results in a reduction in bone formation are polyaromatic hydrocarbons (PAHs). PAHs have been identified to be both carcinogenic and teratogenic, and can also lead to a decrease in osteoblastogenesis through the induction of endogenous ROS, as well as through the induction of p53, which can lead to apoptosis [van der Vos and Coffer, 2008; Almeida et al, 2007]. Formation of endogenous ROS can result in oxidative stress. This suggests that PAHs can induce ROS, which can then lead to modification of the Wnt signaling pathway during osteogenesis.

Video and Image Analysis in a Biological World

Biological evidence has been built on the back bone of images. Pioneers in cell biology, such as Anton van Leeuwenhoek, the inventor of microscopes, and Robert Hook, who first confirmed the existence of cells, have relied heavily upon simple drawings to catalog the evidence for their claims. Recent advances in both microscopy and computers have led to a new revolution in cell biology. This is the advent of analysis based on observations that can be derived from microscopy images or micrographs. The hope is to develop novel methods that are not only high-throughput and automated, but also accurate. Methods such as the one presented on this dissertation are a step toward revolutionizing the field of cell biology, as well as toxicology. For now, this is an introduction to computer vision or machine learning for creating tools designed to analyze biological events, such as bone differentiation.

New innovation in microscopy, such as robotics, has allowed for automated imaging opportunities, such as the Nikon Biostation Series. The Biostation Series is a phase contrast microscope built inside an incubator with robotics to allow for high-throughput automated imaging in both phase contrast or fluorescence mode. The amount of data that can be collected from this method can be staggering. Thus, there is a need for innovation in computational analysis of these captured biological events to reduce the workload and increase the objectivity of the results [Yu et al, 2002]. Bioimage informatics methods, such as object detection, motion analysis, and morphometric feature measurements, can offer a powerful solution [Yu et al, 2002; Wilk et al, 2013; Danuser, 2011; Murphy, 2011]. In order to create automated methods to analyze data in a high throughput manner, methods have to be created specifically for a given task. This

can be accomplished through machine learning [Myers, 2012; Eliceiri et all, 2012; Cherkassky, 2009]. Machine learning is conducted in two phases. The first phase is the training phase, in which a series of sample data are used to develop the relationship or features in the data that will be recognized by the computer during data analysis. As a cooking metaphor, this is the phase in which a recipe for a dish is made. The second phase is when the computer applies these newly learned parameters and applies them into new data to obtain measurements to predict certain properties based on the new data sets [Myer, 2012, Eliceiri et al, 2012; Domingos, 2012]. Through machine learning new methods for image analysis can be applied on large quantities of biological micrograph images to obtain measurements and data in an accurate, automated, and high-throughput manner.

Objective of this Thesis

In this dissertation, I aim to examine the teratogenic effects of tobacco products, which are environmental toxicants, on bone development. Most studies involving tobacco have been focused on three main areas of human health: cardiovascular and respiratory health, as well as tobacco's carcinogenic nature. Although there has been suggestive evidence that tobacco may affect development and bone health, the consequences of smoking on bone development during pregnancy are unknown. This thesis aims to close this gap in knowledge by applying a human embryonic stem cell *in vitro* osteogenesis model combined with a newly developed *in vitro* teratogenicity assay to screen a set of tobacco products. This set will include conventional cigarette products,

but also some harm-reduction products, which have been designed to reduce cancer risk in smokers.

Since there are limited reports on the ability of human pluripotent stem cells to differentiate into bone cells, I will first have to transfer a mouse-cell-based protocol to human embryonic stem cells. These cells are chosen as their *in vitro* differentiation mimics all stages of *in utero* development. Secondly, I will need to develop an image-based calcification assay and assess its sensitivity in uncovering different degrees of calcification between different stem cell cultures.

References

1. O'Rahilly, R.,Müller ,F. The development of the neural crest in the human. J. Anat.: 2007, 211(3);335-51
2. https://embryology.med.unsw.edu.au/embryology/index.php?title=Timeline_human_development
3. O'Rahilly,R, Muller, F, Meyer, DB. The human vertebral column at the end of the embryonic period proper. 1. The column as a whole. J. Anat.: 1980, 131(Pt 3);565-75
4. http://www.cdc.gov/ncbddd/birthdefects/index.html
5. Gilbert-Barness E. Teratogenic causes of malformations. Ann Clin Lab Sci. 2010 Spring;40(2):99-114.
6. Brent RL. The cause and prevention of human birth defects: what have we learned in the past 50 years? Congenit Anom (Kyoto) 2001;41:3-21.
7. Cook, MJ and Fairweather, FA. Methods used in teratogenic testing *Lab Anim October 1, 1968 2: 219-228*
8. Kochhar DM. *In vitro* testing of teratogenic agents using mammalian embryos. Teratog Carcinog Mutagen. 1980;1(1):63-74.
9. Fantel AG. Culture of whole rodent embryos in teratogen screening. Teratog Carcinog Mutagen. 1982;2(3-4):231-42
10. Schumann J. Teratogen screening: state of the art. Avicenna J Med Biotechnol. 2010 Jul;2(3):115-21

11. van der Valk T, van der Meijden A. Toxicity of scorpion venom in chick embryo and mealworm assay depending on the use of the soluble fraction versus the whole venom. Toxicon. 2014 Sep;88:38-43.

12. Kim M, Son J, Park MS, Ji Y, Chae S, Jun C, Bae JS, Kwon TK, Choo YS, Yoon H, Yoon D, Ryoo J, Kim SH, Park MJ, Lee HS. *In vivo* evaluation and comparison of developmental toxicity and teratogenicity of perfluoroalkyl compounds using Xenopus embryos. Chemosphere. 2013 Oct;93(6):1153-60.

13. Casarini L, Franchini A, Malagoli D, Ottaviani E. Evaluation of the effects of the marine toxin okadaic acid by using FETAX assay. Toxicol Lett. 2007 Mar 8;169(2):145-51.

14. Memon S, Pratten M. Effects of multivitamins and known teratogens on chick cardiomyocytes micromass culture assay. Iran J Basic Med Sci. 2013 Sep;16(9):996-1003.

15. Hurst H, Clothier RH, Pratten M. An evaluation of the chick cardiomyocyte micromass system for identification of teratogens in a blind trial. Reprod Toxicol. 2009 Dec;28(4):503-10.

16. Zou P, Xing L, Tang Q, Liu R, Hao W. Comparative evaluation of the teratogenicity of genistein and genistin using rat whole embryo culture and limbud micromass culture methods. Food Chem Toxicol. 2012 Aug;50(8):2831-6.

17. de Jong E, van Beek L, Piersma AH. Comparison of osteoblast and cardiomyocyte differentiation in the embryonic stem cell test for predicting embryotoxicity *in vivo*. Reprod Toxicol. 2014 Sep;48:62-71.

18. zur Nieden NI, Kempka G, Ahr HJ. Molecular multiple endpoint embryonic stem cell test--a possible approach to test for the teratogenic potential of compounds. Toxicol Appl Pharmacol. 2004 Feb 1;194(3):257-69.

19. Weissman IL, Anderson DJ, Gage F. Stem and progenitor cells: origins, phenotypes, lineage commitments, and transdifferentiations. Annu Rev Cell Dev Biol. 2001;17:387-403.

20. Smith AG. Embryo-derived stem cells: of mice and men. Annu Rev Cell Dev Biol. 2001;17:435-62.

21. Houck JC, Sharma VK, Hayflick L. Functional failures of cultured human diploid fibroblasts after continued population doublings. Proc Soc Exp Biol Med. 1971 May;137(1):331-3.

22. Hayflick L. The biology of human aging. Am J Med Sci. 1973 Jun;265(6):432-45.

23. Hayflick L.. The longevity of cultured human cells. J Am Geriatr Soc. 1974 Jan;22(1):1-12.

24. Sherr CJ, DePinho RA. Cellular senescence: mitotic clock or culture shock? Cell. 2000 Aug 18;102(4):407-10.

25. Shay JW, Wright WE. Hayflick, his limit, and cellular ageing. Nat Rev Mol Cell Biol. 2000 Oct;1(1):72-6.

26. Iscove NN, Nawa K. Hematopoietic stem cells expand during serial transplantation *in vivo* without apparent exhaustion. Curr Biol. 1997 Oct 1;7(10):805-8.

27. Kau CL, Turpen JB. Dual contribution of embryonic ventral blood island and dorsal lateral plate mesoderm during ontogeny of hemopoietic cells in Xenopus laevis. J Immunol. 1983 Nov;131(5):2262-6.

28. Medvinsky AL, Samoylina NL, Müller AM, Dzierzak EA. An early pre-liver intraembryonic source of CFU-S in the developing mouse. Nature. 1993 Jul 1;364(6432):64-7.

29. Medvinsky A, Dzierzak E. Definitive hematopoiesis is autonomously initiated by the AGM region. Cell. 1996 Sep 20;86(6):897-906.

30. Barker N, Ridgway RA, van Es JH, van de Wetering M, Begthel H, van den Born M, Danenberg E, Clarke AR, Sansom OJ, Clevers H. Crypt stem cells as the cells-of-origin of intestinal cancer. Nature. 2009 Jan 29;457(7229):608-11.

31. van der Flier LG, Clevers H. Stem cells, self-renewal, and differentiation in the intestinal epithelium. Annu Rev Physiol. 2009;71:241-60.

32. Liu S, Dontu G, Wicha MS. Mammary stem cells, self-renewal pathways, and carcinogenesis. Breast Cancer Res. 2005;7(3):86-95.

33. Prater MD, Petit V, Alasdair Russell I, Giraddi RR, Shehata M, Menon S, Schulte R, Kalajzic I, Rath N, Olson MF, Metzger D, Faraldo MM, Deugnier MA, Glukhova MA, Stingl J. Mammary stem cells have myoepithelial cell properties. Nat Cell Biol. 2014 Aug 31.

34. Sanada F, Taniyama Y, Azuma J, Yuka II, Iwabayashi M, Morishita R, Taniyama Y, Azuma J, Rakugi H, Morishita R. Endothelial progenitor cells in clinical settings. J Stem Cells. 2014;9(2):117-25.

35. Phinney DG, Prockop DJ. Concise review: mesenchymal stem/multipotent stromal cells: the state of transdifferentiation and modes of tissue repair—current views. Stem Cells. 2007 Nov;25(11):2896-902.

36. Shi S, Bartold PM, Miura M, Seo BM, Robey PG, Gronthos S. The efficacy of mesenchymal stem cells to regenerate and repair dental structures. Orthod Craniofac Res. 2005 Aug;8(3):191-9.

37. Alvarez-Buylla A, Seri B, Doetsch F. Identification of neural stem cells in the adult vertebrate brain. Brain Res Bull. 2002 Apr;57(6):751-8.

38. Bjornson CR, Rietze RL, Reynolds BA, Magli MC, Vescovi AL. Turning brain into blood: a hematopoietic fate adopted by adult neural stem cells *in vivo*. Science. 1999 Jan 22;283(5401):534-7.

39. Sieber-Blum M, Hu Y. Epidermal neural crest stem cells (EPI-NCSC) and pluripotency. Stem Cell Rev. 2008 Dec;4(4):256-60.

40. Kruger GM, Mosher JT, Bixby S, Joseph N, Iwashita T, Morrison SJ. Neural crest stem cells persist in the adult gut but undergo changes in self-renewal, neuronal subtype potential, and factor responsiveness. Neuron. 2002 Aug 15;35(4):657-69.

41. Murrell W, Féron F, Wetzig A, Cameron N, Splatt K, Bellette B, Bianco J, Perry C, Lee G, Mackay-Sim A. Multipotent stem cells from adult olfactory mucosa. Dev Dyn. 2005 Jun;233(2):496-515.

42. Jiang Y, Jahagirdar BN, Reinhardt RL, Schwartz RE, Keene CD, Ortiz-Gonzalez XR, Reyes M, Lenvik T, Lund T, Blackstad M, Du J, Aldrich S, Lisberg A, Low WC, Largaespada DA, Verfaillie CM. Pluripotency of mesenchymal stem cells derived from adult marrow. Nature. 2002 Jul 4;418(6893):41-9.

43. Papaioannou V. Stem cells and Differentiation. Differentiation. 2001 Oct;68(4-5):153-4.

44. Hadjantonakis A, Papaioannou V. The stem cells of early embryos. Differentiation. 2001 Oct;68(4-5):159-66.

45. Duplomb L, Dagouassat M, Jourdon P, Heymann D. Concise review: embryonic stem cells: a new tool to study osteoblast and osteoclast differentiation. Stem Cells. 2007 Mar;25(3):544-52.

46. Rousselle AV, Heymann D. Osteoclastic acidification pathways during bone resorption. Bone. 2002 Apr;30(4):533-40.

47. Aguila HL, Rowe DW. Skeletal development, bone remodeling, and hematopoiesis. Immunol Rev. 2005 Dec;208:7-18.

48. Blair HC, Zaidi M, Schlesinger PH. Mechanisms balancing skeletal matrix synthesis and degradation. Biochem J. 2002 Jun 1;364(Pt 2):329-41.

49. Heng BC, Cao T, Stanton LW, Robson P, Olsen B. Strategies for directing the differentiation of stem cells into the osteogenic lineage *in vitro*. J Bone Miner Res. 2004 Sep;19(9):1379-94.

50. Buttery LD, Bourne S, Xynos JD, Wood H, Hughes FJ, Hughes SP, Episkopou V, Polak JM. Differentiation of osteoblasts and *in vitro* bone formation from murine ,embryonic stem cells. Tissue Eng. 2001 Feb;7(1):89-99.

51. Chae HJ, Chae SW, Kang JS, Bang BG, Han JI, Moon SR, Park RK, So HS, Jee KS, Kim HM, Kim HR. Effect of ionizing radiation on the differentiation of ROS 17/2.8 osteoblasts through free radicals. J Radiat Res. 1999 Dec;40(4):323-35.

52. Petersson CJ, Holmer NG, Johnell O. Electrical stimulation of osteogenesis: studies of the cathode effect on rabbit femur. Acta Orthop Scand. 1982 Oct;53(5):727-32.

53. Yonemori K, Matsunaga S, Ishidou Y, Maeda S, Yoshida H. Early effects of electrical stimulation on osteogenesis. Bone. 1996 Aug;19(2):173-80.

54. Lee JH, McLeod KJ. Morphologic responses of osteoblast-like cells in monolayer culture to ELF electromagnetic fields. Bioelectromagnetics. 2000; 21(2):129-36.

55. Zelzer E, Glotzer DJ, Hartmann C, Thomas D, Fukai N, Soker S, Olsen BR. Tissue specific regulation of VEGF expression during bone development requires Cbfa1/Runx2. Mech Dev. 2001 Aug;106(1-2):97-106.

56. Nakashima K, Zhou X, Kunkel G, Zhang Z, Deng JM, Behringer RR, de Crombrugghe B. The novel zinc finger-containing transcription factor osterix is required for osteoblast differentiation and bone formation. Cell. 2002 Jan 11;108(1):17-29.

57. Katagiri T, Takahashi N. Regulatory mechanisms of osteoblast and osteoclast differentiation. Oral Dis. 2002 May;8(3):147-59.

58. McClelland Descalzo DL, Ehnes DD, zur Nieden NI. Stem cells for osteodegenerative diseases: current studies and future outlook. Regen Med. 2014 Mar;9(2):219-30. doi: 10.2217/rme.13.100.

59. Sottile V, Thomson A, McWhir J. *In vitro* osteogenic differentiation of human ES cells. Cloning Stem Cells. 2003;5(2):149-55.

60. Bielby RC, Boccaccini AR, Polak JM, Buttery LD. *In vitro* differentiation and *in vivo* mineralization of osteogenic cells derived from human embryonic stem cells. Tissue Eng. 2004 Sep-Oct;10(9-10):1518-25.

61. zur Nieden NI, Kempka G, Ahr HJ. *In vitro* differentiation of embryonic stem cells into mineralized osteoblasts. Differentiation. 2003 Jan;71(1):18-27.

62. van Leeuwen JP, van Driel M, van den Bemd GJ, Pols HA. Vitamin D control of osteoblast function and bone extracellular matrix mineralization. Crit Rev Eukaryot Gene Expr. 2001;11(1-3):199-226.

63. Valenti MT, Zanatta M, Donatelli L, Viviano G, Cavallini C, Scupoli MT, Dalle Carbonare L. Ascorbic acid induces either differentiation or apoptosis in MG-63 osteosarcoma lineage. Anticancer Res. 2014 Apr;34(4):1617-27.

64. Rogers JJ, Young HE, Adkison LR, Lucas PA, Black AC Jr. Differentiation factors induce expression of muscle, fat, cartilage, and bone in a clone of mouse pluripotent mesenchymal stem cells. Am Surg. 1995 Mar;61(3):231-6.

65. Beresford JN, Bennett JH, Devlin C, Leboy PS, Owen ME. Evidence for an inverse relationship between the differentiation of adipocytic and osteogenic cells in rat marrow stromal cell cultures. J Cell Sci. 1992 Jun;102 (Pt 2):341-51.

66. Notoya K, Nagai H, Oda T, Gotoh M, Hoshino T, Muranishi H, Taketomi S, Sohda T, Makino H. Enhancement of osteogenesis *in vitro* and *in vivo* by a novel osteoblast differentiation promoting compound, TAK-778. J Pharmacol Exp Ther.1999 Sep;290(3):1054-64.

67. Trettner S, Findeisen A, Taube S, Horn PA, Sasaki E, zur Nieden NI. Osteogenic induction from marmoset embryonic stem cells cultured in feeder-dependent and feeder-independent conditions. Osteoporos Int. 2014 Apr;25(4):1255-66.

68. Karp JM, Ferreira LS, Khademhosseini A, Kwon AH, Yeh J, Langer RS. Cultivation of human embryonic stem cells without the embryoid body step enhances osteogenesis *in vitro*. Stem Cells. 2006 Apr;24(4):835-43.

69. Lee NK, Sowa H, Hinoi E, Ferron M, Ahn JD, Confavreux C, Dacquin R, Mee PJ, McKee MD, Jung DY, Zhang Z, Kim JK, Mauvais-Jarvis F, Ducy P, Karsenty G. Endocrine regulation of energy metabolism by the skeleton. Cell. 2007 Aug 10;130(3):456-69.

70. Nielsen LB, Pedersen FS, Pedersen L. Expression of type III sodium-dependent phosphate transporters/retroviral receptors mRNAs during osteoblasts differentiation. Bone. 2001 Feb;28(2):160-6.

71. Choi JY, Lee BH, Song KB, Park RW, Kim IS, Sohn KY, Jo JS, Ryoo HM. Expression patterns of bone-related proteins during osteoblastic differentiation in MC3T3-E1 cells. J Cell Biochem. 1996 Jun 15;61(4):609-18.

72. Nakashima K, Zhou X, Kunkel G, Zhang Z, Deng JM, Behringer RR, de Crombrugghe B. The novel zinc finger-containing transcription factor osterix is required for osteoblast differentiation and bone formation. Cell. 2002 Jan 11;108(1):17-29.

73. Kasugai S, Nagata T, Sodek J. Temporal studies on the tissue compartmentalization of bone sialoprotein (BSP), osteopontin (OPN), and SPARC protein during bone formation *in vitro*. J Cell Physiol. 1992 Sep;152(3):467-77.

74. Addison WN, Masica DL, Gray JJ, McKee MD. Phosphorylation-dependent inhibition of mineralization by osteopontin ASARM peptides is regulated by PHEX cleavage. J Bone Miner Res. 2010 Apr;25(4):695-705.

75. Azzopardi PV, O'Young J, Lajoie G, Karttunen M, Goldberg HA, Hunter GK. Roles of electrostatics and conformation in protein-crystal interactions. PLoS One. 2010 Feb 19;5(2):e9330.

76. Hunter GK, O'Young J, Grohe B, Karttunen M, Goldberg HA. The flexible polyelectrolyte hypothesis of protein-biomineral interaction. Langmuir. 2010 Dec 21;26(24):18639-46.

77. Choi ST, Kim JH, Kang EJ, Lee SW, Park MC, Park YB, Lee SK. Osteopontin might be involved in bone remodelling rather than in inflammation in ankylosing spondylitis. Rheumatology (Oxford). 2008 Dec;47(12):1775-9.

78. Inoue D, Kido S, Matsumoto T. Transcriptional induction of FosB/DeltaFosB gene by mechanical stress in osteoblasts. J Biol Chem. 2004 Nov 26;279(48):49795-803.

79. Eferl R, Hoebertz A, Schilling AF, Rath M, Karreth F, Kenner L, Amling M, Wagner EF. The Fos-related antigen Fra-1 is an activator of bone matrix formation. EMBO J. 2004 Jul 21;23(14):2789-99.

80. Price PA, Otsuka AA, Poser JW, Kristaponis J, Raman N. Characterization of a gamma-carboxyglutamic acid-containing protein from bone. Proc Natl Acad Sci U S A. 1976 May;73(5):1447-51.

81. Noda M, Yoon K, Prince CW, Butler WT, Rodan GA. Transcriptional regulation of osteopontin production in rat osteosarcoma cells by type beta transforming growth factor. J Biol Chem. 1988 Sep 25;263(27):13916-21.

82. Fisher LW, Robey PG, Tuross N, Otsuka AS, Tepen DA, Esch FS, Shimasaki S, Termine JD. The Mr 24,000 phosphoprotein from developing bone is the NH2-terminal propeptide of the alpha 1 chain of type I collagen. J Biol Chem. 1987 Oct 5;262(28):13457-63.

83. Urist MR, Huo YK, Brownell AG, Hohl WM, Buyske J, Lietze A, Tempst P,Hunkapiller M, DeLange RJ. Purification of bovine bone morphogenetic protein by hydroxyapatite chromatography. Proc Natl Acad Sci U S A. 1984 Jan;81(2):371-5.

84. Legros R, Balmain N, Bonel G. Age-related changes in mineral of rat and bovine cortical bone. Calcif Tissue Int. 1987 Sep;41(3):137-44.

85. Field RA, Riley ML, Mello FC, Corbridge MH, Kotula AW. Bone composition in cattle, pigs, sheep and poultry. J Anim Sci. 1974 Sep;39(3):493-9.

86. Moester MJ, Schoeman MA, Oudshoorn IB, van Beusekom MM, Mol IM, Kaijzel EL, Löwik CW, de Rooij KE. Validation of a simple and fast method to quantify *in vitro* mineralization with fluorescent probes used in molecular imaging of bone. Biochem Biophys Res Commun. 2014 Jan 3;443(1):80-5.

87. Meloan SN, Puchtler H (1985) Chemical mechanisms of staining methods: von Kossa's technique. What von Kossa really wrote and a modified reaction for selective demonstration of inorganic phosphate. J Histotechol 8:11–13

88. zur Nieden NI, Davis LA, Rancourt DE. Comparing three novel endpoints for developmental osteotoxicity in the embryonic stem cell test. Toxicol Appl Pharmacol. 2010 Sep 1;247(2):91-7.

89. U.S. Department of Health and Human Services. The Health Consequences of Smoking—50 Years of Progress. A Report of the Surgeon General. Atlanta: U.S. Department of Health and Human Services, Centers for Disease Control and Prevention, National Center for Chronic Disease Prevention and Health Promotion, Office on Smoking and Health, 2014 [accessed 2014 Feb 6].

90. Centers for Disease Control and Prevention. QuickStats: Number of Deaths from 10 Leading Causes—National Vital Statistics System, United States, 2010. Morbidity and Mortality Weekly Report 2013: 62(08);155 [accessed 2014 Feb 6].

91. http://www.cdc.gov/tobacco/osh/index.htm

92. U.S. Department of Health and Human Services. How Tobacco Smoke Causes Disease: What It Means to You. Atlanta: U.S. Department of Health and Human Services, Centers for Disease Control and Prevention, National Center for Chronic

Disease Prevention and Health Promotion, Office on Smoking and Health, 2010 [accessed 2014 Feb 6].

93. U.S Department of Health and Human Services. How Tobacco Smoke Causes Disease: The Biology and Behavioral Basis for Smoking-Attributable Disease: A Report of the Surgeon General, 2010.
94. Mayer B. How much nicotine kills a human? Tracing back the generally accepted lethal dose to dubious self-experiments in the nineteenth century. Arch Toxicol. 2014 Jan;88(1):5-7.
95. “Nicotinic acetylcholine receptors: Introduction". *IUPHAR Database*. International Union of Basic and Clinical Pharmacology. Retrieved 1 September 2014.
96. Malenka RC, Nestler EJ, Hyman SE (2009). "Chapter 9: Autonomic Nervous System". In Sydor A, Brown RY. *Molecular Neuropharmacology: A Foundation for Clinical Neuroscience* (2nd ed.). New York: McGraw-Hill Medical. p. 234.
97. Hukkanen J, Jacob P 3rd, Benowitz NL. Metabolism and disposition kinetics of nicotine. Pharmacol Rev. 2005 Mar;57(1):79-115.
98. Gerdhem P, Obrant KJ. Effects of cigarette-smoking on bone mass as assessed by dual-energy X-ray absorptiometry and ultrasound. Osteoporos Int. 2002 Dec;13(12):932-6.
99. Behnke M, Smith VC; Committee on Substance Abuse; Committee on Fetus and Newborn. Prenatal substance abuse: short- and long-term effects on the exposed fetus. Pediatrics. 2013 Mar;131(3):e1009-24.
100. Benowitz NL, Hukkanen J, Jacob P 3rd. Nicotine chemistry, metabolism, kinetics and biomarkers. Handb Exp Pharmacol. 2009;(192):29-60.

101. Marie PJ, Haÿ E. Cadherins and Wnt signalling: a functional link controlling bone formation. Bonekey Rep. 2013 Apr 17;2:330.
102. Walker LM, Preston MR, Magnay JL, Thomas PB, El Haj AJ. Nicotinic regulation of c-fos and osteopontin expression in human-derived osteoblast-like cells and human trabecular bone organ culture. Bone. 2001 Jun;28(6):603-8.
103. Need AG, Kemp A, Giles N, Morris HA, Horowitz M, Nordin BE. Relationships between intestinal calcium absorption, serum vitamin D metabolites and smoking in postmenopausal women. Osteoporos Int. 2002 Jan;13(1):83-8.
104. Devasagayam TP, Tilak JC, Boloor KK, Sane KS, Ghaskadbi SS, Lele RD. Free radicals and antioxidants in human health: current status and future prospects. J Assoc Physicians India. 2004 Oct;52:794-804.
105. Iyer S, Ambrogini E, Bartell SM, Han L, Roberson PK, de Cabo R, Jilka RL, Weinstein RS, O'Brien CA, Manolagas SC, Almeida M. FOXOs attenuate bone formation by suppressing Wnt signaling. J Clin Invest. 2013 Aug 1;123(8):3409-19.
106. Monroe DG, McGee-Lawrence ME, Oursler MJ, Westendorf JJ. Update on Wnt signaling in bone cell biology and bone disease. Gene. 2012 Jan 15;492(1):1-18.
107. Clevers H, Nusse R. Wnt/β-catenin signaling and disease. Cell. 2012 Jun 8;149(6):1192-205.
108. Rodda SJ, McMahon AP. Distinct roles for Hedgehog and canonical Wnt signaling in specification, differentiation and maintenance of osteoblast progenitors. Development. 2006 Aug;133(16):3231-44.
109. Essers MA, de Vries-Smits LM, Barker N, Polderman PE, Burgering BM, Korswagen HC. Functional interaction between beta-catenin and FOXO in oxidative stress signaling. Science. 2005 May 20;308(5725):1181-4.

110. Kenyon C, Chang J, Gensch E, Rudner A, Tabtiang R. A C. elegans mutant that lives twice as long as wild type. Nature. 1993 Dec 2;366(6454):461-4.

111. Lin K, Dorman JB, Rodan A, Kenyon C. daf-16: An HNF-3/forkhead family member that can function to double the life-span of Caenorhabditis elegans. Science. 1997 Nov 14;278(5341):1319-22.

112. Ogg S, Paradis S, Gottlieb S, Patterson GI, Lee L, Tissenbaum HA, Ruvkun G. The Fork head transcription factor DAF-16 transduces insulin-like metabolic and longevity signals in C. elegans. Nature. 1997 Oct 30;389(6654):994-9.

113. van der Vos KE, Coffer PJ. FOXO-binding partners: it takes two to tango. Oncogene. 2008 Apr 7;27(16):2289-99.

114. Almeida M, Han L, Martin-Millan M, O'Brien CA, Manolagas SC. Oxidative stress antagonizes Wnt signaling in osteoblast precursors by diverting beta-catenin from T cell factor- to forkhead box O-mediated transcription. J Biol Chem. 2007 Sep 14;282(37):27298-305.

115. Yu D, Berlin JA, Penning TM, Field J. Reactive oxygen species generated by PAH o-quinones cause change-in-function mutations in p53. Chem Res Toxicol. 2002 Jun;15(6):832-42.

116. Wilk A, Waligórski P, Lassak A, Vashistha H, Lirette D, Tate D, Zea AH, Koochekpour S, Rodriguez P, Meggs LG, Estrada JJ, Ochoa A, Reiss K. Polycyclic aromatic hydrocarbons-induced ROS accumulation enhances mutagenic potential of T-antigen from human polyomavirus JC. J Cell Physiol. 2013 Nov;228(11):2127-38.

117. Danuser G. Computer vision in cell biology. Cell. 2011 Nov 23;147(5):973-8.

118. Murphy RF. An active role for machine learning in drug development. Nat Chem Biol. 2011 Jun;7(6):327-30.

119. Myers G. Why bioimage informatics matters. Nat Methods. 2012 Jun 28;9(7):659-60.

120. Eliceiri KW, Berthold MR, Goldberg IG, Ibáñez L, Manjunath BS, Martone ME, Murphy RF, Peng H, Plant AL, Roysam B, Stuurman N, Swedlow JR, Tomancak P, Carpenter AE. Biological imaging software tools. Nat Methods. 2012 Jun 28;9(7):697-710.

121. Cherkassky V, Ma Y. Another look at statistical learning theory and regularization. Neural Netw. 2009 Sep;22(7):958-69.

122. Bishop, C. M. (2006). *Pattern recognition and machine learning* (Vol. 1, p. 740). New York: springer.

123. Domingos, P. (2012). A few useful things to know about machine learning. *Communications of the ACM*, *55*(10), 78-87.

124. Tarca AL, Carey VJ, Chen XW, Romero R, Drăghici S. Machine learning and its applications to biology. PLoS Comput Biol. 2007 Jun;3(6):e116.

125. de Ridder D, de Ridder J, Reinders MJ. Pattern recognition in bioinformatics. Brief Bioinform. 2013 Sep;14(5):633-47.

Chapter 2: Video-Based Calcification Assay: A Novel Method for Kinetic Analysis of Functional Properties of Osteoblasts in Live Cultures

Abstract

Calcification in osteogenic cultures is traditionally measured with calcium-sensitive reagents that are toxic to living cells. Therefore, these measurements typically terminate the cultures and as a result do not allow the kinetic analysis of calcification *in vitro*. In this paper, we demonstrate that calcification from developing osteoblasts derived from pluripotent stem cells can be quantified from time-lapse images to provide such kinetic data. The video-based calcification assay used the natural properties of emerging osteoblasts to appear as dark clusters in culture, thereby abrogating the use of chemical reagents entirely. In addition, the true kinetic nature of the image-based assay allowed the development of a new parameter for characterizing calcification outputs of emerging osteoblasts in culture: the rate of calcification. The video-based calcification assay has been tested to determine if toxicants hinder calcification of osteoblasts derived from pluripotent stem cells and to compare the differences in calcification yield and kinetics between different pluripotent stem cell lines. Through the extraction of video data, this method is widely adaptable to other types of stem cells and calcifying cells in culture.

Introduction

The field of cell biology is about to enter a revolution. The improvement in microscopy along with the increase in computing power and reduction of cost of

computers in the last decade led to the development of novel image-based technology to extract and quantify data from micrograph images. The aim of this paper is to add to the growing body of work regarding image analysis of micrographs to analyze biologically relevant events in a cell.

Video Informatics refers to programs that allow for automated extraction and retrieval of information embedded in dynamic images in an automated manner [Talbot et al, 2014]. Several programs have been developed to quantify information from both the cellular level [Yarrow et al, 2004; Gough et al, 2011, Buggenthin et al, 2013; Battich et al, 2013, Schmid et al, 2013] and the whole organism level [Vogt et al, 2009, Guan et al, 2014]. These programs range from tasks that describe cell morphology and cell density [Buggenthin et al, 2013; Zhong et al, 2012] to even describing changes in transcription [Battich et al, 2013], as well as automate traditional assays, such as the scratch assay to detect cell migration [Yarrow et al, 2014; Gough et al, 2011]. Image-based analysis is versatile and has potential to be used for other types of studies, including quantifying functional properties of cells that are involved in the formation of bone.

In the body, bone formation is conducted through the incorporation of hydroxyapatite, a mineral composed of calcium and phosphate, into the bone extracellular matrix (ECM), in a process called calcification facilitated by osteoblasts. These osteoblasts emerge from the differentiation of stem cells, which can be mimicked *in vitro* [Buttery et al 2001; zur Nieden et al; 2003; Sottile et al, 2003; Ding et al; 2012]. In culture, calcification can be confirmed by staining for markers found specifically in the bone matrix, such as osteocalcin (OCN) [Boskey, 1996, Rutledge et al, 2014]. In addition, identification of calcium in the matrix is typically accomplished by calcium specific stains, such as von Kossa [Puchtler, 1969; Rungby, 1993]. However, these methods are only

qualitative. Typically, quantifying calcium from osteogenically induced cultures is measured through a reagent based assay utilizing either fluorescent (i.e. calcein, coelenterazine, dehydrocalcein fluo-3, fura-2, indo-1 and rhod-2) or absorbent calcium sensitive dyes (e.g. Arsenazo III, 2,2'-bisbenzenearsonic acid, Alizarin Red) that are excellent at detecting and quantifying intracellular and matrix-bound calcium, respectively [Choi et al, 2011; Davis et al, 2011; Kim et al, 2012]. As the latter category quantifies the amount of deposited calcium, these dyes can be used to characterize the success of osteogenesis between different sources of stem cell lines [Palmieri et al 2008; Pilz et al 2011], the effects of growth factors [Kawaguchi et al, 2005], morphogens [Zeng et al, 2007; De Rosa et al, 2011], toxicants [Koskela et al, 2012; Korkalainen et al, 2009], or chemicals [Kawaguchi et al, 2005; Bielby et al, 2004].

The disadvantage of these calcium-sensitive dyes is that they typically require the sacrifice of the culture. Thus, novel methods for quantifying calcium from live cultures without destroying them are of great importance for studies involving developing osteoblasts. A few studies have begun quantifying calcium deposition of osteoblasts in culture by adding the calcium-sensitive fluorescent dye calcein into the medium [Uchimura et al, 2003]. The fluorescent dye incorporated into the mineralized matrix and allowed for tracing of calcification as it emerged. Our lab has used the physical dark appearance of calcified matrix in culture from bright-field images to quantify the amount of calcium deposited without destroying the cultures, thus enabling time course studies [zur Nieden et al, 2007]. This signature dark appearance of calcified matrix is the cornerstone in the development of the image-based calcification assay presented in this paper.

Materials and Methods

Culture of human pluripotent stem cells

H9 human embryonic stem cells (hESCs) were obtained from WiCell; Riv4 and Riv9 human induced pluripotent stem cells (hiPSCs) were a kind gift of the University of California Riverside's Stem Cell Core Facility. All cells were cultured on Matrigel (BD Biosciences) treated culture plates in mTeSR 1 medium (Stem Cell Technologies) at 37^{o}C with 5% CO_2. Colonies were passaged every 5 days using accutase and a cell scraper.

Osteogenic Induction of human pluripotent stem cells

Osteogenesis was induced in culture from confluent pluripotent cells by addition of control differentiation medium (CDM, Dulbecco's Modified Eagle Medium containing 15% fetal bovine serum (FBS, Atlanta Biologicals), 1% (v/v) non-essential amino acids, penicillin/streptomycin and 0.1 mM β-mercaptoethanol. Osteogenic differentiation medium composed of CDM supplemented with $1.2x10^{-7}$ M 1,25$\alpha(OH)_2$ Vitamin D_3 (VD3; Calbiochem), 0.1mM β-glycerophosphate (βGP), and 20.8 μg/ml ascorbic acid (AA) was used from day 5 of differentiation onward.

Toxicity studies

Tobacco extract was made by incubating 10 g of Camel Snus in 100 ml of DMEM with 15% FBS overnight. The extract was centrifuged at 450×g for 10 min at room

temperature and the supernatant again centrifuged at 13,000×g for 1 hour to remove finer tobacco debris. The pH was adjusted to 7.4 and the extract filter sterilized.

Tobacco-specific nitrosamines, N'-nitrosonornicotine (NNN; Toronto Research Chemicals) were created at 48mM stock concentration by diluting the compound in DMEM. Compounds were diluted $4.8 \times E^{-6}$, $4.8 \times E^{-8}$, $4.8 \times E^{-10}$, $4.8 \times E^{-12}$, $4.8 \times E^{-14}$.

Immunohistochemistry

Cells were rinsed with phosphate buffered saline (PBS) and fixed in 4% paraformaldehyde at 4°C for 1 hour. Fixed cells were permeabilized with 0.1% Triton X-100/PBS and stained with anti-OCN (AbCam; AB1857) in 4% FBS/PBS overnight at 4°C. A secondary anti-rabbit IgG conjugated to Alexa Fluor 546 (Invitrogen; A10040) in 10% FBS/PBS was incubated for 2 hours at room temperature. Cultures were counterstained with 4',6-diamidino-2-phenylindole (DAPI) and visualized using a Nikon Eclipse Ti microscope.

Cytochemical staining

Fixed cells were stained with 2% (w/v) Alizarin Red solution for 5 min and then washed with PBS followed by increasing concentrations of ethanol (70%, 80%, 90%, 100%). For von Kossa stain, cultures were stained with 5% silver nitrate solution under a strong light source for one hour. Cultures were washed three times with water and fixed with 5% sodium thiosulfate for 2 min.

Detection of calcium

In order to quantify calcium content, cells were lysed with radio-immunoprecipitation assay (RIPA) buffer (1% NP40, 0.5% sodium deoxycholate, 0.1%SDS, in PBS). The cell lysate was assayed with Arsenazo III (Genzyme) and the change in absorbance measured at 655nm in an iMark microplate reader (BioRad). Absorbances were compared to a $CaCl_2$ calcium standard and total calcium content normalized to the total protein content determined by a Lowry assay as described [Davis et al, 2011].

Image acquisition

Differentiating cultures were placed inside the Nikon Biostation CT, a hybrid and automated incubator that contains a phase contrast microscope and maintains the culture at 37^{o}C with 5% CO_2. Phase contrast images were taken every 12h for a period of 15 to 20 days from 10 separate areas within the culture plate. Images were assembled to create time-lapse videos.

Image analysis

Time lapse videos were analyzed using Matrix Laboratory (MatLab) program, designed to automatically segment calcified areas from the individual phase contrast images from the time-lapse video using a manual threshold for pixels with an intensity value of 33 or less. These pixels were removed to create segmented images of calcified

regions. Remaining pixels were counted to quantify the degree of calcification from each image. Concentration response curves for tobacco toxicants were obtained by normalizing the calcium pixel counts of each concentration at t_x from a treated sample with the calcified pixel counts at t_x from an untreated sample represented as percentage. The amount of calcified pixels from each video image at t_x were subtracted from the amount of calcified pixels at t_0 and divided by the hours of elapsed time to determine the calcification rate.

Statistics

All experiments were run in biological triplicate. Calcium assays were run in technical quintuplicate and video bioinformatics assessment was performed from a total of 30 areas within three independent culture wells. Statistical assessment was performed with a t-test when appropriate (http://www.graphpad.com/quickcalcs/ttest1/) or One-Way ANOVA with Holm-Sidak posthoc test when multiple groups were compared (SigmaPlot). A p-value below 0.05 was considered significant.

Results

Development of an Image-Based Calcification Assay for Quantifying Osteogenesis from Time-Lapse Videos of Developing Pluripotent Stem Cell-Derived Osteoblasts

As calcification is the most fundamental property of functional osteoblasts, the goal of this study was to develop a novel method of quantifying this process in culture

using serial image analysis. We based this study on the *in vitro* model of human embryonic stem cell (hESC) osteogenesis. This is an excellent model as these cells are able to self-renew indefinitely and capable of tri-lineage differentiation. Previous studies in mouse have demonstrated that ESCs can be directed to yield osteoblasts [Buttery et al, 2001, zur Nieden et al, 2003]. Human derived ESCs (hESCs) can also become osteoblasts when induced with dexamethasone [Sottile et al, 2003] or, alternatively, with 1,25$\alpha(OH)_2$ vitamin D_3 (VD_3) [Ding et al 2012].

In culture, calcification from emerging osteoblasts possesses a distinct appearance when viewed under phase-contrast microscopy (Fig. 1A). This signature appearance is seen as dense black clusters that result from the inability of light to pass through calcified matrix. These areas are immuno-positive for osteocalcin (OCN), a bone-specific protein found in the bone matrix, and are composed of calcium as determined by Alizarin Red and von Kossa staining (Fig. 1A). These dense black areas were not present when osteogenic factors were withheld from the media (denoted as control (Fig. 1B)).

This criterion of osteogenic cultures in phase contrast images was then exploited to measure calcification as hESCs differentiate. Live cultures of hESCs were imaged as time-lapse videos using the Nikon Biostation CT to follow their commitment into the osteogenic lineage while in culture. The collected phase contrast micrographs were processed in sequence to segment out the calcified regions of interest from the background. In definition, an image is made up of pixels arranged in a matrix. In an 8-bit image, these pixels range from 0 to 256 value of pixel intensity with 0 being defined as the darkest shade of black and 256 representing the brightest shade of white. The pixel values found in between are commonly described as gray scale. This is important as this

property of the image in conjunction with the black appearance of calcification allowed us to segment areas of calcification from phase contrast images using thresholding. Initially, Gaussian Mixture Model and Otsu Thresholding segmentation techniques were applied to create an automated threshold to isolate calcified areas from images. These methods rely on finding threshold values that separate two Gaussian Curves, however most of the images produced by the machine contained too many gray areas resulting in a singular Gaussian Curve.

Therefore, a manual threshold limit was identified as a pixel intensity value of 33 or less. The application of this manual threshold on all images led to the retention of pixels that made up the calcified areas on the micrographs. Remaining pixels were then quantified to represent the degree of calcification (Fig. 1C). When comparing to images from the control cultures, application of this segmentation method resulted in little to no extracted data (Fig. 1B, C).

This image based quantification method was then compared to the traditional method of quantifying calcium using Arsenazo III reagent. The image-based quantification showed a ~20-fold increase in calcium content between osteogenic and the non-osteogenic cultures (Fig. 1C) displaying a similar increasing trend in calcification as was found with the reagent based assay. However, the reagent based assay seemed to be 100 times more sensitive than the image-based assay.

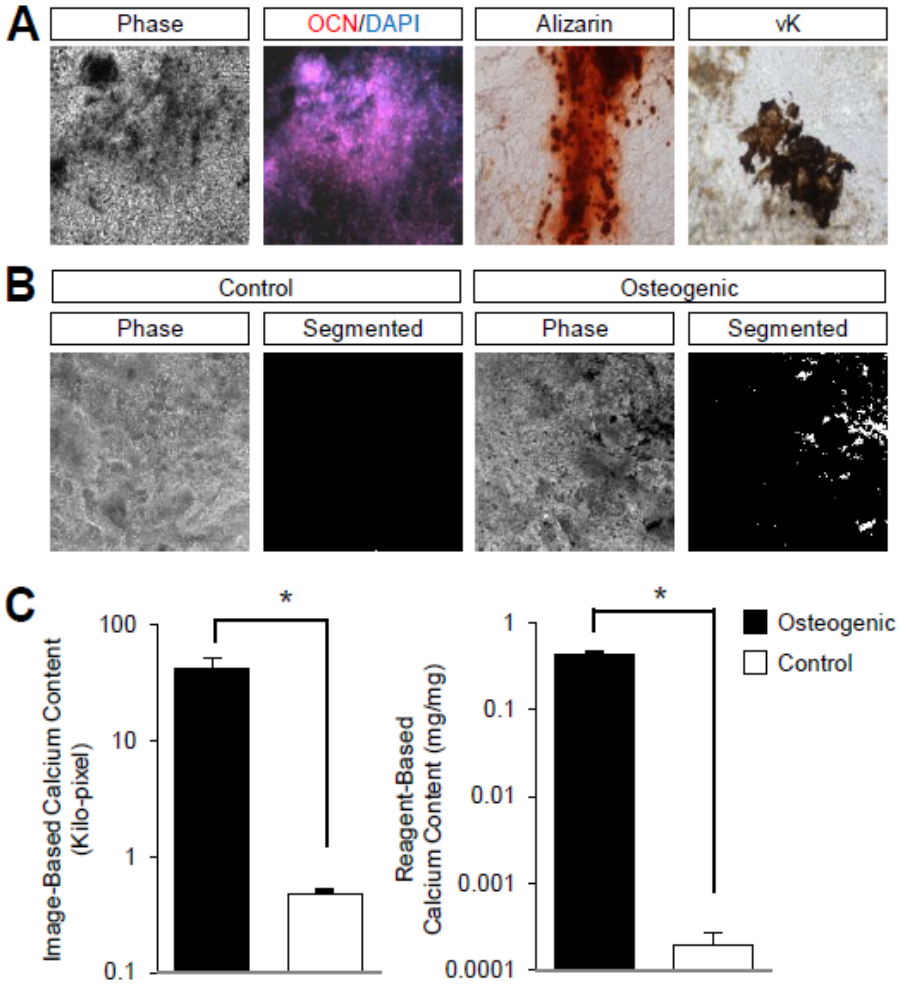

Fig. 1: Development of an image-based calcification assay. (A) Osteogenic differentiation of human ESC (H9 line) was confirmed by immunocytochemistry of the bone matrix marker, Osteocalcin (OCN), and calcification of matrix was confirmed by Alizarin Red S (Alizarin) and von Kossa (vK) staining. (B) Calcified matrix from phase contrast micrographs of osteogenic and non-osteogenic (control) cultures was segmented by thresholding pixels with a value of 33 or less. (C) Image-based measurement of calcification represented as number of segmented kilo-pixels. (D) Calcium content of cultures determined using Arsenazo III. *p<0.5, student's t-test.

Comparison of Pluripotent Stem Cell Lines to Assess Aptness for Osteogenesis using the Image-Based Calcification Assay

In order to show that the lesser sensitivity of the image-based assay was not causing problems, we next applied it to characterize and compare the suitability of other pluripotent stem cell lines as a cellular source for osteoblasts with application in toxicity studies or regenerative medicine. The osteogenic potential of two different human induced pluripotent stem cell (hiPSC) lines, Riv4 and Riv9, was contrasted to that of H9 hESCs based on calcium quantification using time-lapse videos of the osteogenic process. Human iPSCs were induced to commit to an osteogenic lineage with the same osteogenic protocol used for hESCs. These hiPSC lines exhibited typical dense black regions, the signature of calcification in culture (Fig. 2A). These black regions were composed of calcium embedded in the osteogenic ECM as confirmed by both Alizarin Red and von Kossa stainings, as well as immunocytochemistry for OCN (Fig. 2A). Using the image-based calcification assay to define the calcification process in hiPSCs, the image segmentation illustrated that both Riv4 and Riv9 hiPSCs exhibited a lower osteogenic output than H9 hESCs (Fig. 2B-D). In addition, the hiPSCs began to calcify earlier than the H9 hESCs. However, the key difference leading to the higher calcification yield in hESCs was the steeper incline in calcification seen in the early differentiation days. In contrast, the Riv lines displayed a flatter slope in their calcification output that also plateaued earlier (Fig. 2C, D).

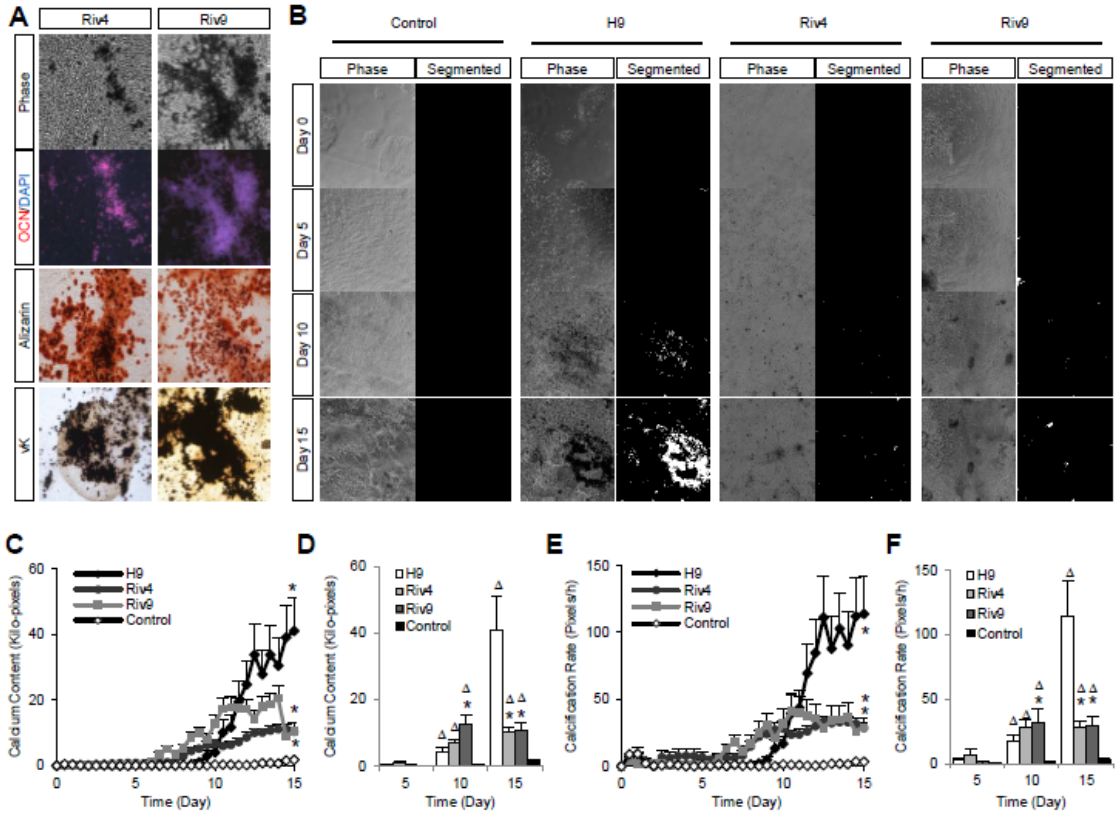

Fig. 2: Osteogenic differentiation and calcification in human Riv4 and Riv9 iPSC lines. (A) Calcification as a result of emergence of osteoblasts was verified by immune reactivity against an anti-OCN antibody. Presence of calcium was detected with Alizarin Red S (Alizarin) and von Kossa (vK) staining. (B) Detection of calcified areas in images from osteogenic hiPSC cultures based on segmentation compared to hESCs. (C, D) Calcium content of the different cell lines measured at 12h intervals from live cultures (C) and at specific days 5, 10 and 15 of the differentiation period (D). (E, F) Calcification rate of each cell line based on the amount of calcification added in a given hour. *p<0.05, One-Way ANOVA, n=3.

To quantify the notion that the difference in osteogenic output between these different types of pluripotent stem cells may be founded in differential differentiation kinetics, we next determined the calcification rate of the cultures from the time-lapse video, a property that is not readily available from the classic reagent-based method of quantifying calcium in culture. The calcification rate was deduced from the calcium

content in pixels measured at t_x from t_0 and divided by the hours passed. This calculation resulted in the number of pixels added every hour. Based on this calcification rate, we were able to determine that the amount of calcification added to the ECM of hESCs accelerated as time progressed, while the addition of calcium in both Riv lines only minimally changed over time (Fig. 3E, F) confirming the notion that the higher calcification yield from H9 hESCs was due to a faster calcification rate ($p = 0.0001$). Thus, this study has shown that the image-based calcification assay can be used to successfully compare two different types of pluripotent stem cells and characterize their potential to produce osteoblasts as will be relevant to the comparison of source material used for replenishing bone cells for regenerative medicine as well as for toxicological studies.

Pixel Intensity versus Pixel Count

We next evaluated whether the assessment of pixel intensity rather than using an average pixel count increased the sensitivity of our method. When both methods were contrasted (Fig 3A,B), only the pixel count picked up the difference between the non-osteogenic and osteogenic cultures, not the overall pixel intensity. Additionally, only the pixel count showed the reduction in calcification in the hiPSC line

This suggests that our approach of using pixel counts is better and more sensitive as opposed to quantifying calcification based on changes in pixel intensity.

When we charted the pixel count at each gray value intensity against its corresponding pixel intensity, it became apparent that hESCs not only calcify more, but

also more intensely compared to hiPSCs, a feature that was equally well detected by the calcification rate as described above.

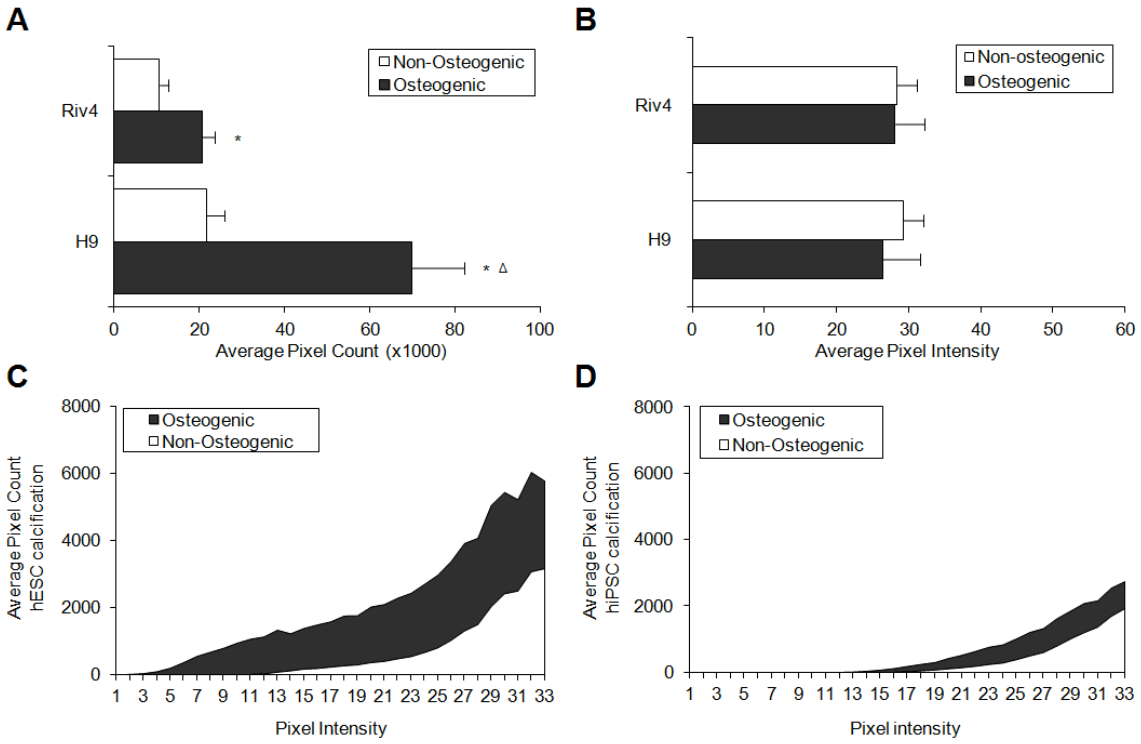

Fig. 3: Pixel count is a more representative measurement compared to pixel intensity after manual threshold segmentation. (A) Comparison of calcification in hESCs (H9) and hiPSC (Riv4) based on pixel counts at d15 of differentiation against a non-osteogenic culture. *P<0.05, One Way ANOVA compared to non-osteogenic, $^{\Delta}P$<0.05, One Way ANOVA compared to Riv4. (B) Comparison of calcification properties based on differences in pixel intensities. (C, D) Differences in calcification between osteogenic and non-osteogenic cultures derived from (C) hESCs and (D) hiPSCs by charting the pixel counts for each pixel intensity value.

Determining Effects of Toxicants on Bone Development: A Toxicological Study on Tobacco Extracts

Since the pixel count was very well capable of detecting differences between the hESCs and hiPSCs, we concluded that the image-based assay was sensitive enough to

differentiate different calcification levels. We tested this experimentally by treating differentiating hESC cultures with different concentrations of a test chemical, which we suspected to be teratogenic to differentiating osteoblasts. Our group has previously shown that calcification assays from still images can be used to accurately determine the teratogenic effects of chemicals on osteoblasts developing from pluripotent stem cells [zur Nieden et al, 2010]. Using tobacco smoke extract as a teratogenic chemical blend, we focused here on the changes in calcification that arise from addition of the toxicant to osteogenically differentiating hESC cultures. Tobacco has an effect on a wide range of human diseases, including osteoporosis [Yuhara et al, 1999], as well as having the potential to affect human development, especially during the embryonic period [Feltes et al, 2013].

Photomicrographs derived from key time-points of time-lapse videos created from osteogenically differentiating hESCs treated with whole tobacco extract revealed no differences in calcification at low doses (Fig. 4A). However, at concentrations higher than 1%, no overt calcium deposition was observed indicating a reduction in calcification caused by chemical treatment. The image-based calcification assay was then used to quantify calcium deposition. At the lowest dose of 0.001% of tobacco, calcium content measured twice as high compared to untreated samples, but then declined with increasing concentrations of tobacco to reveal no significant differences at the 0.1% dose ($p=0.103$) (Fig. 4B). In line with these findings, the calcification rate of the lower doses showed a faster calcification profile (Fig 4C). Typically, toxicity assays will normalize the effect in any given endpoint to the untreated control [Kuske et al, 2012]. Normalizing the calcification output of tobacco treated sample to the untreated sample,

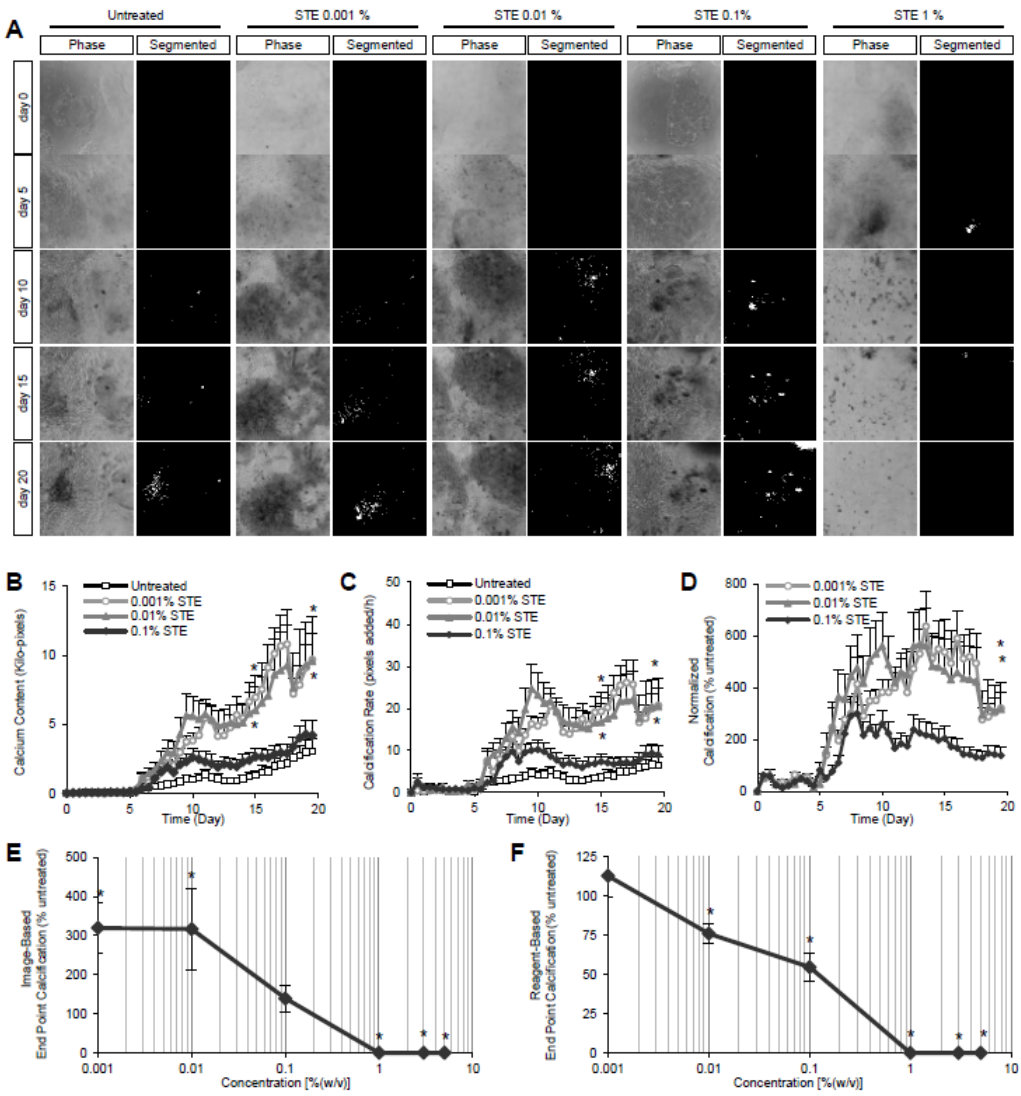

Fig. 4: Time-lapse images and segmentation of calcified regions in osteogenic hESC cultures treated with Camel Snus tobacco extract (%w/v). (A) Images show a decrease in the amount of calcification observed at 0.1% and cell death at 1%. (B) Image-based calcification measured every 12h. (C) Calcification rate calculated from images of tobacco treated samples. (D) Normalized image-based calcification data. (E, F) Concentrations-response curves determined using videobioinformatics (E) and a reagent-based calcium assay (F). *p<0.05, One-Way ANOVA, n=3.

the image based program detected differences between various tobacco concentrations again supporting the notion that lower doses of tobacco increased calcification (Fig. 4E, F).

Next, a concentration response curve was generated from the endpoint of the calcification curves (day 20) calculated with the image-based calcification assay (Fig. 4E) and the half-maximal inhibition of differentiation (ID_{50}) determined to be 0.5%. A concentration-response curve generated from data obtained with the traditional dye-based calcification assay revealed a similar ID_{50} value of 0.2% (Fig. 4F) suggesting that the image-based analysis is equally sensitive to detect appropriate ID_{50} concentration ranges.

We further aimed to confirm this notion by testing individual components of tobacco. Tobacco is a complex mixture of at least 5000 chemicals that are toxic and carcinogenic [Hecht, 2014] and it is still undetermined which of these chemicals are teratogenic. One of the most recognized components found in tobacco with widely accepted detriments to human health are tobacco specific nitrosamines (TSNAs), including N'-nitrosonornicotine (NNN) and 4-(methylnitro-samino)-1-(3-pyridyl)-1-butanone (NNK) [Hecht, 2014; Xue et al, 2014]. NNK revealed to have no effect on osteoblast differentiation (data not shown), but visual inspection of the segmentation of calcified areas in images of NNN treated cells suggested that NNN had a concentration-dependent effect on calcification (Fig. 5A), which was confirmed with the pixel count analysis (Fig. 5B). However, calcification rates did not reveal a dose-dependent change suggesting that calcification rate was not altered specifically in low-dose treatments of NNN (Fig. 5C). Comparison of the image-based calcification assay (Fig. 5E) and the reagent-based method (Fig 5F) confirmed the dose-dependent decline in calcification as a result of NNN treatment.

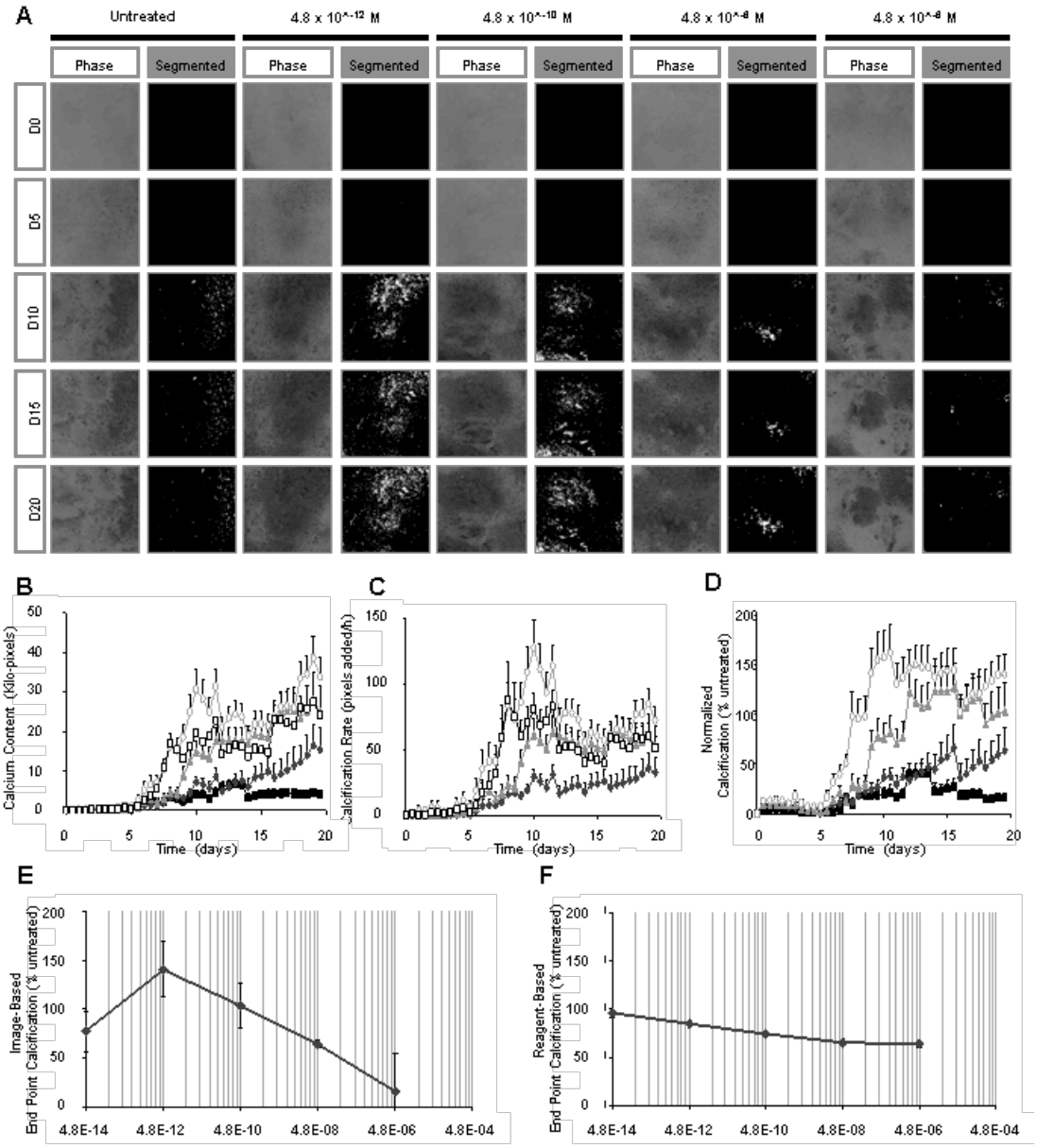

Fig. 5: Video bioinformatics time-lapse images and calcium segmentation to study effects of NNN calcification during hESC osteogenesis. (A) No detrimental effects of NNN on calcification could be detected in the tested range. (B) Time-course calcification of NNN treated osteogenically differentiating hESCs as shown every 12 hours. (C) Calcification rates of representative concentrations at 12h intervals. (D) Calcification of NNN-treated samples normalized to the untreated control. (E) Concentration-response calcification curve generated using image-quantified calcium measurement. (F) Arsenazo III based endpoint calcification curve.

Together, this data provided evidence that the image-based calcification assay can be used to identify toxicants that hinder calcification of osteoblasts derived from hESC cultures *in vitro*. It can also be used to generate calcification curves to identify half-maximal inhibitory concentrations of these chemicals with respect to the formation of bone in culture. In this particular study, whole tobacco smoke extract led to a reduction of osteogenic output and may thus affect the *de novo* bone formation of hESCs in culture.

Discussion

Cell biology relies heavily on the use of images. They provide evidence for most observations made in studies involving cellular behavior, changes in morphology, as well as expression of cell-specific molecular markers. However, images also contain information that is typically not quantified due to the various range of difficulty involving their extraction, such as cell counts, cell size, tracking movement and levels of expression of specific markers [Osman et al, 2013; Kaakinen et al, 2014]. In addition, the quantification of these traits requires a great deal of man power and time in order to accomplish satisfactory comparisons [Osman et al 2013]. Thus, image analysis if performed is often used on small scale using a limited number of images to process. However, obtaining quantifiable data from single images alone is rather limited. Cells are living organisms that participate in dynamic events during their lifespan, in the form of movement, division, morphological change, and response to the environment. Thus, studies that factor in these vibrant changes in the form of time-lapse or video-based studies would be more relevant for cell biology.

In this study, we have demonstrated that image analysis and quantification of data can be performed from a series of time-lapsed images in the form of videos. Moreover, this study illustrates that image-based analysis can be used to quantify calcification of osteoblasts derived from human ESCs and characterize the differences in calcification between related cell lines or in response to environmental toxicants. This testifies to the untapped potential of quantifiable data from images or videos to be used to understand dynamic cellular events.

Mineralization and calcification due to the bone-forming capability of osteoblasts is a dynamic event both *in vivo* and *in vitro.* Traditional methods of quantifying the amount of calcium deposits in culture require the use of calcium sensitive dyes, such as Arsenazo III or Alizarin Red S. The method presented here offers several advantages in both a biological and a technical sense.

One biological advantage is that it capitalizes on using the unique facet of mature osteoblasts to incorporate calcium into the extracellular matrix. Calcification of osteoblasts derived from hESCs has a particularly black appearance when viewed with phase contrast optics. This appearance of calcified areas had been previously documented to be characteristic to the formation of bone nodules *in vitro* [Buttery et al, 2001; zur Nieden et al, 2003; Sottile et al, 2003; Ding et al, 2012]. Due to this distinguishable appearance extracting the information corresponding to a calcified area through segmentation allowed us to threshold only the pixels that comprise the mineralized areas in the image. Therefore, the image-based calcification assay does not require the addition of calcium sensitive reagents, which could be toxic to live cultures [Barnard et al, 1995]. As such, Arsenazo III has been identified to inhibit calcium transport and ATP hydrolysis [Harman and Maxwell, 1995]. Because of their cytotoxic

nature traditional quantifications of calcium with dyes are typically terminal experiments. Therefore, such *in vitro* measurement of calcium is only a snap-shot of how much calcification there is at the time a sample is measured. Any time-course assay used to assess the calcium deposition in live cultures hence, requires measuring different samples at different stages of the calcification process. The technique is thus inherently variable and, as a consequence, prevents the observation of calcification as a complete process. In contrast, the time-lapsed image based calcification assay that is presented in this study analyzes the complete calcification process as a whole.

A potential problem with this video-based assay is the requirement of special equipment, such as the Nikon Biostation CT, used in this study. However, the program does not require the use of such expensive machines in order for the program to be utilized. The program can be used with phase-contrast images. The only draw back is that images taken from different machines have different quality in terms of amount of brightness and contrast, thus it is important to redefine the manual threshold of the video-based calcification assay. Videos are also not a requirement for the assay to be performed, though the time component as a result of using a video is a key component for other parameters, such as calcification rate. Phase contrast images are more than enough to determine ID_{50} and IC_{50} by calcification and viability curve using these methods.

Finally, in the course of developing this image-based calcification assay, we characterized a novel kind of calcification measurement: the calcification rate, which is defined as the amount of calcium – in the form of pixels corresponding to segmented calcium – added into the matrix over time. This method determined that hESCs exhibited a greater, yet delayed level of calcification than hiPSCs and that the osteoblasts derived

from hESCs had a faster calcification rate than the hiPSCs. This suggested that even though hESC-derived osteoblasts emerged later, they compensated by having a faster rate of calcification resulting in a higher degree of calcified matrix in culture by the end of the study.

Conclusion

Overall, the image-based calcification assay presented here is a notable update to the classic reagent-based assay for quantifying the degree of calcification in culture. Automated segmentation of calcified regions in images without the aid of toxic calcium sensitive dyes brings with it several biological and technical advantages of using this technique over the reagent-based method: it is more cost effective, is automatable and amenable to high-throughput. Ultimately, this method can be used to generate calcification curves and identify ID_{50} of toxicants on osteogenesis with simple variation in the protocol (Fig. 6).

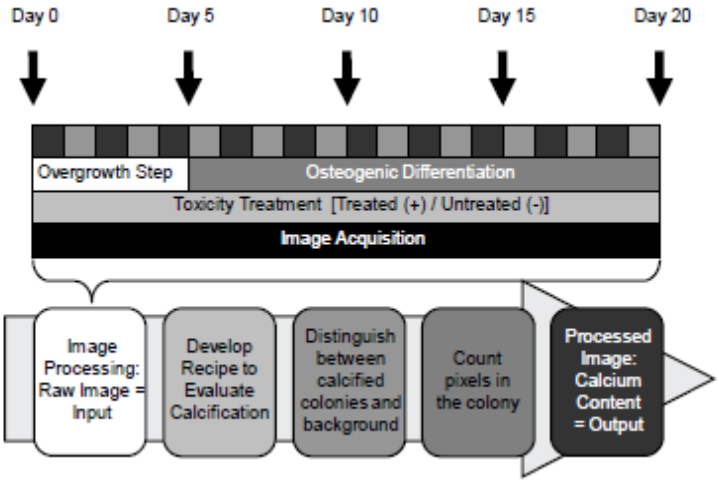

Fig. 6: Schematic overview of image acquisition and data processing for video bioinformatic measurement of calcification. Cells are induced to undergo osteogenic differentiation through an overgrowth approach followed by addition of osteogenic factors on day 5. Differentiation is captured by time-lapse imaging every 12h for a period of 20 days using a Nikon Biostation CT. Time-lapse images are preprocessed to minimize noise from images. Calcification from images is segmented via a manual threshold of pixel value set at 33 using MatLab. Numbers of segmented pixels representing calcified regions are quantified representing the amount of calcification from each time point of the time-lapse imaging

References

1. Talbot P, zur Nieden NI, Lin S, Martinez IKC, Guan B, and Bhanu B. (2014). Use of Video Bioinformatics Tools in Stem Cell Toxicology. In: Handbook of Nanotoxicology, Nanomedicine and Stem Cell Use in Toxicology. Sahu SC and Casciano D, eds. John Wiley & Sons, Ltd, pp 379-402.
2. Yarrow JC. Perlman ZE, Westwood NJ, and Mitchison TJ. (2004). A high-throughput cell migration assay using scratch wound healing, a comparison of image-based readout methods. BMC Biotechnol. 4: 21.
3. Gough W, Hulkower KI, Lynch R, McGlynn P, Uhlik M, Yan L, and Lee JA. (2011). A quantitative, facile, and high-throughput image-based cell migration method is a robust alternative to the scratch assay. J Biomol Screen 16(2): 155-163.
4. Buggenthin F, Marr C, Schwarzfischer M, Hoppe PS, Hilsenbeck O, Schroeder T, and Theis FJ. (2013). An automatic method for robust and fast cell detection in bright field images from high-throughput microscopy. BMC Bioinformatics. 14: 297.
5. Battich N, Stoeger T, and Pelkmans L. (2013). Image-based transcriptomics in thousands of single human cells at single-molecule resolution. Nat Methods. 10(11): 1127-1133.
6. Schmid B, Shah G, Scherf N, Weber M, Thierbach K, Campos CP, Roeder I, Aanstad P, and Huisken J. (2013). High-speed panoramic light-sheet microscopy reveals global endodermal cell dynamics. Nat Commun. 4: 2207.
7. Vogt A, Cholewinski A, Shen X, Nelson SG, Lazo JS, Tsang M, and Hukriede NA. (2009). Automated image-based phenotypic analysis in zebrafish embryos. Dev Dyn. 238(3): 656-663.

8. Guan BX, Lin S, Talbot P, and Bhanu B. (2014). Bio-driven cell region detection in human embryonic stem cell assay. IEEE/ACM Transactions on Computational Biology and Bioinformatics.
9. Zhong Q, Busetto AG, Fededa JP, Buhmann JM, and Gerlich DW. (2012). Unsupervised modeling of cell morphology dynamics for time-lapse microscopy. Nat Methods 9(7): 711-713.
10. Buttery LD, Bourne S, Xynos JD, Wood H, Hughes FJ, Hughes SP, Episkopou V, and Polak JM. (2001). Differentiation of osteoblasts and in vitro bone formation from murine embryonic stem cells. Tissue Eng. 7(1): 89-99.
11. zur Nieden NI, Kempka G, and Ahr HJ. (2003). In vitro differentiation of embryonic stem cells into mineralized osteoblasts. Differentiation 71(1): 18-27.
12. Sottile V, Thomson A, and McWhir J. (2003). In vitro osteogenic differentiation of human ES cells. Cloning Stem Cells 5(2): 149-155.
13. Ding H, Keller KC, Martinez IK, Geransar RM, zur Nieden KO, Nishikawa SG, Rancourt DE, and zur Nieden NI. (2012). NO-β-catenin crosstalk modulates primitive streak formation prior to embryonic stem cell osteogenic differentiation. J Cell Sci. 125(Pt 22): 5564-5577.
14. Boskey AL. (1996). Matrix proteins and mineralization: an overview. Connect Tissue Res. 35(1-4): 357-363.
15. Rutledge KE, Cheng Q, Pryzhkova M, Harris G, Jabbarzadeh E. (2014). Enhanced differentiation of human embryonic stem cells on ECM-containing osteomimetic scaffolds for bone tissue engineering. Tissue Eng Part C Methods. [Epub ahead of print, doi:10.1089/ten.tec.2013.0411]

16. Puchtler H, Meloan SN, and Terry MS. (1969). On the history and mechanism of alizarin and alizarin red S stains for calcium. J Histochem Cytochem. 17(2): 110-124.

17. Rungby J. (1993). The von Kossa reaction for calcium deposits: silver lactate staining increases sensitivity and reduces background. Histochem J. 25(6): 446-451.

18. Choi YJ, Lee JY, Lee SJ, Chung CP, and Park YJ. (2011). Alpha-adrenergic blocker mediated osteoblastic stem cell differentiation. Biochem Biophys Res Commun. 416(3-4): 232-238.

19. Davis LA, Dienelt A, and zur Nieden NI. (2011). Absorption-based assays for the analysis of osteogenic and chondrogenic yield. Methods Mol Biol. 690: 255-272.

20. Kim BS, Kim HJ, Kim JS, You YO, Zadeh H, Shin HI, Lee SJ, Park YJ, Takata T, Pi SH, Lee J, and You HK. (2012). IFITM1 increases osteogenesis through Runx2 in human alveolar-derived bone marrow stromal cells. Bone 51(3): 506-514.

21. Palmieri A, Pezzetti F, Graziano A, Riccardo D, Zollino I, Brunelli G, Martinelli M, Arlotti M, and Carinci F. (2008). Comparison between osteoblasts derived from human dental pulp stem cells and osteosarcoma cell lines. Cell Biol Int. 32(7): 733-738.

22. Pilz GA, Ulrich C, Ruh M, Abele H, Schäfer R, Kluba T, Bühring HJ, Rolauffs B, and Aicher WK. (2011). Human term placenta-derived mesenchymal stromal cells are less prone to osteogenic differentiation than bone marrow-derived mesenchymal stromal cells. Stem Cells Dev. 20(4): 635-646.

23. Kawaguchi J, Mee PJ, and Smith AG. (2005). Osteogenic and chondrogenic differentiation of embryonic stem cells in response to specific growth factors. Bone 36(5): 758-769.

24. Zeng Q, Li X, Beck G, Balian G, Shen FH. (2007). Growth and differentiation factor-5(GDF-5) stimulates osteogenic differentiation and increases vascular endothelial growth factor (VEGF) levels in fat-derived stromal cells in vitro. Bone 40(2): 374-381.

25. De Rosa A. Tirino V, Paino F, Tartaglione A, Mitsiadis T, Feki A, d'Aquino R, Laino L, Colacurci N, and Papaccio G. (2011). Amniotic fluid-derived mesenchymal stem cells lead to bone differentiation when cocultured with dental pulp stem cells. Tissue Eng Part A 17(5-6): 645-653.

26. Koskela A, Viluksela M, Keinänen M, Tuukkanen J, and Korkalainen M. (2012). Synergistic effects of tributyltin and 2,3,7,8-tetrachlorodibenzo-p-dioxin on differentiating osteoblasts and osteoclasts. Toxicol Appl Pharmacol. 263(2): 210-217.

27. Korkalainen M. Kallio E, Olkku A, Nelo K, Ilvesaro J, Tuukkanen J, Mahonen A, and Viluksela M. (2009). Dioxins interfere with differentiation of osteoblasts and osteoclasts. Bone. 4(6): 1134-1142.

28. Bielby RC, Boccaccini AR, Polak JM, and Buttery LD. (2004). In vitro differentiation and in vivo mineralization of osteogenic cells derived from human embryonic stem cells. Tissue Eng. 10(9-10): 1518-1525.

29. Uchimura E, Machida H, Kotobuki N, Kihara T, Kitamura S, Ikeuchi M, Hirose M, Miyake J, and Ohgushi H. (2003). In-situ visualization and quantification of mineralization of cultured osteogenetic cells. Calcif Tissue Int. 73(6): 575-583.

30. zur Nieden NI, Price FD, Davis LA, Everitt RE, Rancourt DE. (2007). Gene profiling on mixed embryonic stem cell populations reveals a biphasic role for beta-catenin in osteogenic differentiation. Mol Endocrinol. 21(3): 674-685.

31. zur Nieden NI, Davis LA, and Rancourt DE. (2010). Comparing three novel endpoints for developmental osteotoxicity in the embryonic stem cell test. Toxicol Appl Pharmacol. 247(2): 91-97.

32. Yuhara S, Kasagi S, Inoue A, Otsuka E, Hirose S, and Hagiwara H. (1999). Effects of nicotine on cultured cells suggest that it can influence the formation and resorption of bone. Eur J Pharmacol. 383(3): 387-393.

33. Feltes BC, de Faria Poloni J, Notari DL, and Bonatto D. (2013). Toxicological effects of the different substances in tobacco smoke on human embryonic development by a systems chemo-biology approach. PLoS One 8(4): e61743.

34. Kuske B, Pulyanina PY, and zur Nieden NI. (2012). Embryonic stem cell test: stem cell use in predicting developmental cardiotoxicity and osteotoxicity. Methods Mol Biol. 889: 147-179.

35. Hecht SS. It is time to regulate carcinogenic tobacco-specific nitrosamines incigarette tobacco. Cancer Prev Res (Phila). 2014 Jul;7(7):639-47.

36. Xue J, Yang S, Seng S. Mechanisms of Cancer Induction by Tobacco-Specific NNK and NNN. Cancers (Basel). 2014 May 14;6(2):1138-56.

37. Osman OS, Selway JL, Kępczyńska MA, Stocker CJ, O'Dowd JF, Cawthorne MA, Arch JR, Jassim S, and Langlands K. (2013). A novel automated image analysis method for accurate adipocyte quantification. Adipocyte 2(3): 160-164.

38. Kaakinen M, Huttunen S, Paavolainen L, Marjomäki V, Heikkilä J, and Eklund L. (2014). Automatic detection and analysis of cell motility in phase-contrast time-

lapse images using a combination of maximally stable extremal regions and Kalman filter approaches. J Microsc. 253(1): 65-78.

39. Barnard DL, Fairbairn DW, O'Neill KL, Gage TL, and Sidwell RW. (1995). Anti-human cytomegalovirus activity and toxicity of sulfonated anthraquinones and anthraquinone derivatives. Antiviral Res. 28(4): 317-329.

40. Harman AW, and Maxwell MJ. (1995). An evaluation of the role of calcium in cell injury. Annu Rev Pharmacol Toxicol. 35: 129-144.

Chapter 3: Harm-reduction Tobacco Products are More Teratogenic to Differentiating Osteoblasts than Conventional Products

Abstract

Tobacco smoking has been implicated in an array of health related diseases including those that affect the adult bone. However, little is known regarding the impact of conventional and harm reduction tobacco smoke on bone tissue as it develops in the embryo. In order to assess the effect of tobacco products on developing bone tissue, human embryonic stem cells were differentiated into osteoblasts and concomitantly exposed to various concentrations of either mainstream or sidestream smoke solutions from two conventional and three harm reduction brands of cigarettes and two types of smokeless tobacco. Differentiation inhibition was determined by calcium assays on osteogenically differentiating cells and compared to the cytotoxicity of the tobacco smoke solution or extract.

Exposure to mainstream smoke from conventional and additive-free cigarettes caused no inhibition of cell viability and calcification of the osteogenic cultures, while sidestream smoke concentration-dependently revealed 100% cell death. Osteogenically differentiating cells were more sensitive to harm-reduction products than to conventional products. Here, a teratogenic effect was found for the highest mainstream concentration tested. In sidestream smoke treated cultures, mineralization was completely retarded at sub-toxic concentrations lower than those determined to be cytotoxic for conventional products. Reducing the content of combustion products by using extracts from smokeless chewing tobacco did not alleviate the teratogenic effect.

In summary, though perceived as safer, harm reduction cigarettes and chewing tobacco were more potent in inhibiting osteogenesis than conventional cigarettes. These results potentially suggest low bone mineral density of the embryo if exposed to environmental smoke during development.

Introduction

Since the early 1900, the American tobacco market has been flooded by a great variety of cigarettes. Among the most popular brands of cigarettes are Marlboro Red and Camel, which are preferred by smokers around the world. The growing body of evidence that acknowledges the detrimental effect of tobacco on the human body has been astounding. Cigarette use has been hailed as the leading cause of preventable death in the world. The most well known of the adverse health consequences of tobacco use are cancer, cardiovascular diseases, and respiratory complications. Moreover, cigarette smoking has been suggested to have adverse effects on bone tissue. For example, smoking increases the occurrence of developing osteopathies, such as osteoporosis (Ayo-Yusuf and Olutola, 2014; Iqbal et al., 2013; Brook et al., 2012) and Legg-Calve-Perthes Disease (Daniel et al., 2012) and has been implicated in delayed healing of fractured bones (Sloan et al., 2010; Moghaddam-Alvandi et al., 2012).

Often underappreciated, tobacco use by women may also adversely affect pregnancy outcomes and impairs the health of the unborn (Soares and Melo, 2008; DiFranza et al., 2004). Among other environmental factors it also accounts for the high frequencies of congenital anomalies in infants (Stillerman et al., 2008). Limited research

in young adults and immature animals suggests a detrimental effect of tobacco on bone during growth (Iwaniec et al., 2000).

The increasing health consciousness by consumers has led the tobacco industry to release products that were once marketed as “harm-reduction” or “light” versions of their conventional products. These products typically contained less tar, nicotine, or other chemical additives that are would otherwise be inhaled by the smoker. While the beneficial impact of harm-reduction cigarettes on the frequency of smoking-related cancer deaths is still being debated, it is even less clear whether the reduction of nicotine and tar content is sufficient to eliminate any teratogenic side effects on developing bone.

Studies to understand the effects of a teratogen are typically performed using rodent animal models, such as mice or rats (Balansky et al., 1992; Givi et al., 2013). These types of studies require the sacrifice of animals, and are often non-cost effective. In this current paper, human ESCs (hESCs) differentiating into osteoblasts were utilized to test seven well-known brands of both conventional and harm-reduction cigarettes available on the market in a manner relatable to effects seen in developing human bone tissue. Typical studies involving tobacco mainly focus on the effects on mainstream smoke only (Balansky et al., 1992; Van Miert et al., 2008). Here, teratogenic effects of both the mainstream and sidestream smoke generated by cigarettes were determined. Our data revealed sidestream smoke to be more teratogenic than mainstream smoke on differentiating osteogenic hESC cultures in all tested brands. The teratogenic effect of sidestream smoke from conventional cigarettes was due to the general cytotoxicity of the smoke solution. In addition, we have determined that smoke from harm-reduction cigarettes showed true teratogenicity even at sub-toxic concentrations in both the

mainstream and the sidestream preparations. These data support the idea that tobacco has more detrimental effects on human health outside the big three categories: cancer, respiratory, and heart disease, and that harm-reduction products may not be less harmful than conventional products.

Materials and Methods

hESC culture

The commercially available hESC H9 line was acquired from WiCell (WiCell Research Institute). The hESCs were maintained in mTeSR® medium (Stem Cell Technologies) and kept in an undifferentiated state at 37°C in a humid 5% CO_2 environment. Pluripotent colonies were passaged every 5 days upon reaching 70% confluency by dissociating cells with accutase and a cell scraper. Cells were allowed to attach on Matrigel (BD Biosciences) treated culture plates.

Osteogenic differentiation

At confluency, pluripotent colonies were induced to undergo osteogenesis with control differentiation medium (DMEM (Gibco) containing 15% FBS (Atlanta), 1% non-essential amino acids (NEAA; Gibco), 1:200 penicillin/streptomycin (Gibco), and 0.1mM β-mercaptoethanol (Sigma)) for 5 days as described (Sparks et al., 2014). Subsequently, control differentiation medium was supplemented with osteogenic factors: 0.1 mM β-glycerophosphate (βGP; Sigma), 50 µg/ml ascorbic acid (AA; Sigma), and 1.2x10-7 M 1,25(OH)2 Vitamin D3 (VD3; Calbiochem).

Production of smoke solution

Commercially available popular conventional (Marlboro Red and Camel) and harm reduction (Marlboro Gold, Camel Blue, and American Spirits) brands of cigarettes were purchased from a local retail dealer and used to make mainstream (MS) and sidestream (SS) smoke solutions with a method described previously in detail (Knoll et al., 1995; Knoll and Talbot, 1998). Smoke solutions were generated using a University of Kentucky smoking machine that took a 2.2 second puff of MS every minute. MS smoke solution was generated by pulling 30 puffs of MS smoke through 10 ml of DMEM culture medium. During MS smoke production, SS smoke solution was produced by collecting the smoke that burned off the end of the cigarette and pulling it through 10 ml of DMEM. SS smoke was collected continuously, while MS smoke was collected during each puff.

Both MS and SS solutions were made at concentrations of 3 puff equivalents (PE). One PE of MS smoke is the amount of smoke in one puff that dissolves in 1 ml of culture medium. For SS smoke, one PE is the amount of SS smoke that dissolves in 1 ml of culture medium during one minute of burning. Immediately after preparation, smoke solutions were filtered through a 0.2 micron Acrodisc® PSF Syringe Filter (Pall Corporation, Port Washington, NY), aliquoted into sterile Eppendorf tubes, and stored in a -80°C freezer until used.

Desired PEs were acquired through serial dilutions and experiments were done using either MS or SS at concentrations as indicated and an untreated control. Osteogenic differentiation of hESCs was induced as described above and cultures were treated with smoke solutions through the 20 day duration of differentiation. Smoke solutions were replenished with each media change.

Derivation of Snus Tobacco Extract

Tobacco extract was created at 10% (v/v) in DMEM. Resulting solution was centrifuged for 10 min at 450 × g, to remove large debris. Supernatant was collected an centrifuged at 13,000 × g for 1 h, to remove finer debris. pH was adjusted to 7.4 and extract sterilized through a 0.45μm filter. FBS was added to a final concentration of 15%.

Osteogenic Viability assay

Culture viability was determined by 3-[4,5-dimethylthiazol-2-yl]-2,5-diphenylterazolium bromide (MTT) assay. Briefly, cells were incubated with MTT (120 mg/ml) at 37°C for 3 h. After the supernatant was removed, 0.04 mol/L HCl in isopropanol was added to each well and the optical density of the solution was read at 595 nm in an iMark™ microplate reader (BIO-RAD). As the generation of the blue product is proportional to the dehydrogenase activity, a decrease in the absorbance at 595 nm provided a direct measurement of the number of viable cells.

Calcium assay

For quantification of calcium in the cell matrix, cells were harvested in radioimmunoprecipitation (RIPA) buffer. Calcium content was normalized to the total protein content of the sample from RIPA protein using the Lowry method as previously described (Davis et al., 2011). Calcium deposition was determined based on calcium ions (Ca^{2+}) reacting with Arsenazo III (Genzyme) to form a purple Ca-Arsenazo III

complex, which was measured at 655 nm. The concentration of total calcium in the sample was calculated based on a $CaCl_2$ standard (Davis et al., 2011).

Statistical analysis

Lowest concentrations at which calcification or cell viability dropped below the untreated control were identified with One-Way ANOVA. Correlations between pairs of IC_{50}/ID_{50} values were assessed with a paired student's t-test (GraphPad QuickCalcs). For all conducted tests, p-values below 0.05 were considered significant.

Results

In order to assess the hazardous effects of smoking on developing bone tissue, we compare here the potency of mainstream and sidestream smoke of conventional and harm-reduction tobacco products to induce differentiation defects in human embryonic stem cells undergoing differentiation into osteoblasts.

Mainstream Smoke from Conventional Tobacco is Neither Cytotoxic nor Teratogenic to Differentiating Osteogenic Cultures

First, mainstream (MS) smoke of two conventional brands of cigarettes was tested to determine their teratogenic effects on the formation of bone tissue. For this, human ESCs that were induced to undergo osteogenic differentiation (Sparks et al., 2014) were used as an *in vitro* model for embryonic bone development. Mainstream

smoke was obtained from the two commercially leading brands of cigarettes: Marlboro Red and Camel, and hESCs treated during the entire differentiation period. Each product was screened at five different concentrations to generate a concentration-response curve.

Cell survival upon tobacco exposure was then measured using an MTT assay after 20 days of culture, at which point these cultures express marker genes and proteins of mature osteoblasts (Sparks et al., 2014). Neither product revealed any adverse effects on mitochondrial dehydrogenase activity (Fig. 1A and B).

As osteoblasts emerge from the culture they begin to form nodules made out of calcified extracellular matrix (Sparks et al., 2014). This process is unique only to bone forming cells in the body. Next, this functional characteristic of bone tissue was assayed via the quantification of calcium ions deposited into the matrix. Similarly to the MTT assay results, neither tobacco smoke solution showed any overt inhibition of calcification, as assessed using Arsenazo III, a reagent-based assay, for measuring calcium contents in samples (zur Nieden et al., 2010; Davis et al., 2011) (Fig. 1A and B). Together, these results suggest that mainstream smoke has no observable effect on neither viability nor functional calcification of osteogenic cultures at any of the concentrations tested.

Sidestream Smoke from Conventional Tobacco Demonstrates Harmful Effects on Human Osteoblast Differentiation

Since mainstream smoke showed no observable changes in either cell survival or functional calcification in the emerging hESC-derived osteoblasts, we next focused our attention on the second type of smoke generated from cigarettes: sidestream smoke

(SS), which is found to be 80% enriched in second hand smoke. Using the previously described method and concentrations, hESCs were induced to differentiate into osteoblasts with concomitant treatment with smoke solution made from sidestream smoke of Marlboro Red and Camel cigarettes.

In contrast to the MS smoke solution, in both Marlboro Red and Camel SS smoke solutions cell death of the entire population was observed at 0.1 and 0.3 PE, respectively (Fig. 2). The functional calcification assay showed similar results to the cell viability assessment for each of the products. The noted inhibition of differentiation and viability upon exposure of the cells to SS smoke solutions were in stark contrast to the respective curves found for MS smoke solutions, which had shown no effect.

Harm-reduced Tobacco Products are more Harmful to Differentiating Osteoblasts than Conventional Products

In order to evaluate whether cigarettes that evidently contain less carcinogens cause less harm also in differentiating cells, American Spirit cigarettes were then tested. These cigarettes were established in 1982 and popularized by their catchy slogans defining their brand as “All Natural”, “Organic”, and “100% Additive-Free,” which captivated more health conscious smokers. MS smoke solution from American Spirits cigarette showed no observable changes in both the calcification and cell viability assays compared to the untreated cells (Fig. 3A). In contrast, American Spirit sidestream smoke revealed teratogenicity at 0.3 PE. Thus, these results were similar to the screen of the conventional versions for both the Marlboro and Camel brands in that no observable and quantifiable inhibitory effects were noted.

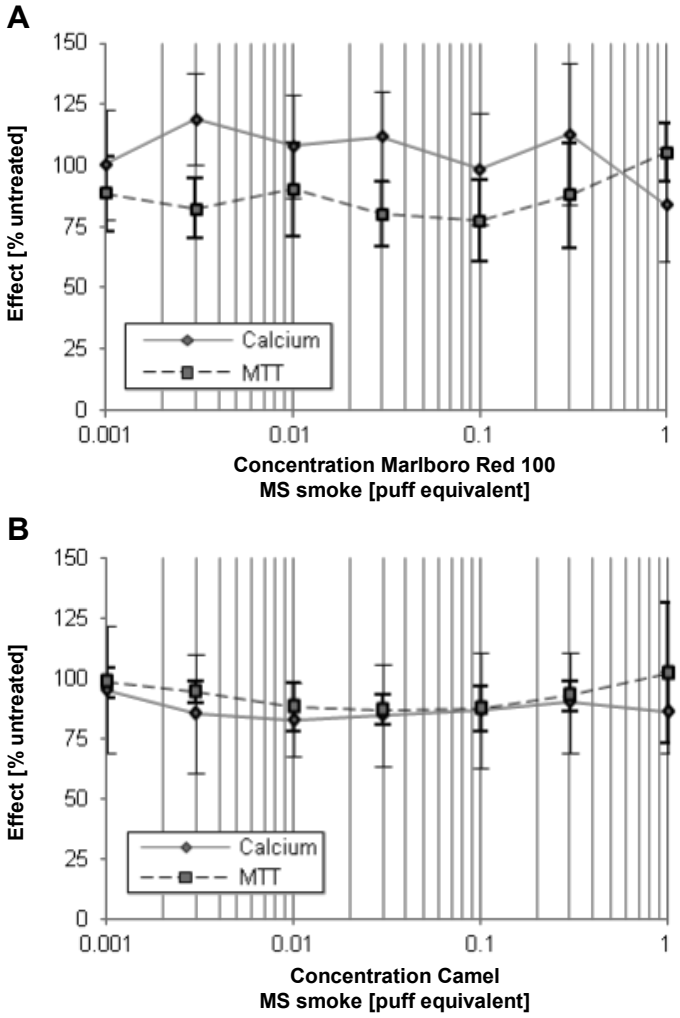

Fig. 1: Effects of mainstream smoke of conventional cigarette brands on osteoblast differentiation. Human ESCs were treated with different concentrations of smoke solution and scored for effects on calcium deposit using Arsenazo III and on viability using an MTT assay. A) Marlboro Red 100 mainstream smoke solution. B) Camel mainstream smoke solution. MS, mainstream; MTT, mitochondrial dehydrogenase activity assay.

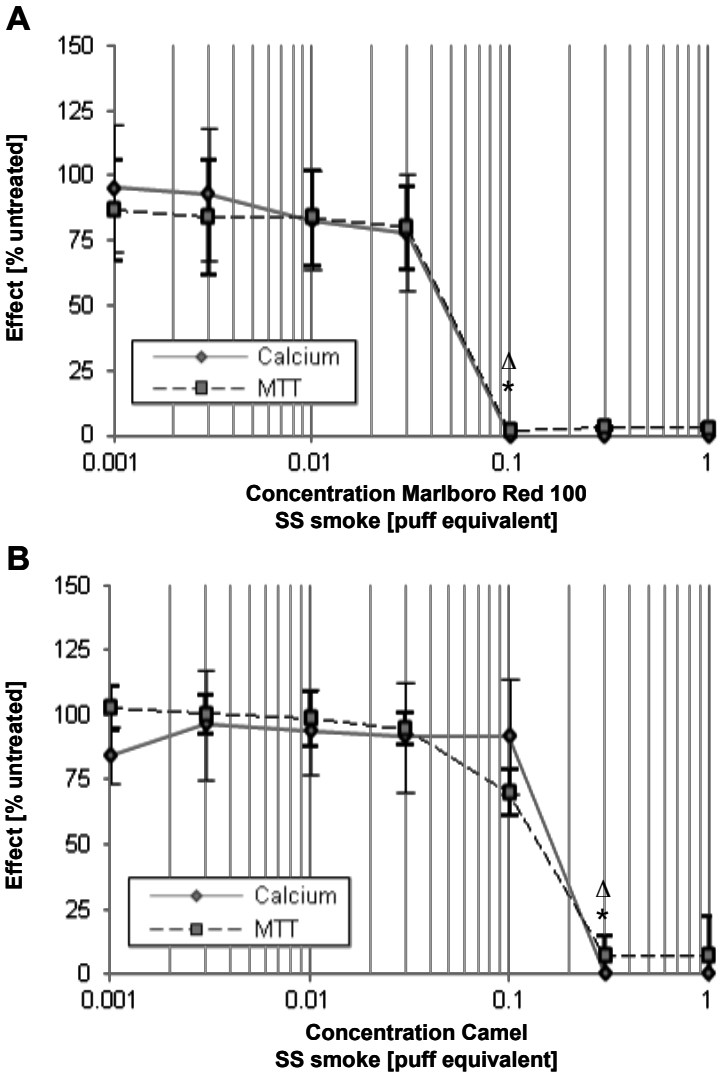

Fig. 2: Effects of treatment with Camel mainstream smoke on osteoblasts formation. Calcification was measured with calcium assay and viability of osteogenic cultures examined with MTT assay. Δp<0.05, One-Way ANOVA, lowest concentration statistically significant below the untreated control in the calcium assay. *p<0.05, One-Way ANOVA, lowest concentration statistically significant below the untreated control in the MTT assay. SS, side stream; MTT, mitochondrial dehydrogenase activity assay.

Marlboro Gold and Camel Blue cigarettes, previously marketed as light cigarettes, were then screened with hESCs to determine their teratogenic effects on the formation of bones. Again, both MS and SS smoke were tested in five concentrations per cigarette type. In contrast to MS smoke from the conventional brands, which showed no adverse effect, calcification of the hESC-derived osteoblasts was inhibited at the highest concentration tested (1 PE), while no effects on cell viability were noted (Fig. 3B, C). Similarly, Marlboro Gold and Camel Blue SS smoke both ablated calcification at 0.1 PE and caused a reduction in cell viability at 0.3 PE down to 6% viable cells (Fig. 3B, C). This further eludes to the idea that SS smoke from any cigarette has more adverse effects on bone health than MS smoke. However, these data also suggest that "harm-reduction" or "light" versions of popular brands may be more detrimental to differentiating osteogenic cells than conventional products.

Smokeless Tobacco Products are Detrimental to Osteogenically Differentiating hESCs

Due to the harmful effects on osteogenically developing cells that we found with smoke solutions of tobacco products, we next set to investigate whether the lack of combustion of the tobacco would contribute to reducing its adverse health effect on these cells. For example, chewing tobacco is used by putting a wad of tobacco inside the cheek, either contained in a paper pouch or not. We tested extracts of Marlboro and Camel chewing tobacco made in DMEM on osteogenically differentiating hESCs as described above and found that extracts of chewing tobacco also inhibited calcification

of hESCs in a concentration-dependent manner (Fig. 4A and B). These inhibitory effects were noted at sub-toxic concentrations.

Teratogenesis of SS Tobacco Smoke Solutions from Conventional Brands is Based on their General Cytotoxicity

In order to classify the tested chemical blends in SS smoke from Marlboro Red100, Camel and American Spirits, as teratogenic, we next contrasted the IC_{50} and ID_{50} values that we obtained from the concentration-response curves (Table 1). Only if the reduction in functional output (ID_{50}) and the reduction in survival of the culture (IC_{50}) are relatively different can the chemical be assigned to be teratogenic. In those cases, inhibition of differentiation would be found at concentrations that are not cytotoxic. In contrast, when the IC_{50} and ID_{50} fall close together, the teratogenic effect of the chemical or chemical blend may be due to a direct effect of the chemical towards the developmental process.

In order to identify these subtle differences, we have next charted the obtained IC_{50} values against the ID_{50} values (Fig. 5A). This comparison of the ID_{50} and IC_{50} for the tested conventional products revealed that the observed IC_{50} values were very similar to the ID_{50} values of the same tobacco product. The p-values that were obtained by comparing both of these concentrations with a paired t-test were above the significance cut-off of 0.05 (Fig. 5B). This indicated that the decrease in the amount of calcification upon addition of conventional SS smoke into the osteogenic cultures correlated well with the decrease in cell viability. Consequently, the decrease in the amount of calcified

matrix was likely due to a cytotoxic effect that led to the eradication of a viable osteoblast-like population.

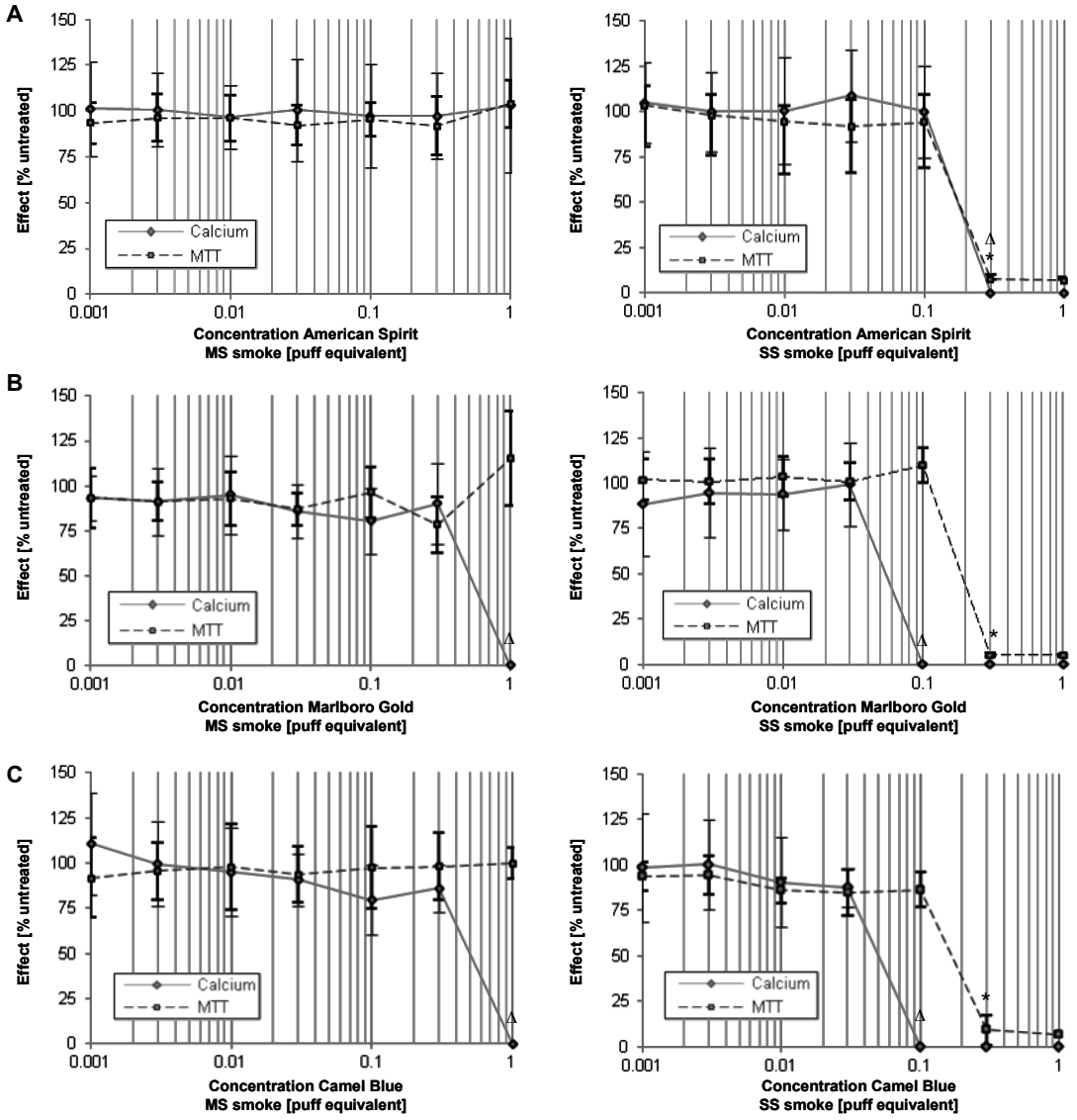

Fig. 3: Effects of harm-reduction cigarette smoke on developing osteoblasts. A) Calcification and viability screen for mainstream smoke generated from harm-reduction cigarette products using Arsenazo III and MTT assay, respectively. B) Sidestream smoke calcification and cell survival screen for the harm-reduction tobacco product indicated. $^{\Delta}p<0.05$, One-Way ANOVA, lowest concentration statistically significant below the untreated control in the calcium assay. *p<0.05, One-Way ANOVA, lowest concentration statistically significant below the untreated control in the MTT assay. MS, mainstream; MTT, mitochondrial dehydrogenase activity assay; SS, side stream.

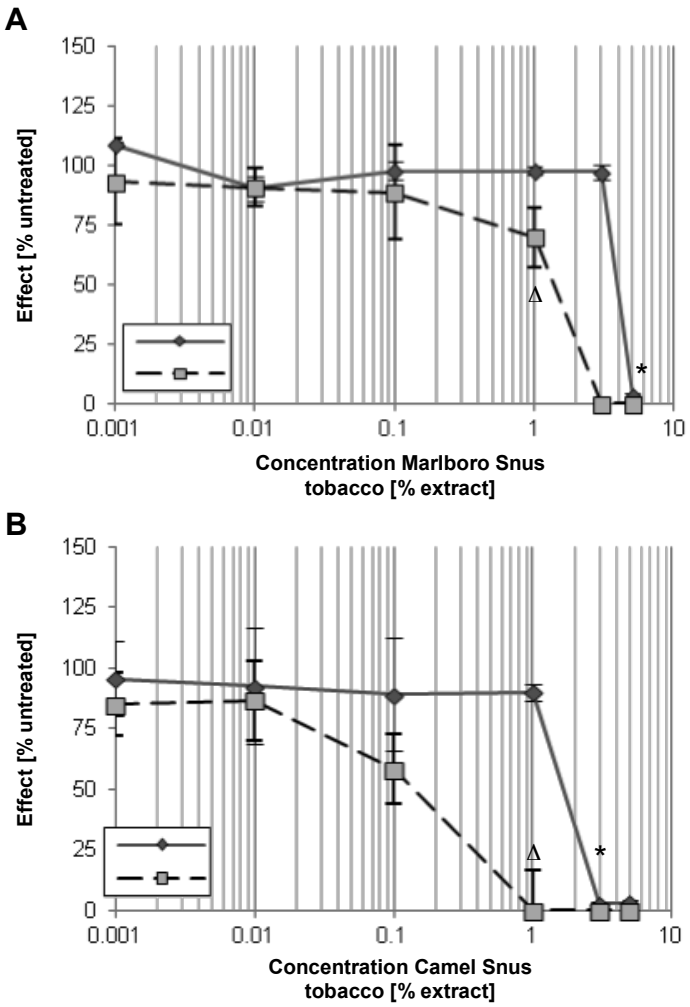

Fig. 4: Extracts from chewing tobacco concentration-dependently inhibit hESC calcification below cytotoxic threshold. Calcification and viability screen for A) Marlboro and B) Camel Snus using Arsenazo III and MTT assay, respectively. ᵃp<0.05, One-Way ANOVA, lowest concentration statistically significant below the untreated control in the calcium assay. *p<0.05, One-Way ANOVA, lowest concentration statistically significant below the untreated control in the MTT assay. MTT, mitochondrial dehydrogenase activity assay.

The same similarity between the IC_{50} and ID_{50} was found for American Spirit SS cigarette smoke (Fig. 5A, B). Treatment with SS smoke solution from American Spirit led to a decrease in the total amount of calcification based on a cytotoxic effect on the osteogenic cultures.

MS and SS Tobacco Smoke Solutions from Harm-reduction Brands are Teratogenic to Differentiating Osteogenic Cultures

The described relationship between the IC_{50} and the ID_{50} is in contrast to what was observed for Marlboro Gold, Camel Blue both the mainstream and sidestream smoke solutions, and Snus tobacco, which all showed a decrease in osteogenic output, but at subtoxic concentrations (Fig. 5A, B). For example, at 1 PE MS smoke, cell viability was still around the 100% mark, but calcification already absent. The IC_{50} concentrations were statistically different from the ID_{50} values (Fig. 5B) suggesting that the harm-reduction products are truly teratogenic to the differentiating osteoblasts.

In conclusion, conventional products, but also those with reduced levels of additives showed cytotoxicity that caused teratogenicity to the developing osteoblasts. Among the seven products tested, our study revealed two harm-reduction products, Marlboro Gold and Camel Blue, to be the most harmful to developing osteoblasts, followed by Snus tobacco.

		MS			SS/Extract		
Type of tobacco	**Brand**	**IC_{50}**	**ID_{50}**	**Toxicity**	**IC_{50}**	**ID_{50}**	**Toxicity**
Conventional	*Marlboro*	1	1	Cytotoxic	0.036±0.018	0.043±0.007	Cytotoxic
	Camel	1	1	Cytotoxic	0.137±0.095	0.175±0.03	Cytotoxic
Additive-free	*American Spirit*	1	1	Cytotoxic	0.180±0.023	0.17±0.012	Cytotoxic
Harm-reduction (less tar/less nicotine)	*Marlboro Gold*	1	0.473±0.067	Teratogenic	0.195±0.01	0.056±0.009	Teratogenic
	Camel Blue	1	0.487±0.021	Teratogenic	0.167±0.006	0.049±0.002	Teratogenic
Harm-reduction (no combustion)	*Marlboro Snus*				4±0.1	1.267±0.25	Teratogenic
	Camel Snus				1.63±0.25	0.137±0.047	Teratogenic

Table 1: List of IC_{50} and ID_{50} values determined from concentration-response curves for all tobacco products grouped by mainstream and sidestream smoke (cigarettes) or extract (chewing tobacco)

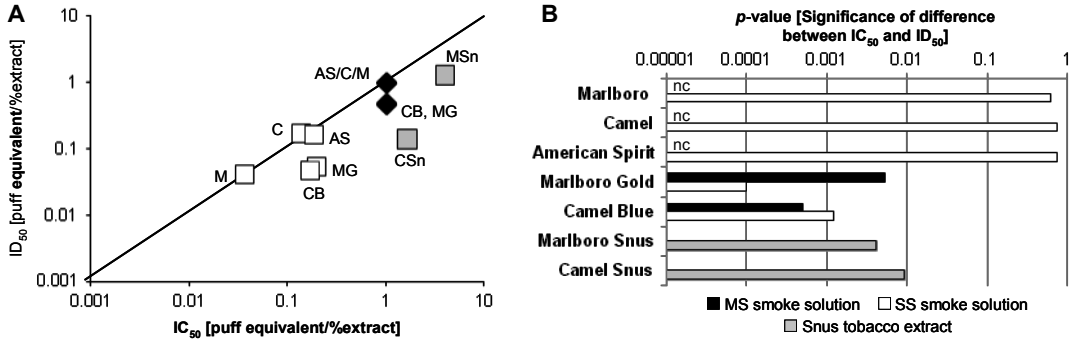

Fig. 5: Comparison of IC_{50} and ID_{50} of conventional and harm reduction products. (A) Linear regression analysis charting IC_{50} values against ID_{50} values. (B) Graph charting the p-values obtained when comparing IC_{50} and ID_{50} concentrations from three independent experiments for the respective products by One-Way ANOVA. AS, American Spirit; C, Camel; CB, Camel Blue; CSn, Camel Snus; M, Marlboro Red 100; MG, Marlboro Gold; MS, mainstream; MSn, Marlboro Snus; nc, not computed;SS,sidestream.

Discussion

This paper demonstrated that use of tobacco products can lead to changes in osteogenic development. We used a modified embryonic stem cell test (zur Nieden and Baumgartner, 2010) that uses human embryonic stem cells, instead of mouse embryonic stem cells, and directed their differentiation through an osteogenic lineage. This was used as a model that we confidently believe to be a highly representative model of human embryonic bone development to determine the toxicological effect of tobacco products on human bone health.

One outcome of our study was the finding that SS smoke always showed detrimental effects at lower concentrations than MS smoke. From our results, it can be argued that mainstream smoke appears to hinder neither the functionality nor the viability of developing osteoblasts in the culture. The inverse is true for sidestream

smoke for it exhibited effects on both the calcification, as well as the survivability of the osteogenic cultures. Despite of its importance to second hand smoke there have only been a limited number of studies that determined the effect of SS smoke alone. Instead, most studies that determine the effect of second hand smoke use whole smoke, which is a combination of MS smoke exhaled by the smoker and SS smoke. The few studies that did investigate the two different types of smokes separately also found that SS smoke was more potent than MS smoke, in very diverse endpoint assays such as content of free radical species, damage to IVF outcome, sperm motility and attachment ability of peri-implantation embryonic cells (Valavanidis and Haralambous, 2001; Neal et al., 2005; Lin et al., 2009; 2010; Polyzos et al., 2009).

One of these previous studies also suggested that harm-reduction products are more potent in attributing harm than conventional products. Lin and colleagues showed that the ability of human embryonic stem cells to attach to a substratum was severely impaired by exposure to harm-reduction products, while conventional products had milder outcomes (Lin et al., 2010). Although this was the first study to evaluate the health of unspecialized pluripotent stem cells in response to tobacco, it did not allow any conclusions as to the potential impairment of differentiation events. Simply extending their findings to differentiating cells may not be straightforward, since undifferentiated cells exhibit altered metabolic, transcriptional and epigenetic states than differentiated cells (Bibikova et al., 2006; Liu et al., 2006; Han et al., 2014) that could potentially dictate their responses to toxicants.

Thus, in this study, harm-reduction brands were compared to their conventional counterparts to determine if these products do confer a reduced harm on differentiating tissues, using bone health as an example. Similarly to the previous findings our data

suggested that harm-reduction products are more teratogenic than conventional products to differentiating osteoblasts, as exposure demonstrated cytotoxic and in some concentrations teratogenic effects on calcification.

These results are alarming given that the general public historically perceived harm-reduction products to lower the health risk involved in smoking. This was a response by tobacco companies on the growing body of work that provided a causal link between smoking and cancer (Wynder and Graham, 1950; Doll and Hill, 1952; Hammond and Horn, 1958). These products came to be known as “Light” versions of the conventional cigarettes and constitute 85% of the US cigarette market (Federal Trade Commission cigarette report). Another example are cigarettes that have reduced ingredients that contribute to the overall detrimental effects of the cigarette smoke, for example American Spirits.

Ironically, our findings render harm reduction products that are marketed as a safer alternative to conventional products to be harmful. Indeed, already in 1997 prospective mortality studies performed by Thun and Heath (1997) revealed an increase rather than a decrease in smoking associated health risks over a 20 year period after the introduction of low nicotine low tar cigarettes, which also suggested that harm-reduction products were not truly reducing harm. Based on these and other studies in 2009 deceptive tobacco marketing descriptors such as light,” “low,” or “mild' were banned by the Family Smoking Prevention and Tobacco Control Act (www.fda.org). Today, such products are hidden under a color code and include Marlboro Gold and Camel Blue, which were tested here.

In vitro, the fact that harm-reduction products inhibited osteogenesis more severely than conventional products may be explained by the alteration in chemical

composition associated with the process of the lowering of tar and nicotine. Depending on the type of tobacco leaf processed, other constituents found in the complex chemical blend of cigarette smoke, such as nitrate, nitrogen oxide and tobacco-specific nitrosamines, may be enriched (Hoffmann and Hoffmann, 1997). Individually, all of those chemicals have been shown to cause adverse health effects in mammalian cells (Nayak et al., 1989; Fujinaga et al., 1989; Sasaki et al., 2008; Zeman et al., 2011).

Given that harm-reduction smokers compensate for the amount of delivered nicotine by smoking a larger number of cigarettes or by inhaling deeper (Burns and Benowitz, 2001), it is likely that concentrations of such chemicals are even higher in mothers that cannot quit smoking while pregnant and that their harmful effects are compounded in their unborn fetuses. In fact, a recent pragmatic trial suggested that nicotine replacement therapies often drawn on to quit smoking during pregnancy, deliver inadequate nicotine levels, as measured by urine cotinine levels, to actually aid in smoking cessation (Bowker et al., 2014). Consequently, addicted smoking women, who become pregnant, may be unsuccessful in quitting, exposing their children.

Our data is also relevant to pregnant women, who do not smoke themselves, but expose their fetuses to a smoking environment. Even in countries with extensive tobacco control policies, this is still a relevant concern. For example, in New York, a city with comprehensive tobacco control policies, almost 50% of nonsmoking pregnant women had elevated cotinine levels (Hawkins et al., 2014) suggesting that their bodies and thus their fetuses had been exposed to second hand smoke. It is likely that these exposure levels would be exacerbated in countries that do not yet or not as extensively control tobacco use in public places. Therefore, our data may inform policy makers about yet another adverse health outcome of smoking.

Conclusion

In a recent press release international experts on tobacco policies have urged the World Health Organization to embrace harm-reduction products to promote better health (Torjesen, 2014). However, based on our evidence, it is clear that harm-reduction products may not be as safe as they are being marketed out to be. Hence, our data advises pregnant women to abstain from smoking completely rather than to switch to these products.

References

1. Ayo-Yusuf, O.A., and Olutola, B.G. (2014) Epidemiological association between osteoporosis and combined smoking and use of snuff among South African women. *Niger J Clin Pract*. 17(2), 174-177.
2. Iqbal, J., Sun, L., Cao, J., Yuen, T., Lu, P., Bab, I., Leu, N.A., Srinivasan, S., Wagage, S., Hunter, C.A., Nebert, D.W., Zaidi, M., and Avadhani, N.G. (2013) Smoke carcinogens cause bone loss through the aryl hydrocarbon receptor and induction of Cyp1 enzymes. *Proc Natl Acad Sci U S A*. 110(27), 11115-11120.
3. Brook, J.S., Balka, E.B., and Zhang, C. (2012) The smoking patterns of women in their forties: their relationship to later osteoporosis. *Psychol Rep*. 110(2), 351-362.
4. Daniel, A.B., Shah, H., Kamath, A., Guddettu, V., and Joseph, B. (2012) Environmental tobacco and wood smoke increase the risk of Legg-Calvé-Perthes disease. *Clin Orthop Relat Res*. 470(9), 2369-2375.
5. Sloan, A., Hussain, I., Maqsood, M., Eremin, O., and El-Sheemy, M. (2010) The effects of smoking on fracture healing. *Surgeon*. 8(2), 111-116.
6. Moghaddam-Alvandi, A., Zimmermann, G., Hammer, K., Bruckner, T., Grützner, P.A., and von Recum, J. (2013) Cigarette smoking influences the clinical and occupational outcome of patients with tibial shaft fractures. *Injury*. 44(11), 1670-1671.
7. Soares, S.R., and Melo, M.A. (2008) Cigarette smoking and reproductive function. *Curr Opin Obstet Gynecol* 20(3), 281-291.

8. DiFranza, J.R., Aligne, C.A., and Weitzman, M. (2004) Prenatal and postnatal environmental tobacco smoke exposure and children's health. *Pediatrics* 113(4 Suppl), 1007-1015

9. Stillerman, K.P., Mattison, D.R., Giudice, L.C., and Woodruff, T.J. (2008) Environmental exposures and adverse pregnancy outcomes: a review of the science. *Reprod Sci*. 15(7), 631-650.

10. Iwaniec, U.T., Fung, Y.K., Cullen, D.M., Akhter, M.P., Haven, M.C., and Schmid, M. (2000) Effects of nicotine on bone and calciotropic hormones in growing female rats. *Calcif Tissue Int* 67, 68-74

11. Balansky, R.B., D'Agostini, F., Zanacchi, P., and De Flora, S. (1992) Protection by N-acetylcysteine of the histopathological and cytogenetical damage produced by exposure of rats to cigarette smoke. *Cancer Lett*. 64(2), 123-131.

12. Givi, M.E., Blokhuis, B.R., Da Silva, C.A., Adcock, I., Garssen, J., Folkerts, G., Redegeld, F.A., and Mortaz, E. (2013) Cigarette smoke suppresses the surface expression of c-kit and FcεRI on mast cells. *Mediators Inflamm*. 2013, 813091.

13. Van Miert, E., Vanscheeuwijck, P., Meurrens, K., Gomm, W., and Terpstra, P.M. (2008) Evaluation of the micronucleus assay in bone marrow and peripheral blood of rats for the determination of cigarette mainstream-smoke activity. *Mutat Res*. 652(2), 131-138.

14. Knoll, M., Shaoulian, R., Magers, T., and Talbot, P. (1995) Ciliary beat frequency of hamster oviducts is decreased in vitro by exposure to solutions of mainstream and sidestream cigarette smoke. *Biol Reprod* 53, 29-37.

15. Knoll, M., and Talbot, P. (1998) Cigarette smoke inhibits oocyte cumulus complex pick-up by the oviduct in vitro independent of ciliary beat frequency. *Reprod Toxicol.* 12, 57-68

16. Sparks, N.R.L., Martinez I.K.C., zur Nieden, N.I. Lineage tracing and replicate analysis reveals low osteogenic yield in human induced pluripotent stem cells correlated with differential Twist1 expression. Stem Cells, under review

17. Davis, L.A., Dienelt, A., and zur Nieden, N.I. (2011) Absorption-based assays for the analysis of osteogenic and chondrogenic yield. *Methods Mol Biol*. 690, 255-272.

18. zur Nieden, N.I., Davis, L.A., and Rancourt, D.E. (2010) Comparing three novel endpoints for developmental osteotoxicity in the embryonic stem cell test. *Toxicol Appl Pharmacol.* 247(2), 91-97.

19. zur Nieden, N.I., and Baumgartner, L. (2010) Assessing developmental osteotoxicity of chlorides in the embryonic stem cell test. *Reprod Toxicol*. 30(2), 277-283.

20. Valavanidis, A., and Haralambous, E. (2001) A comparative study by electron paramagnetic resonance of free radical species in the mainstream and sidestream smoke of cigarettes with conventional acetate filters and 'bio-filters'. *Redox Rep*. 6(3), 161-171.

21. Neal, M.S., Hughes, E.G., Holloway, A.C., and Foster, W.G. (2005) Sidestream smoking is equally as damaging as mainstream smoking on IVF outcomes. *Hum Reprod*. 20(9), 2531-2535.

22. Lin, S., Fonteno, S., Weng, J.H., and Talbot, P. (2010) Comparison of the toxicity of smoke from conventional and harm reduction cigarettes using human embryonic stem cells. *Toxicol Sci*. 118(1), 202-212.

23. Lin, S., Tran, V., and Talbot, P. (2009) Comparison of toxicity of smoke from traditional and harm-reduction cigarettes using mouse embryonic stem cells as a novel model for preimplantation development. *Hum Reprod*. 24(2), 386-397.

24. Polyzos, A., Schmid, T.E., Piña-Guzmán, B., Quintanilla-Vega, B., and Marchetti, F. (2009) Differential sensitivity of male germ cells to mainstream and sidestream tobacco smoke in the mouse. *Toxicol Appl Pharmacol*. 237(3), 298-305.

25. Bibikova, M., Chudin, E., Wu, B., Zhou, L., Garcia, E.W., Liu, Y., Shin, S., Plaia, T.W., Auerbach, J.M., Arking, D.E., Gonzalez, R., Crook, J., Davidson, B., Schulz, T.C., Robins, A., Khanna, A., Sartipy, P., Hyllner, J., Vanguri, P., Savant-Bhonsale, S., Smith, A.K., Chakravarti, A., Maitra, A., Rao, M., Barker, D.L., Loring, J.F., and Fan, J.B. (2006) Human embryonic stem cells have a unique epigenetic signature. *Genome Res*. 16(9), 1075-1083.

26. Liu, Y., Shin, S., Zeng, X., Zhan, M., Gonzalez, R., Mueller, F.J., Schwartz, C.M., Xue, H., Li, H., Baker, S.C., Chudin, E., Barker, D.L., McDaniel, T.K., Oeser, S., Loring, J.F., Mattson, M.P., and Rao, M.S. (2006) Genome wide profiling of human embryonic stem cells (hESCs), their derivatives and embryonal carcinoma cells to develop base profiles of U.S. Federal government approved hESC lines. *BMC Dev Biol*. 6, 20.

27. Han, S., Auger, C., Thomas, S.C., Beites, C.L., and Appanna, V.D. (2014) Mitochondrial biogenesis and energy production in differentiating murine stem cells: a functional metabolic study. *Cell Reprogram*. 16(1), 84-90.

28. Wynder, E.L., and Graham, E.A. (1950) Tobacco smoking as a possible etiologic factor in bronchiogenic carcinoma; a study of 684 proved cases. *J Am Med Assoc*. 143(4), 329-336.

29. Doll, R., and Hill, A.B. (1952) A study of the aetiology of carcinoma of the lung. *Br Med J*. 2(4797), 1271-1286.

30. Hammond, E.C., and Horn, D. (1958) Smoking and death rates; report on forty-four months of follow-up of 187,783 men. I. Total mortality. *J Am Med Assoc*. 166(10), 1159-1172.

31. Thun, M.J., and Heath, C.W. Jr. (1997) Changes in mortality from smoking in two American Cancer Society prospective studies since 1959. *Prev Med*. 26(4), 422-426.

32. Hoffmann, D., and Hoffmann, I. (1997) The changing cigarette, 1950-1995. *J Toxicol Environ Health*. 50(4), 307-364.

33. Nayak, B.N., Ray, M., and Persaud, T.V. (1989) Maternal and fetal chromosomal aberrations in mice following prenatal exposure to subembryotoxic doses of lead nitrate. *Acta Anat* (Basel). 135(2), 185-188.

34. Fujinaga, M., Baden, J.M., and Mazze, R.I. (1989) Susceptible period of nitrous oxide teratogenicity in Sprague-Dawley rats. *Teratology*. 40(5), 439-444.

35. Sasaki, S., Sata, F., Katoh, S., Saijo, Y., Nakajima, S., Washino, N., Konishi, K., Ban, S., Ishizuka, M., and Kishi, R. (2008) Adverse birth outcomes associated with maternal smoking and polymorphisms in the N-Nitrosamine-metabolizing enzyme genes NQO1 and CYP2E1. *Am J Epidemiol*. 167(6), 719-726.

36. Zeman, C., Beltz, L., Linda, M., Maddux, J., Depken, D., Orr, J., and Theran, P. (2011) New questions and insights into nitrate/nitrite and human health effects: a retrospective cohort study of private well users' immunological and wellness status. *J Environ Health*. 74(4), 8-18.

37. Burns, D.M., and Benowitz, N.L. (2001). Public health implications of changes in cigarette design and marketing. In: US Department of Health and Human Services monograph 13, Risks associated with smoking cigarettes with low machine-measured yields of tar and nicotine, pp1-12.

38. Bowker, K.A., Lewis, S., Coleman, T., Vaz, L.R., and Cooper, S. (2014) Comparison of cotinine levels in pregnant women while smoking and when using nicotine replacement therapy. *Nicotine Tob Res*. 16(6), 895-898.

39. Hawkins, S.S., Dacey, C., Gennaro, S., Keshinover, T., Gross, S., Gibeau, A., Lulloff, A., and Aldous, K.M. (2014) Secondhand Smoke Exposure Among Nonsmoking Pregnant Women in New York City. *Nicotine Tob Res*. Mar 31. [Epub ahead of print]

40. Torjesen, I. (2014) Tobacco control policies should embrace harm reduction products, nicotine experts say. *BMJ*. 348, g3604.

Chapter 4: A Video-Based Assay as a Novel Method for Identifying Teratogenic Effects of Tobacco on Bone Development

Abstract

The 1st trimester of embryonic development is considered to be the period in which most of organ development occurs. Due to this intricate development and rapid growth, this period is also the most susceptible to teratogens or embryotoxicants. Typically, teratogens cause congenital diseases that affect an organism starting from birth. Thus, it is important to identify potential teratogens that are naturally found in the environment and could harm the developing embryo if exposed. In this paper, we developed a novel method of teratogenic testing for effects towards bone differentiation that takes advantage of innovations in microscopy and imaging technology and analysis. Using human embryonic stem cells undergoing osteogenesis as an *in vitro* model of embryonic bone development, we classified the teratogenic effects of commercially available conventional and harm-reduction tobacco products. Using the degree of calcification as a differentiation endpoint and confluency and debris count as endpoint for cell growth, both from time-lapse phase contrast images, we created a novel method to determine the teratogenic effects of tobacco smoke. Using this assay we have identified that sidestream smoke generated from tobacco smoke is more potent than mainstream smoke in inhibiting osteogenic differentiation, results that we have also obtained with a classic reagent-based assay. We have also determined that sidestream smoke is cytotoxic to differentiating osteogenic cultures as revealed by our novel method and verified by reagent method. Our results suggest that video-based analysis is equally

predictive as reagent-based testing of environmental toxicants, thus eliminating the need for the use of reagents and reducing the number of samples needed to perform the test. This method has a quicker turn-around time because it is more sensitive than conventional methods, allowing us to create a calcification curve as early as d10.

Introduction

In 1957, thalidomide has been widely prescribed to pregnant women to relieve symptoms of morning sickness [Franks et al, 2004]. This drug was later taken off the market in 1961 due to its teratogenic effects that resulted in serious birth defects in children whose mothers took thalidomide during their first trimester [Franks et al, 2004]. It was initially thought to be safe because this drug did not show any harmful effects in animal studies conducted with rats [Franks et al, 2004]. In this modern era, teratogenic studies are still being conducted using live animal models [Cook and Fairweather, 1968; Kochlar, 1980; Fantel, 1982; Schumann, 2010], along with *in vitro* methods testing with whole embryos from chicken [van der Valk and van der Meijden, 2014] and frogs [Kim et al, 2013; Casarini et al, 2007] and micromass test [Memon and Pratten, 2013; Hurst et al, 2009, Zou et al, 2012; Minta et al, 2005] and are slowly beginning to be replaced by stem cell assays, such as the embryonic stem cell test (EST) [de Jong et al, 2014; zur Nieden et al, 2004]. Most of these tests assess the teratogenicity of a chemical or drug in the developing embryo as a whole. However, teratogenesis can alter specific stages of development or distinct events during development, including skeletal deformities through defects in bone formation. Thus, a system that uses one type of endpoint to represent all different types of development in the body may not be sufficient.

We previously updated the EST to allow for direct comparison of effects of chemical compounds on human bone development. This was accomplished by substituting the mouse embryonic stem cell model with embryonic stem cells (ESCs) derived from human blastocysts [chapter 3]. Using human cells instead of those from the mouse will eliminate species-species differences during comparisons. In addition, we also modified the differentiation protocol of the original EST to yield osteogenic cells rather than cardiomyocyte cells. This allows the test to directly compare the perceived effects to the target process of bone development. This is important since an estimated 6000 babies in the United States are affected by musculoskeletal congenital birth defects each year. Most of these are due to exposure to environmental teratogens [zur Nieden et al, 2003; zur Nieden et al 2004]. One example of a prevalent environmental teratogen is cigarette or tobacco smoke.

In a previous study, we have used a human ESC-based EST to determine the teratogenic effects of different tobacco products on the differentiation of osteoblast, the cells responsible for secreting the bone matrix [chapter 3]. These results showed that sidestream smoke generated by from cigarettes was more harmful to osteogenic differentiation than the mainstream smoke, which burns off the tip of the cigarette. In addition, we found that harm-reduction products did not lower damage to bone health compared to conventional products of the same brand.

Teratogenic studies on bone differentiation, such as this, are performed using known and acceptable methods for quantifying calcium deposits, by emerging osteoblasts in culture, often through the use of chemical or reagent-based assays [zur Nieden et al, 2003; zur Nieden et al 2004]. This is also true when determining cell viability of the culture, the second endpoint in the EST, by assessing mitochondrial

health typically performed with an MTT assay. Although predictive, such reagent-based assays have some fundamental flaws. Since they require the sacrifice of the culture, calcification and MTT assay are performed from separate samples, yet the result of on assay is put into relation to the other. This can result in technical inaccuracies that affect the predictivity of the assay. In addition, the conventional reagent-based way of testing requires a substantial length of time and may include man-based errors.

We have previously demonstrated that we can reliably quantify calcium content in osteogenic cultures from time-lapse phase contrast images using video-based calcification tools [chapter 2]. In this study, our video-based assay was used to determine changes in hESCs as they differentiate into osteoblasts while exposed to tobacco products. In addition, an image based parameter was developed that allowed conclusions as to the viability of the cultures from the same image. Using this completely image-based automated method, we were able to confirm the results of our previous screen suggesting accuracy of the new method, while simultaneously reducing the length of the assay by 10 days.

Materials and Methods

hESC culture

The commercially available hESC H9 line was acquired from WiCell (WiCell Research Institute). The hESCs were maintained in mTeSR® medium (Stem Cell Technologies) and kept in an undifferentiated state at 37°C in a humid 5% CO_2 environment. Pluripotent colonies were passaged every 5 days upon reaching 70%

confluency. This is performed by dissociating cells with accutase and passages at a lower density on Matrigel (BD Biosciences) treated culture plates.

Osteogenic differentiation

Upon culture confluency, pluripotent colonies were induced to undergo osteogenesis with control differentiation medium of Dulbecco's modified Eagle's medium (DMEM; Gibco) containing 15% FBS (Atlanta), 1% non-essential amino acids (NEAA; Gibco), 1:200 penicillin/streptomycin (Gibco), and 0.1mM β-mercaptoethanol (Sigma) for 5 days as described (Sparks et al., 2014). Subsequently, control differentiation medium was supplemented with osteogenic factors: 0.1 mM β-glycerophosphate (βGP; Sigma), 50 µg/ml ascorbic acid (AA; Sigma), and $1.2x10^{-7}$ M $1,25(OH)_2$ Vitamin D_3 (VD3; Calbiochem).

Production of smoke solution

Commercially available popular conventional (Marlboro Red and Camel) and harm reduction (Marlboro Gold, Camel Blue, and American Spirits) brands of cigarettes were purchased from a local retail dealer and used to make mainstream (MS) and sidestream (SS) smoke solutions with a method described previously in detail (Knoll et al., 1995; Knoll and Talbot, 1998). Smoke solutions were generated using a University of Kentucky smoking machine that took a 2.2 second puff of MS every minute. MS smoke solution was generated by pulling 30 puffs of MS smoke through 10 ml of DMEM culture medium. During MS smoke production, SS smoke solution was produced by collecting

the smoke that burned off the end of the cigarette and pulling it through 10 ml of DMEM. SS smoke was collected continuously, while MS smoke was collected during each puff. Both MS and SS solutions were made at concentrations of 3 puff equivalents (PE). One PE of MS smoke is the amount of smoke in one puff that dissolves in 1 ml of culture medium. For SS smoke, one PE is the amount of SS smoke that dissolves in 1 ml of culture medium during one minute of burning. Immediately after preparation, smoke solutions were filtered through a 0.2 micron Acrodisc® PSF Syringe Filter (Pall Corporation, Port Washington, NY), aliquoted into sterile Eppendorf tubes, and stored in a -80°C freezer until used.

Desired PEs were acquired through serial dilutions and experiments were done using either MS or SS at concentrations as indicated and an untreated control. Osteogenic differentiation of hESCs was induced as described above and cultures were treated with smoke solutions through the 20 day duration of differentiation. Smoke solutions were replenished with each media change.

Osteogenic Viability assay

Viability was determined by 3-[4,5-dimethylthiazol-2-yl]-2,5-diphenylterazolium bromide (MTT) assay. Briefly, cells were incubated with MTT (120 mg/ml) at 37°C for 3 h. After the supernatant was removed, 0.04 mol/L HCl in isopropanol was added to each well and the optical density of the solution was read at 595 nm in an iMark™ microplate reader (BIO-RAD). As the generation of the blue product is proportional to the dehydrogenase activity, a decrease in the absorbance at 595 nm provided a measurement of the number of viable cells.

Calcium assay

For quantification of calcium in the cell matrix, cells were harvested in radioimmunoprecipitation (RIPA) buffer. Calcium deposition was determined based on calcium ions (Ca^{2+}) reacting with Arsenazo III (Genzyme) to form a purple Ca-Arsenazo III complex, which was measured at 655 nm. The concentration of total calcium in the sample was calculated based on a $CaCl_2$ standard (Davis et al., 2011) an then normalized to the total protein content of the sample from RIPA protein using the Lowry method (Davis et al., 2011).

Image acquisition

Differentiating cultures were placed inside the Nikon Biostation CT, a hybrid and automated incubator that contains a phase contrast microscope and maintains the culture at 37^{o}C with 5% CO_2. Phase contrast images were taken every 12h for a period of 15 to 20 days from 10 separate areas within the culture plate. Images were assembled to create time-lapse videos.

Image analysis

Time lapse videos were analyzed using Matrix Laboratory (MatLab) program, designed to automatically segment calcified areas from the individual phase contrast images from the time-lapse video using a manual threshold for pixels with an intensity value of 33 or less. These pixels were removed to create segmented images of calcified

regions. Remaining pixels were counted to quantify the degree of calcification from each image. Concentration response curves for tobacco toxicants were obtained by normalizing the calcium pixel counts of each concentration at t_x from a treated sample with the calcified pixel counts at t_x from an untreated sample represented as percentage. The amount of calcified pixels from each video image at t_x were subtracted from the amount of calcified pixels at t_0 and divided by the hours of elapsed time to determine the calcification rate.

Confluency was calculated by segmenting areas that composes cellular colonies. This was obtained by detecting edges of the colonies and filling in areas within the colonies. Confluency is represented as percent coverage by counting the total number of pixels segmented as part of the colonies for each image and normalizing it to the total number of pixels for the image. Debris counts were obtained by segmenting debris using the same edge detection program and combining it with size exclusion of objects that were less than 1000 pixels. These objects were counted in all the time-lapse images and normalized against untreated samples.

Results

Video-Based Assessment of Cytotoxic Effects of Tobacco Products on Cell Viability of Osteogenic Cultures

In a typical EST, the MTT assay is used to assess the viability of a given cell culture treated with a chemical compound. Reduced viability can be a product of different cellular processes, such as increased cell death, lower metabolism, reduced

cell growth or reduced survival. From images, we are able to capture information on the formation of cellular debris, a typical by product of cell death in cultures, and confluency, the ability of cells to divide and completely cover a given area in a plate. Thus, these two parameters were used to assess the effects of mainstream and sidestream smoke of different tobacco products on cell survival of osteogenic cultures. These chemical blends were chosen for testing, since we have a comprehensive prior test set that we had acquired with the MTT assay.

In pursuance of a method to quantify the amount of debris that forms during osteogenic differentiation, debris was segmented from the images using object-based classification through debris size. Since debris is typically smaller in size compared to non-adherent cells on the culture dish, the program was able to differentiate between floating debris versus living cells. Comparison of debris formation as a result of treatment with mainstream and sidestream smoke solution from conventional and harm-reduction tobacco product is shown in Fig 1. Debris formation from osteogenic cultures as a result of exposure to mainstream smoke showed no change in debris formation at any concentration tested (Fig. 1A-E). This suggests that exposure to mainstream smoke was not cytotoxic to osteogenically differentiating hESCs. However, exposure of cells to sidestream smoke revealed an increased susceptibility towards this second type of smoke (Fig 1F-J). For example, the Marlboro and Marlboro Gold products showed increased debris formation at 0.3 and 0.1PE. Camel and Camel Blue brands, as well as American Spirits, showed higher debris counts than the untreated control at 0.3 PE. These results suggest that sidestream smoke is more potent than mainstream smoke in inducing cytotoxicity, a result that we have also obtained with our conventional screen (see chapter 3).

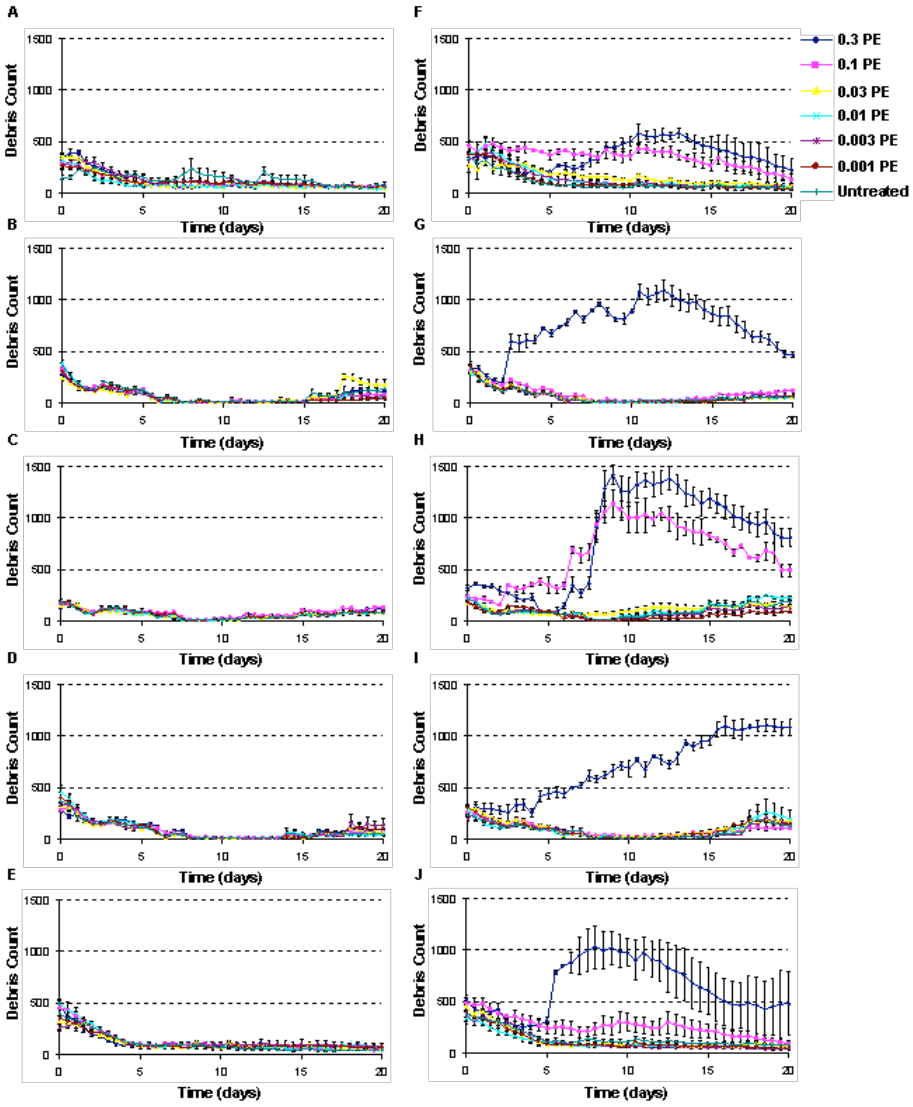

Fig 1 Effects of tobacco product on cell death of osteogenic cultures. Cell death were determined by formation of cellular debris during the culture from time-lapse images. Cellular debris were segmented by size. Debris were defined as aggregation of pixels of about 1000 pixels. Each debris were counted and plotted in the graphs above. Time-lapse images were obtained from tobacco-treated osteogenic culture using mainstream and sidestream smoke from varying tobacco products. Time-lapse images were taken every 12h for a period of 20d. Each experiment is composed of 10 video analyzed. Experiments conducted in triplicates. Data shown are average of 3 experimental replicates. Mainstream treatments are displayed in Fig 6 A-E. Side-stream treatments are shown in Fig 6 F-J. Conventional tobacco products tested are Marlboro Red (A, F), Camel (B,G), and harm-reduced versions are Marlboro Gold (C,H), Camel Blue (D, I), and American Spirits (E).

Debris formation is a feature that may result from increases in apoptosis and therefore can only indirectly infer cell viability. Hence, it is still necessary to utilize a feature that can directly convey viability, such as confluency. In this endpoint, mainstream smoke showed no changes in confluency in any concentrations tested compared to untreated cultures (Fig. 2A-E). As expected from the result of the debris formation analysis brands such as Camel, Camel Blue, American Spirit showed a reduction in confluency at the 0.3 PE concentration of sidestream smoke (Fig. 2F-J). Marlboro and Marlboro Gold revealed to be more cytotoxic compared to the other brands tested as both products showed a decrease in confluency at concentrations as low as 0.1PE of sidestream smoke. This result confirms the idea that sidestream smoke to be more detrimental to cell survival compared to mainstream smoke. These outcome are similar to those that was obtained using a MTT assay, a conventional reagent-based method. Taken together both novel types of viability assessment from images can accurately predict cytotoxicity of tobacco products.

Video-Based Analysis of Effect on Functional Properties of Developing Osteoblasts Treated with Cigarette Smoke from Conventional and Harm Reduction Tobacco Products

Calcification and mineralization of the extracellular matrix are the most fundamental properties of osteoblasts. Previously, we have developed a program that can automatically segment and quantify calcified regions on images and time-lapse videos based on signature appearance and dense black aggregation in the image (chapter 2). In that study, our video-based calcification assay was utilized to assess any

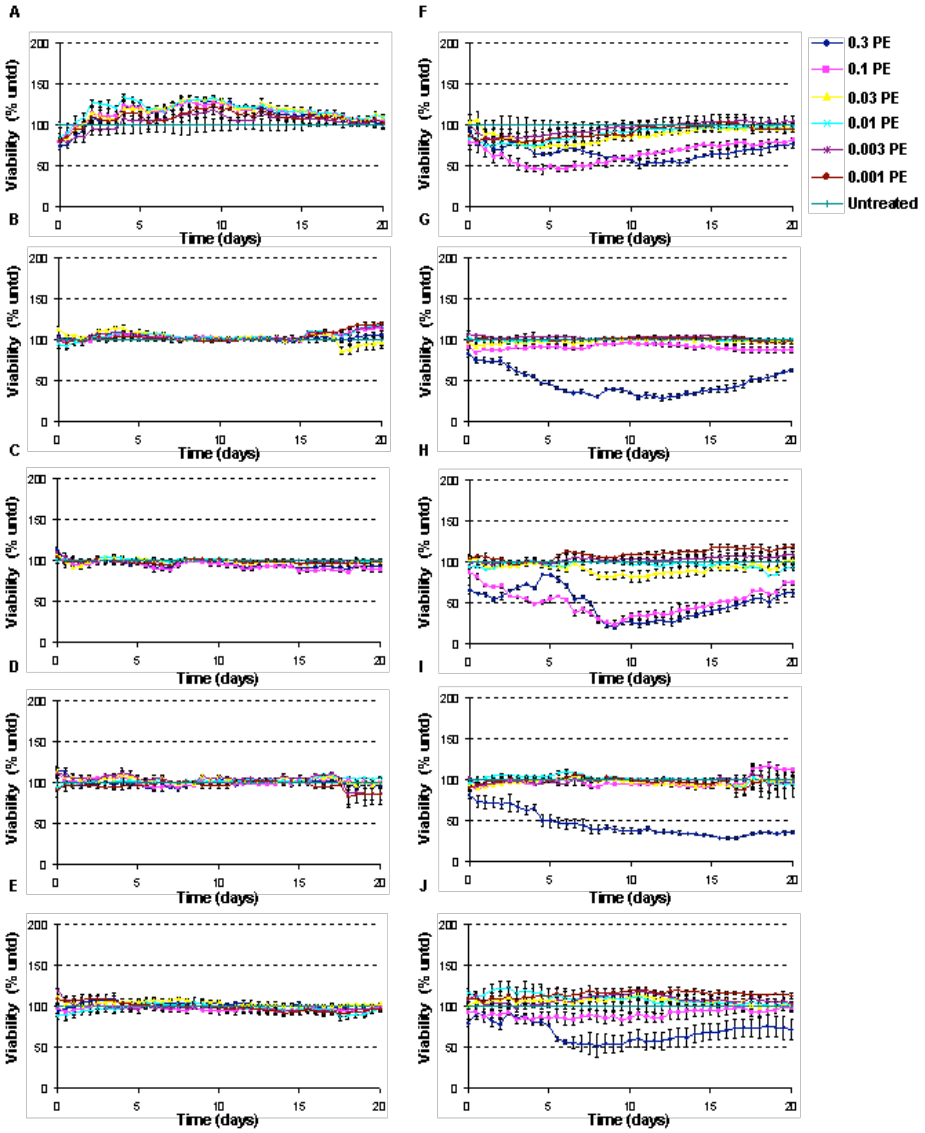

Fig 2 Effects to tobacco product on cell growth of osteogenic culture. Image based assessment of percent confluence of culture on osteogenic culture in the presence of varying concentration from 2 different types smoke solution from several tobacco products. Confluence were determined by segmenting area from time-lapse images. Time lapse images were generated obtained from tobacco treated cultures every 12h for a total of 20 days.Each experiment is composed of 10 time-lapse video for each concentration tested. Experiments were conducted in triplicate. Mainstream treatments are displayed in Fig 6 A-E. Side-stream treatments are shown in Fig 6 F-J. Conventional tobacco products tested are Marlboro Red (A, F), Camel (B,G), and harm-reduced versions are Marlboro Gold (C,H), Camel Blue (D, I), and American Spirits (E,J).

changes in the functional capabilities of developing osteoblasts that has been exposed to whole tobacco extract, or N'-nitrosonornicotine (NNN). Here, we apply this technique to determine the overall calcification and calcification rate from cultures treated with different concentrations of smoke solutions.

Mainstream smoke treatment did not exhibit any changes in the amount of calcification compared to the untreated cultures (Fig. 3A-E). However, the sidestream treatment showed concentrations that are inhibitory to proper osteogenic maturation of osteoblasts: Camel, Camel Blue, and American Spirit showed no measurable calcification at 0.3PE. Marlboro and Marlboro Gold demonstrated no measurable calcification at 0.3PE and 0.1PE, as measured by our video-based calcification assay. Concentrations below 0.1PE for Marlboro and Marlboro Gold, as well as concentrations below 0.3PE for Camel, Camel Blue, and American Spirit showed no significant changes in calcification. Nonetheless, a notable increase in calcification was noticed on sidestream treated osteogenic culture from products, such as Camel, Camel Blue and Marlboro Gold. These increases appear to be most noticeable at the end of the test period and appear to be associated with the highest concentration prior to the lowest lethal concentration for that particular tobacco product.

Calcification rate is a novel parameter that can be quantified using this video-based calcification assay. Our previous studies have suggested that calcification rate adds another dimension for analyzing changes in functional property, which makes this video-based calcification more superior than looking at calcification alone. Mainstream smoke treatment did not produce data suggesting any perturbation on calcium kinetics (Fig. 4A-E). All concentrations tested showed similar kinetic profiles as the untreated control. As expected from data displayed in Figs 1-3, sidestream smoke showed no

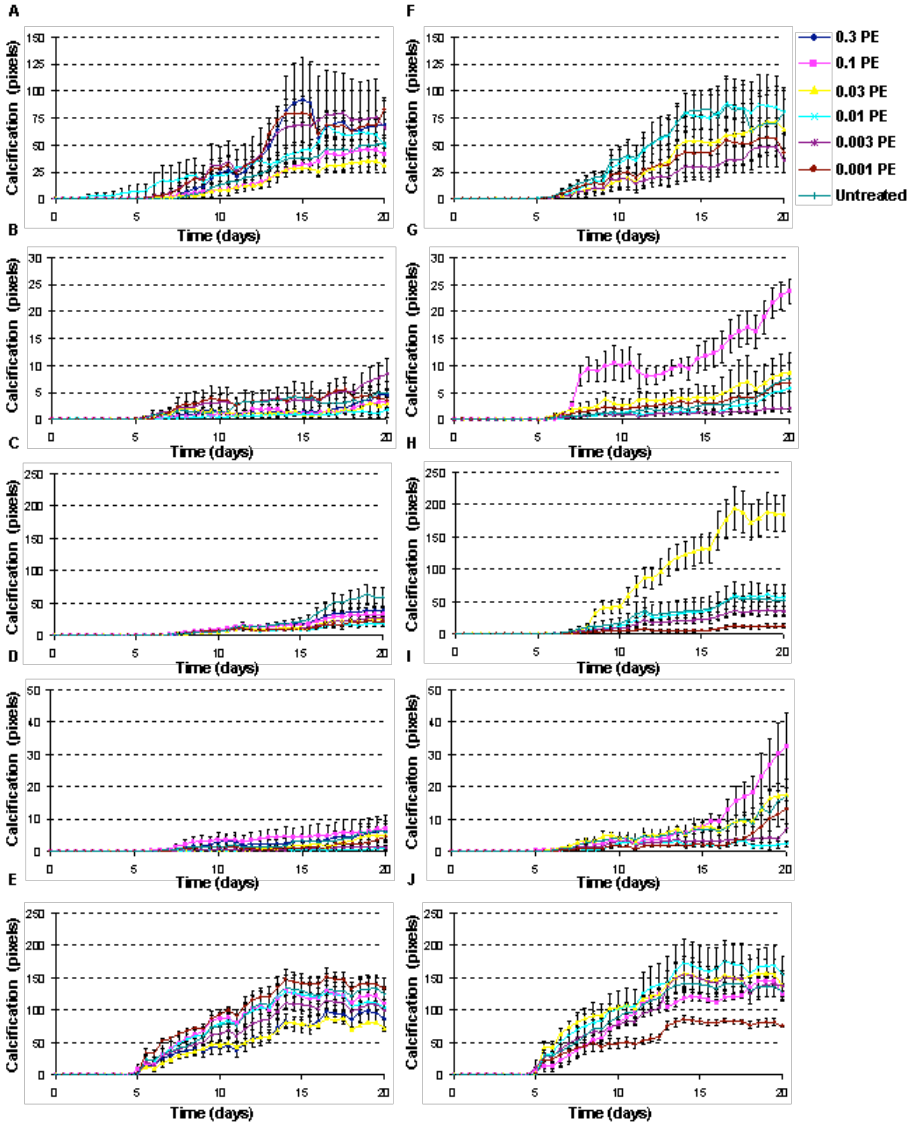

Fig 3. Effects of Tobacco Products on Osteoblasts Calcification. Calcification measurements were measure from time-lapse images of tobacco-treated osteogenic cultures. Cultures were imaged every 12 h for a period of 20 days. Each measurements were obtained from 10 sample videos. Calcified regions were segmented by manual threshold for pixels with a value of 33 or less, counted and ploted on the graph. Experiments were performed in triplicate. Mainstream treatments are displayed in Fig 6 A-E. Side-stream treatments are shown in Fig 6 F-J. Conventional tobacco products tested are Marlboro Red (A, F), Camel (B,G), and harm-reduced versions are Marlboro Gold (C,H), Camel Blue (D, I), and American Spirits (E,J).

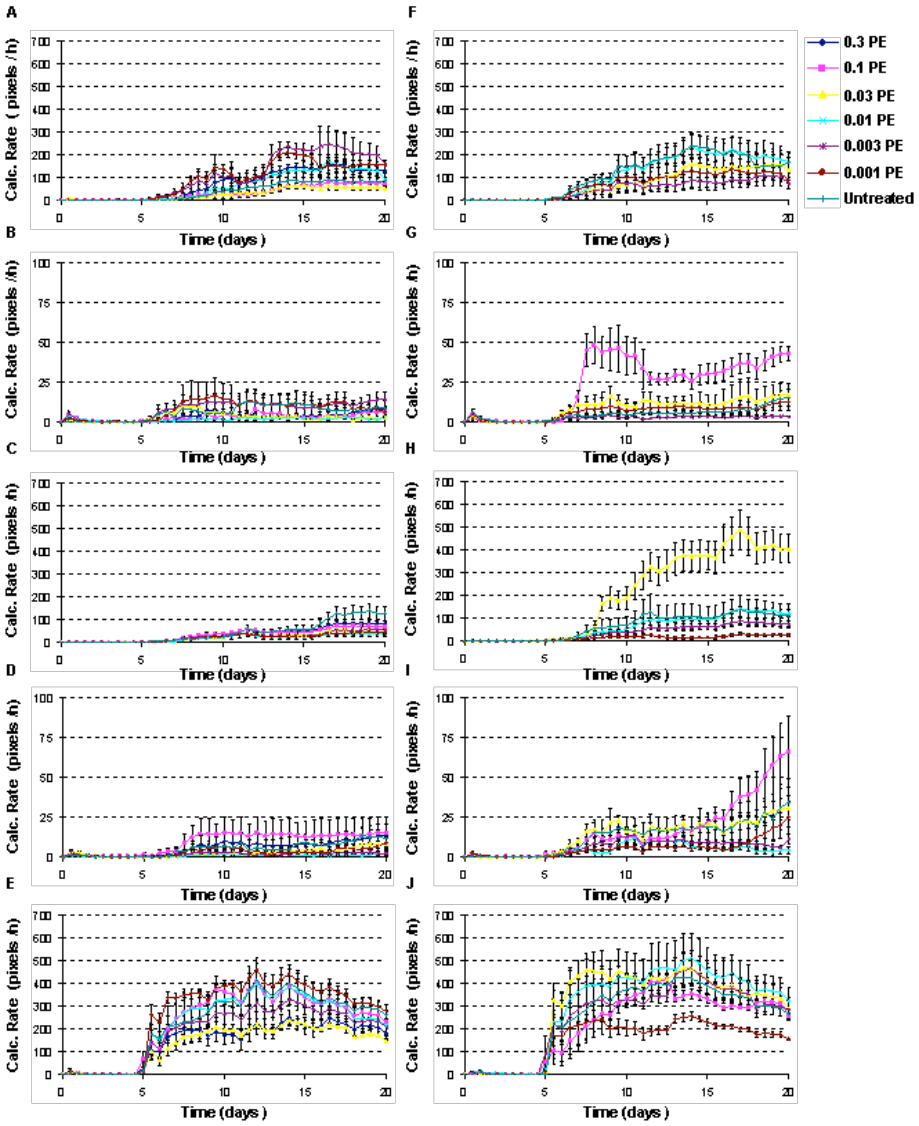

Fig 4. Calcification rate of tobacco-treated osteogenic culture. Osteogenic culture were treated with varying concentrations of tobacco and subjected to time-lapse imaging. Images were obtained every 12h for a treatment period of 20d. Calcified regions were quantified from each images. The rate of calcium deposition were determined by the change in amount of calcification over the amount of time it took for the change. Each measurements were determined from 10 samples. The experiments were repeated as a triplicate. Mainstream treatments are displayed in Fig 6 A-E. Side-stream treatments are shown in Fig 6 F-J. Conventional tobacco products tested are Marlboro Red (A, F), Camel (B,G), and harm-reduced versions are Marlboro Gold (C,H), Camel Blue (D, I), and American Spirits (E,J)

observable calcium rate at concentrations that showed decrease in viability and no measurable calcification.

However, as shown in Fig. 4G, H, and I, some tobacco products showed higher observable levels of calcification rate prior to lethal levels of sidestream smoke. This suggests that the increase in calcification endpoint measurement might be due to an increased rate of calcification. Taken together, our data suggests that calcification is reduced in the sidestream smoke treated from different tobacco products. These calcification data suggest that video-based calcification assay can be used to determine differentiation inhibition as a result of toxicant treatment, such as tobacco.

Novel Video-based Assays Reduce Length to Analysis

From the kinetic analysis of viability and calcification shown in Figs. 1-4, it became apparent that changes were already observable as early as d10 of differentiation. Therefore, calcification and viability values from d10 were utilized to create both a calcification curve and viability curve, in order to determine ID_{50} and IC_{50} values, respectively. Comparison of the ID_{50}, the concentration of treatment that reduced calcification output by 50%, and IC_{50}, the concentration that reduced viability by 50%, obtained from both types of smoke studied, allowed us to categorize the smoke to show no observable effect (NOE), a cytotoxic effect (CYT) and a teratogenic effect (TER). This categorization is shown in table 1 and the video-based teratogenicity assay is displayed in Fig. 5. Mainstream Smoke treatment showed no effect on cell survival and functionality (Fig. 5A-E). This is true for both the conventional products as well as the

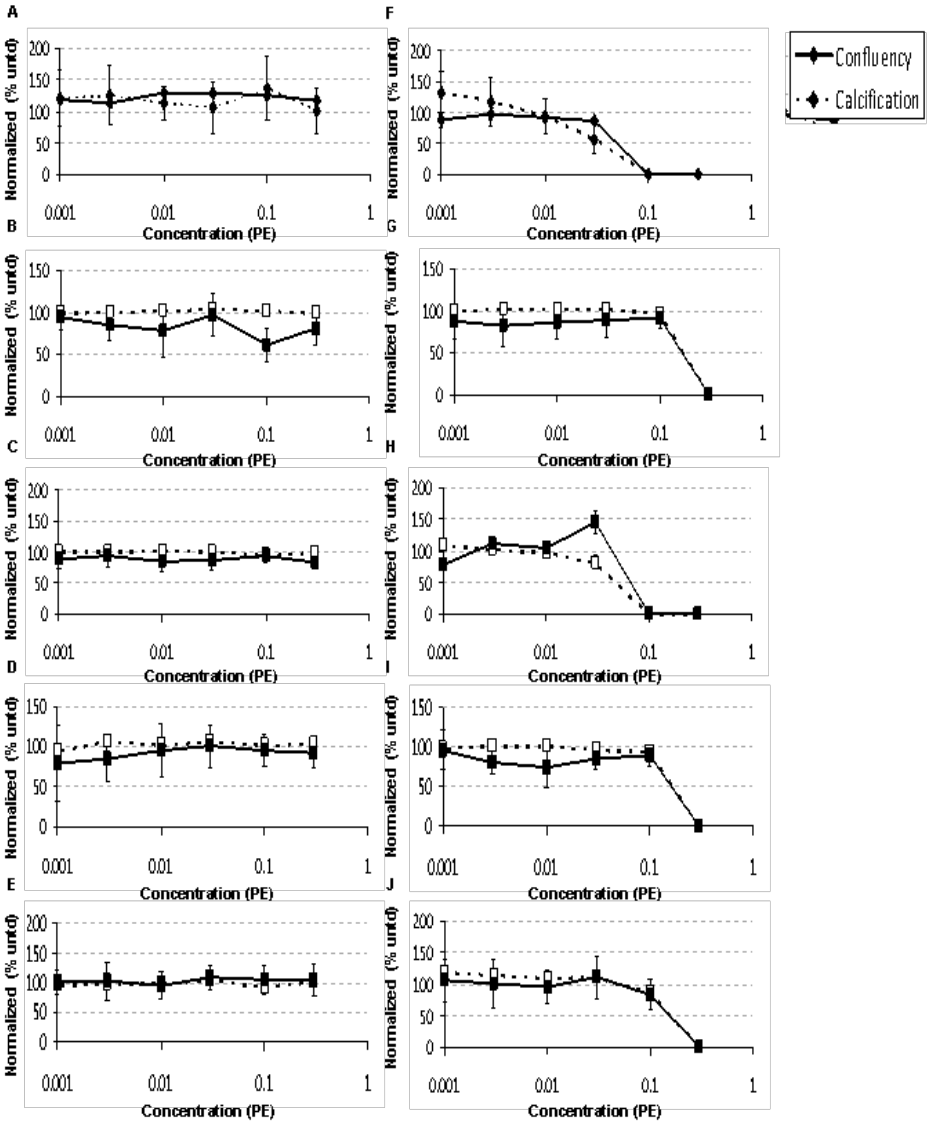

Fig 5 Cytotoxic and teratogenic effects of tobacco products on bone development. Dose-dependent curves were generated to determine effects of various tobacco products on the functional properties of developing bone (calcification) and their overall viability (confluency). Data were taken from day 10 measurements from time-lapse video based data. Measurement for calcium content (black line) was based on quantification of pixels composed of calcified areas in an image. Confluence (dash line) was determined as percent of the area in an image composed of live cell culture. Treated-samples were normalized against untreated control and expressed as %untreated. Mainstream treatments are displayed in Fig 5 A-E. Side-stream smoke treatments are shown in Fig. 5 F-J. Conventional tobacco products tested were Marlboro Red (A, F), Camel (B,G), and harm-reduced versions were Marlboro Gold (C,H), Camel Blue (D, I), and American Spirits (E,J).

		MS			SS		
Type of tobacco	**Brand**	**IC_{50}**	**ID_{50}**	**Toxicity**	**IC_{50}**	**ID_{50}**	**Toxicity**
Conventional	*Marlboro*	Unable to determine	Unable to determine	N/A	0.05	0.04	Cytotoxic
	Camel	Unable to determine	Unable to determine	N/A	0.17	0.17	Cytotoxic
Additive-free	*American Spirit*	Unable to determine	Unable to determine	N/A	0.17	0.16	Cytotoxic
Harm-reduction (less tar/less nicotine)	*Marlboro Gold*	Unable to determine	Unable to determine	N/A	0.05	0.08	Cytotoxic
	Camel Blue	Unable to determine	Unable to determine	N/A	0.17	0.17	Cytotoxic

Table 1: List of IC_{50} and ID_{50} values determined from concentration-response curves for all tobacco products grouped by mainstream and sidestream smoke (cigarettes) .

harm-reduction versions. Thus, we are unable to identify a proper ID_{50} and IC_{50} from this smoke type for any brands tested.

In contrast, exposure of osteogenic cultures to sidestream smoke revealed cytotoxic effects of both conventional (Fig 5 F,G) and harm-reduction products (Fig 5 H,I,J) on osteoblast development. The IC_{50} and ID_{50} curve of the sidestream treatment for all products tested are similar to each other. This suggests that the effect on osteoblasts differentiation exhibited by sidestream smoke treatment is cytotoxic. This means that the decrease in calcification output is due to decrease in viable osteoblasts.

Furthermore, we compared these results from the teratogenicity test that was obtained using our video-based teratogenicity assay with the reagent-based assays used in our previous study in order to determine the predictivity of the entirely video based assay (Fig. 6). Since mainstream smoke did not show and observable effect on calcification and cell survival (Table 1), we opted to display graphical representation the results from the sidestream smoke treatment only. Comparison of both calcification curves (Fig. 6A-E) from the video-based assay and the reagent-based assay showed

similar curves. This is also true for the viability curves obtained by both methods (Fig. 6F-J). Comparison of the results of the video based confluency assay and the reagent based MTT assay showed a closer similarity in results compared to the calcification assay presented above. Taken together, this novel method of determining teratogenicity and comparing it to more well-established reagent-based assays suggests that this video-based teratogenicity assay is a viable alternative to previously known assays.

Discussion

We demonstrate here an innovative and powerful use of video-based analysis to determine the teratogenic effects of tobacco products on the differentiation of osteoblasts. Currently, there are several ways to determine teratogenicity of a given chemical or toxicant. These methods rely on the use of animal models of human diseases or organs, immortalized cell lines, stem cells, and clinical trials [Ko and Gelb, 2014]. These methods can be controversial, such as the requirement for animal sacrifice [Cook and Frank, 1968, Kochhar, 1980; Fantel, 1982; Schumann,2010] or be monetarily expensive, an example is the use of animal trials that requires a large amount of animal samples. It has been debated that the use of human immortalized cell lines or stem cells might be a better model for human development, than animal studies [de Jong et al, 2014, zur Nieden et al, 2004, Seiler and Speilmann, 2011]. In this study, we took advantage of current techniques in toxicology to determine the teratogenic effects of tobacco on bone differentiation.

By modifying the traditional EST [Seiler and Speilmann, 2011] for the use with human embryonic stem cells, we were able to directly predict teratogenicity as detected

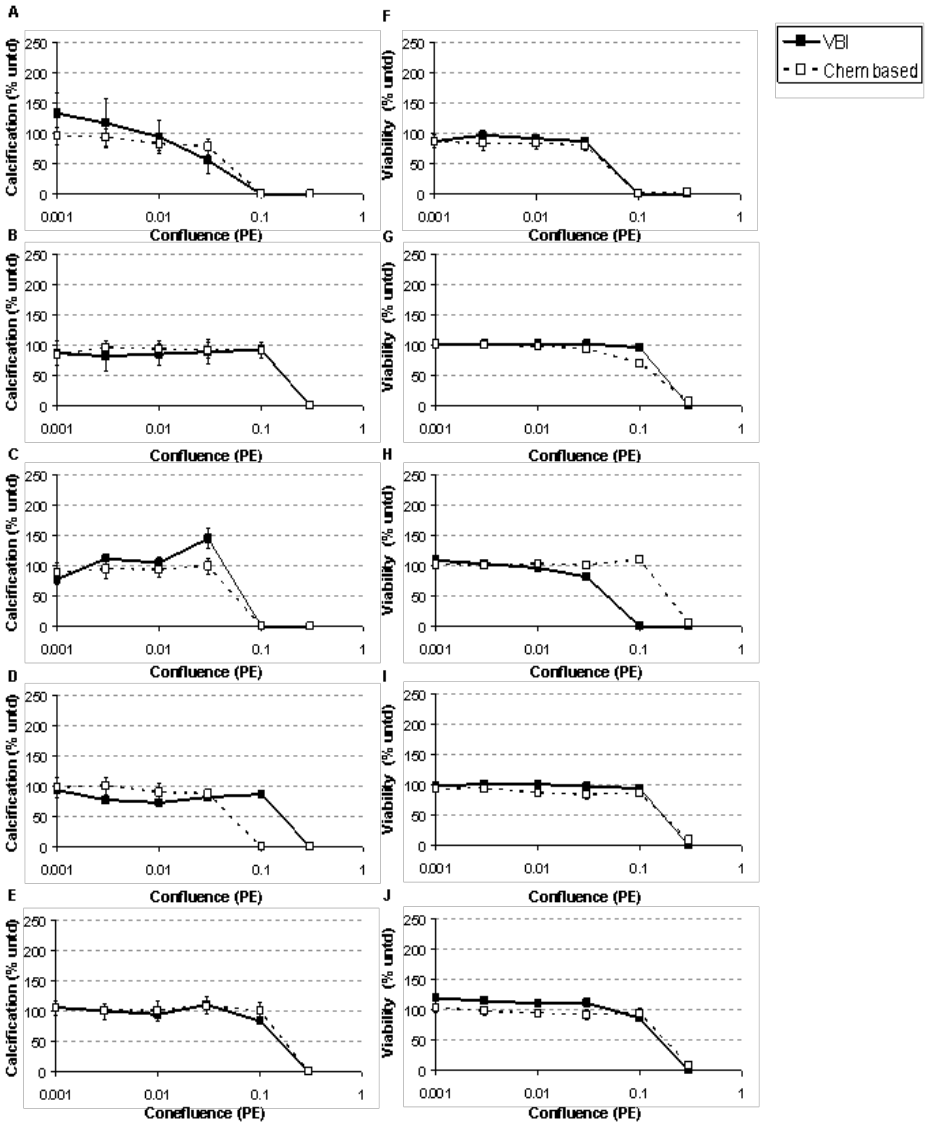

Fig 6: Comparison of dose-dependent calcification curve and viability curve from video-based and reagent based assays. Video-based measurements are represented in black lines and reagent based measurements are shown in dash lines. Comparison of the two teratogenicity assay compared measurements from side-stream smoke treatment from different tobacco products. Calcification curves were displayed in Fig 6 A-E. Viability curve is shown in Fig 6 F-J. Conventional tobacco products tested are Marlboro Red (A, F), Camel (B,G), and harm-reduced versions are Marlboro Gold (C,H), Camel Blue (D, I), and American Spirits (E,J).

in culture to that of *in vivo*, without being concerned about the compounding effects of species to species variation [Franks, 2004]. Directing differentiation of stem cells into osteoblasts, as opposed to the typical cardiomyocyte differentiation, from ESCs has allowed us to directly determine the effects of tobacco on the actual process of bone development [chapter 3]. This modification of the EST represents a vast improvement because it allows interpolation of the *in vitro* data directly to effects on human bone differentiation.

The conventional EST uses reagent-based assays, but these assays are often very time-consuming, require numerous samples for testing, and are expensive. The novel video-based teratogenicity assay developed here has combined the use of human cells and image analysis resulting in several advantages over conventional test methods. For example, video-based assays require less processing time because of their ability to measure changes kinetically, while the reagent based EST typically requires 20 days for testing a chemical. This suggests that the image-based method is more sensitive at determining changes between treated and untreated sample compared to the reagent-based assay.

Furthermore, this assay requires less sample needed to accomplish the assay and reduces variation when comparing calcification (ID_{50}) to viability (IC_{50}). Moreover, the video-based method includes additional parameters for identifying changes in viability and calcification, such as debris count and calcification rate, respectively. This suggests that more characterization can be performed using video-based assay without requiring the use of more samples and comparisons can be done in the same sample resulting in more accurate comparisons. Lastly, since less samples are required to

perform the necessary assays, the assay is expected to be less expensive, because of the reduction in requirement for media and material.

In summary, the video-based assay to establish teratogenic and cytotoxic effects of chemicals on human bone differentiation is highly advantageous over conventional assays. It is a multi-parameter assay, does not require the sacrifice of the culture, and is cost-effective. Its components are versatile and therefore can be easily performed in labs that do not have the equipment used here. Lastly, this method is equally predictive as conventional reagent based assays, at half the time required to perform the test.

References

1. Franks ME, Macpherson GR, Figg WD. Thalidomide. Lancet. 2004 May 29;363(9423):1802-11
2. Margaret J. Cook and Frank A. Fairweather. Methods used in teratogenic testing *Lab Anim October 1, 1968 2: 219-228*
3. Kochhar DM. In vitro testing of teratogenic agents using mammalian embryos. Teratog Carcinog Mutagen. 1980;1(1):63-74.
4. Fantel AG. Culture of whole rodent embryos in teratogen screening. Teratog Carcinog Mutagen. 1982;2(3-4):231-42.
5. Schumann J. Teratogen screening: state of the art. Avicenna J Med Biotechnol. 2010 Jul;2(3):115-21.
6. van der Valk T, van der Meijden A. Toxicity of scorpion venom in chick embryo and mealworm assay depending on the use of the soluble fraction versus the whole venom. Toxicon. 2014 Sep;88:38-43.
7. Kim M, Son J, Park MS, Ji Y, Chae S, Jun C, Bae JS, Kwon TK, Choo YS, Yoon H, Yoon D, Ryoo J, Kim SH, Park MJ, Lee HS. *In vivo* evaluation and comparison of developmental toxicity and teratogenicity of perfluoroalkyl compounds using Xenopus embryos. Chemosphere. 2013 Oct;93(6):1153-60.
8. Casarini L, Franchini A, Malagoli D, Ottaviani E. Evaluation of the effects of the marine toxin okadaic acid by using FETAX assay. Toxicol Lett. 2007 Mar 8;169(2):145-51.

9. Memon S, Pratten M. Effects of multivitamins and known teratogens on chick cardiomyocytes micromass culture assay. Iran J Basic Med Sci. 2013 Sep;16(9):996-1003.
10. Hurst H, Clothier RH, Pratten M. An evaluation of the chick cardiomyocyte micromass system for identification of teratogens in a blind trial. Reprod Toxicol. 2009 Dec;28(4):503-10.
11. Zou P, Xing L, Tang Q, Liu R, Hao W. Comparative evaluation of the teratogenicity of genistein and genistin using rat whole embryo culture and limbud micromass culture methods. Food Chem Toxicol. 2012 Aug;50(8):2831-6.
12. Minta M, Wilk I, Zmudzki J. Inhibition of cell differentiation by quinolones in micromass cultures of rat embryonic limb bud and midbrain cells. Toxicol In Vitro. 2005 Oct;19(7):915-9.
13. de Jong E, van Beek L, Piersma AH. Comparison of osteoblast and cardiomyocyte differentiation in the embryonic stem cell test for predicting embryotoxicity *in vivo*. Reprod Toxicol. 2014 Sep;48:62-71.
14. zur Nieden NI, Kempka G, Ahr HJ. Molecular multiple endpoint embryonic stem cell test--a possible approach to test for the teratogenic potential of compounds. Toxicol Appl Pharmacol. 2004 Feb 1;194(3):257-69.
15. Seiler AE, Spielmann H. The validated embryonic stem cell test to predict embryotoxicity in vitro. Nat Protoc. 2011 Jun 16;6(7):961-78.
16. Rogers JM. Tobacco and pregnancy. Reprod Toxicol. 2009 Sep;28(2):152-60.
17. Jauniaux E, Burton GJ. Morphological and biological effects of maternal exposure to tobacco smoke on the feto-placental unit. Early Hum Dev. 2007 Nov;83(11):699-706.

18. Hernández-Martínez C, Arija Val V, Escribano Subías J, Canals Sans J. A longitudinal study on the effects of maternal smoking and secondhand smoke exposure during pregnancy on neonatal neurobehavior. Early Hum Dev. 2012 Jun;88(6):403-8.

19. Wang Y, Ji J, Liu YJ, Deng X, He QQ. Passive smoking and risk of type 2 diabetes: a meta-analysis of prospective cohort studies. PLoS One. 2013 Jul 26;8(7):e69915.

20. Östenson CG, Hilding A, Grill V, Efendic S. High consumption of smokeless tobacco ("snus") predicts increased risk of type 2 diabetes in a 10-year prospective study of middle-aged Swedish men. Scand J Public Health. 2012 Dec;40(8):730-7.

21. Ospelt C, Camici GG, Engler A, Kolling C, Vogetseder A, Gay RE, Michel BA, Gay S. Smoking induces transcription of the heat shock protein system in the joints. Ann Rheum Dis. 2014 Jul;73(7):1423-6.

22. Lee J, Jeong H, Park EJ, Hwang JW, Bae EK, Ahn JK, Ahn KS, Koh EM, Cha HS. A role for benzo[a]pyrene and Slug in invasive properties of fibroblast-like synoviocytes in rheumatoid arthritis: a potential molecular link between smoking and radiographic progression. Joint Bone Spine. 2013 Dec;80(6):621-5.

23. Agnihotri R, Gaur S. Implications of tobacco smoking on the oral health of older adults. Geriatr Gerontol Int. 2014 Jul;14(3):526-40.

24. Morse DE, Avlund K, Christensen LB, Fiehn NE, Molbo D, Holmstrup P, Kongstad J, Mortensen EL, Holm-Pedersen P. Smoking and drinking as risk indicators for tooth loss in middle-aged Danes. J Aging Health. 2014 Feb;26(1):54-71.

25. Baljoon M. Tobacco smoking and vertical periodontal bone loss. Swed Dent J Suppl. 2005;(174):1-62.

26. Ayo-Yusuf OA, Olutola BG. Epidemiological association between osteoporosis and combined smoking and use of snuff among South African women. Niger J Clin Pract. 2014 Mar-Apr;17(2):174-7.

27. Iqbal J, Sun L, Cao J, Yuen T, Lu P, Bab I, Leu NA, Srinivasan S, Wagage S, Hunter CA, Nebert DW, Zaidi M, Avadhani NG. Smoke carcinogens cause bone loss through the aryl hydrocarbon receptor and induction of Cyp1 enzymes. Proc Natl Acad Sci U S A. 2013 Jul 2;110(27):11115-20.

28. Daniel AB, Shah H, Kamath A, Guddettu V, Joseph B. Environmental tobacco and wood smoke increase the risk of Legg-Calvé-Perthes disease. Clin Orthop Relat Res. 2012 Sep;470(9):2369-75.

29. Brook JS, Balka EB, Zhang C. The smoking patterns of women in their forties: their relationship to later osteoporosis. Psychol Rep. 2012 Apr;110(2):351-62.

30. Akhter MP, Lund AD, Gairola CG. Bone biomechanical property deterioration due to tobacco smoke exposure. Calcif Tissue Int. 2005 Nov;77(5):319-26.

31. Zimmermann G, Henle P, Küsswetter M, Moghaddam A, Wentzensen A, Richter W, Weiss S. TGF-beta1 as a marker of delayed fracture healing. Bone. 2005 May;36(5):779-85.

32. Moghaddam-Alvandi A, Zimmermann G, Hammer K, Bruckner T, Grützner PA, von Recum J. Cigarette smoking influences the clinical and occupational outcome of patients with tibial shaft fractures. Injury. 2013 Nov;44(11):1670-1.

33. Sloan A, Hussain I, Maqsood M, Eremin O, El-Sheemy M. The effects of smoking on fracture healing. Surgeon. 2010 Apr;8(2):111-6.

34. Moghaddam A, Weiss S, Wölfl CG, Schmeckenbecher K, Wentzensen A, Grützner PA, Zimmermann G. Cigarette smoking decreases TGF-b1 serum concentrations after long bone fracture. Injury. 2010 Oct;41(10):1020-5.

35. Martinez IKC, Sparks N, Talbot P, zur Nieden NI. Harm-reduction Tobacco Products are More Teratogenic to Differentiating Osteoblasts than Conventional Products.

36. zur Nieden NI, Kempka G, Ahr HJ. In vitro differentiation of embryonic stem cells into mineralized osteoblasts. Differentiation. 2003 Jan;71(1):18-27.

37. Buttery LD, Bourne S, Xynos JD, Wood H, Hughes FJ, Hughes SP, Episkopou V,Polak JM. Differentiation of osteoblasts and in vitro bone formation from murine embryonic stem cells. Tissue Eng. 2001 Feb;7(1):89-99.

38. Sottile V, Thomson A, McWhir J. In vitro osteogenic differentiation of human ES cells. Cloning Stem Cells. 2003;5(2):149-55.

39. Ding H, Keller KC, Martinez IK, Geransar RM, zur Nieden KO, Nishikawa SG,Rancourt DE, zur Nieden NI. NO-β-catenin crosstalk modulates primitive streak formation prior to embryonic stem cell osteogenic differentiation. J Cell Sci. 2012 Nov 15;125(Pt 22):5564-77.

40. Gao Q, Guo M, Jiang X, Hu X, Wang Y, Fan Y. A cocktail method for promoting cardiomyocyte differentiation from bone marrow-derived mesenchymal stem cells. Stem Cells Int. 2014;2014:162024.

41. Gunewardene N, Bergen NV, Crombie D, Needham K, Dottori M, Nayagam BA. Directing human induced pluripotent stem cells into a neurosensory lineage for auditory neuron replacement. Biores Open Access. 2014 Aug 1;3(4):162-75.

42. Lee LH, Tambasco M, Otsuka S, Wright A, Klimowicz A, Petrillo S, Morris D, Magliocco A, Bebb DG. Digital differentiation of non-small cell carcinomas of the lung by the fractal dimension of their epithelial architecture. Micron. 2014 Jul 28;67C:125-131.

43. Smith ZJ, Gao T, Chu K, Lane SM, Matthews DL, Dwyre DM, Hood J, Tatsukawa K, Heifetz L, Wachsmann-Hogiu S. Single-step preparation and image-based counting of minute volumes of human blood. Lab Chip. 2014 Aug 21;14(16):3029-36.

44. Shimoni R, Pham K, Yassin M, Ludford-Menting MJ, Gu M, Russell SM. Normalized polarization ratios for the analysis of cell polarity. PLoS One. 2014 Jun 25;9(6):e99885.

45. Diener C, Schreiber G, Giese W, del Rio G, Schröder A, Klipp E. Yeast mating and image-based quantification of spatial pattern formation. PLoS Comput Biol. 2014 Jun 26;10(6):e1003690.

46. Le Dévédec SE, Yan K, de Bont H, Ghotra V, Truong H, Danen EH, Verbeek F, van de Water B. Systems microscopy approaches to understand cancer cell migration and metastasis. Cell Mol Life Sci. 2010 Oct;67(19):3219-40.

47. Gough W, Hulkower KI, Lynch R, McGlynn P, Uhlik M, Yan L, Lee JA. A quantitative, facile, and high-throughput image-based cell migration method is a robust alternative to the scratch assay. J Biomol Screen. 2011 Feb;16(2):155-63.

48. Schmid B, Shah G, Scherf N, Weber M, Thierbach K, Campos CP, Roeder I, Aanstad P, Huisken J. High-speed panoramic light-sheet microscopy reveals global endodermal cell dynamics. Nat Commun. 2013;4:2207.

49. Yarrow JC, Perlman ZE, Westwood NJ, Mitchison TJ. A high-throughput cell migration assay using scratch wound healing, a comparison of image-based readout methods. BMC Biotechnol. 2004 Sep 9;4:21.

50. Szalóki N, Doan-Xuan QM, Szöllősi J, Tóth K, Vámosi G, Bacsó Z. High throughput FRET analysis of protein-protein interactions by slide-based imaging laser scanning cytometry. Cytometry A. 2013 Sep;83(9):818-29.

51. Lund FW, Wüstner D. A comparison of single particle tracking and temporal image correlation spectroscopy for quantitative analysis of endosome motility. J Microsc. 2013 Nov;252(2):169-88.

52. Ko HC, Gelb BD. Concise review: drug discovery in the age of the induced pluripotent stem cell. Stem Cells Transl Med. 2014 Apr;3(4):500-9.

53. Martinez IKC, Sparks N, Affeldt III H, Bhanu, B, zur Nieden NI**.** Video-Based Calcification Assay: A Novel Method for Kinetic Analysis of Functional Properties of Osteoblasts in Live Cultures (Chapter 3)

54. Talbot P, Lin S. Mouse and human embryonic stem cells: can they improve human health by preventing disease? Curr Top Med Chem. 2011;11(13):1638-52.

55. Jung EM, Choi YU, Kang HS, Yang H, Hong EJ, An BS, Yang JY, Choi KH, Jeung EB. Evaluation of developmental toxicity using undifferentiated human embryonic stem cells. J Appl Toxicol. 2014 Apr 16.

56. Hong EJ, Jeung EB. Assessment of Developmental Toxicants using Human Embryonic Stem Cells. Toxicol Res. 2013 Dec 31;29(4):221-7.

57. zur Nieden NI, Kempka G, Ahr HJ. *In vitro* differentiation of embryonic stem cells into mineralized osteoblasts. Differentiation. 2003 Jan;71(1):18-27.

58. Knoll M, Talbot P. Cigarette smoke inhibits oocyte cumulus complex pick-up by the oviduct in vitro independent of ciliary beat frequency. Reprod Toxicol. 1998 Jan-Feb;12(1):57-68.

59. Knoll M, Shaoulian R, Magers T, Talbot P. Ciliary beat frequency of hamsteroviducts is decreased in vitro by exposure to solutions of mainstream andsidestream cigarette smoke. Biol Reprod. 1995 Jul;53(1):29-37.

60. Davis LA, Dienelt A, and zur Nieden NI. (2011). Absorption-based assays for the analysis of osteogenic and chondrogenic yield. Methods Mol Biol. 690: 255-272.

Chapter 5: Conclusion

Development is a fundamental aspect in a complex organism. It allows an unspecialized cell to generate a diverse type of organ that comprises of a wide range of tissue type. It is essential to keep this process controlled; otherwise the misregulation of differentiation can lead to many congenital birth defects. An example of this is that the misregulation of osteogenesis can result in brittle bones or improper development of limbs [Rauch and Glorieux,2004; Gautieri et al, 2009; Raisz, 2005]. Most congenital defects occur during the 1st trimester of the gestation period during the development of the embryo. At this stage the developing embryo is susceptible to a wide array of environmental toxicants, such as environmental tobacco smoke or cigarette smoke [http://www.cdc.gov/ncbddd/birthdefects/index.html; Gilbert-Barness, 2010; Brent, 2001.] Understanding the teratogenicity of a toxicant to development such as bone differentiation is extremely important. In addition, development of methods to improve teratogenic testing is also immensely valuable. Thus, in this dissertation a video-based assessment tool was developed to quantify the functional property of osteoblasts and to determine the effects of commercially available conventional and harm-reduction tobacco products on osteogenic differentiation.

Human embryonic stem cells were utilized as a model for human bone development. This pluripotent stem cell line was induced to undergo osteogenesis using an over-growth approach and the media supplementation of osteogenic factors, 1,25 dihydroxy-vitamin D_3, β-glycerophosphate, and ascorbic acid. Based on the calcification of the cultures *in vitro*, which appears as black deposit on the culture dish, a video-based calcification was developed to quantify the calcification output of emerging osteoblasts. This video-based calcification assay was also used to introduce a novel characterization

parameter, the calcification rate, which describes calcification in a kinetic manner. This can only be done using this method because of the unique property of obtaining and measuring calcification from the same sample over time without the need to sacrifice it for analysis. In the first part of this thesis, this new method was used to compare calcification of osteoblasts obtained from different pluripotent stem cells, which had never been done before. Results showed that human induced pluripotent stem cells, an artificial source of pluripotent stem cells with high hopes for regenerative medicine, were less capable of generating osteoblasts than bona fide ESCs, and that already early on in differentiation. Although the lower osteogenic differentiation ability of hiPSCs could potentially put a halt to their use in cell-based therapies, their *in vitro* differentiation may still be exploited in predictive teratogenicity assays, as we show here.

The human osteogenesis *in vitro* model was also used to determine the teratogenic effects of several tobacco products available on the market. These product consisted of well-known conventional products, Marlboro and Camel, as well as their harm-reduction counterpart, Marlboro Gold (Light), Camel Blue (Light) , and American Spirit. These are widely consumed brands, but yet nothing has been previously known about the effects on developing osteoblasts. Our studies reveal here that mainstream smoke showed no observable changes in the ability of stem cells to turn into functional osteoblasts or on their survival ability, even in high doses. However, and important for tobacco regulation, sidestream smoke, which is inhaled involuntarily by bystanders, showed both cytotoxic effects on osteogenesis (conventional tobacco products and American Spirit) as well as teratogenic effects on bone differentiation (harm reduction products). By extension, this would suggest that sidestream smoke is more potent than

mainstream smoke in causing embryonic bone defects and that conventional and harm-reduction tobacco products have different modes of lowering bone differentiation.

Lastly, video-based assay technology was used to update the Embryonic Stem Cell Test to assess teratogenicity of chemicals using videos. A video-based assay to analyze cellular viability was developed and used in conjunction with the video-based calcification assay to create a fully automated quantifiable endpoint assay for teratogenicity. Using this technology, we have again assessed the teratogenic effects of conventional and harm-reduction tobacco products and were able to confirm that sidestream smoke from conventional tobacco products and American Spirits have cytotoxic effect on bone formation, while mainstream smoke had no observable effects on osteogenesis. An additional benefit of this entirely video-based assay was that assessment of teratogenicity was already possible on day 10 of differentiation, which represents a reduction by 10 days and therefore makes the assay more attractive for routine use.

In summary, this study has developed a more accurate method assessing teratogenicity of chemicals because it utilizes the same samples to measure both function and viability. This minimizes differences in results from the analysis of otherwise two different samples as is the case using conventional reagent based assay and therefore increases accuracy and predictivity. This method is also more cost-effective because it does not require the use of reagent to determine change in development, and by minimizes the required cellular material to assess teratogenic effects. Thus, using video and image analysis successfully improved the traditional Embryonic Stem Cell Test for assessing teratogenic effects on bone differentiation.

References

1. Rauch F, Glorieux FH. Osteogenesis imperfecta. Lancet. 2004 Apr 24;363(9418):1377-85.
2. Gautieri A, Uzel S, Vesentini S, Redaelli A, Buehler MJ. Molecular and mesoscale mechanisms of osteogenesis imperfecta disease in collagen fibrils. Biophys J. 2009 Aug 5;97(3):857-65.
3. Raisz LG. Pathogenesis of osteoporosis: concepts, conflicts, and prospects. J Clin Invest. 2005 Dec;115(12):3318-25.
4. http://www.cdc.gov/ncbddd/birthdefects/index.html
5. Gilbert-Barness E. Teratogenic causes of malformations. Ann Clin Lab Sci. 2010 Spring;40(2):99-114.
6. Brent RL. The cause and prevention of human birth defects: what have we learned in the past 50 years? Congenit Anom (Kyoto) 2001;41:3-21.